NISTIR 8331

# Ongoing Face Recognition Vendor Test (FRVT)
# Part 6B: Face recognition accuracy with face masks using post-COVID-19 algorithms

Mei Ngan
Patrick Grother
Kayee Hanaoka

This publication is available free of charge from:
https://doi.org/10.6028/NIST.IR.8331

National Institute of Standards and Technology
U.S. Department of Commerce

NISTIR 8331

# Ongoing Face Recognition Vendor Test (FRVT)
# Part 6B: Face recognition accuracy with face masks using post-COVID-19 algorithms

Mei Ngan
Patrick Grother
Kayee Hanaoka
*Information Access Division*
*Information Technology Laboratory*

This publication is available free of charge from:
https://doi.org/10.6028/NIST.IR.8331

November 2020


U.S. Department of Commerce
*Wilbur L. Ross, Jr., Secretary*

National Institute of Standards and Technology
*Walter Copan, NIST Director and Undersecretary of Commerce for Standards and Technology*

**National Institute of Standards and Technology Interagency or Internal Report 8331**
**Natl. Inst. Stand. Technol. Interag. Intern. Rep. 8331, 83 pages (November 2020)**

**This publication is available free of charge from:**
**https://doi.org/10.6028/NIST.IR.8331**

# Executive Summary

**OVERVIEW**

This is the second of a series of reports on the performance of face recognition algorithms on faces occluded by protective face masks [2] commonly worn to reduce inhalation and exhalation of viruses. Inspired by the COVID-19 pandemic response, this is a continuous study being run under the Ongoing Face Recognition Vendor Test (FRVT) executed by the National Institute of Standards and Technology (NIST). In our first report [8], we tested "pre-pandemic" algorithms that were already submitted to FRVT 1:1 prior to mid-March 2020. This report augments its predecessor with results for more recent algorithms provided to NIST after mid-March 2020. While we do not have information on whether or not a particular algorithm was designed with face coverings in mind, the results show evidence that a number of developers have adapted their algorithms to support face recognition on subjects potentially wearing face masks. The algorithms tested were one-to-one algorithms submitted to the FRVT 1:1 Verification track. Future editions of this document will also report accuracy of one-to-many algorithms.

**WHAT'S NEW**

This report includes

- ▷ Results from evaluating 65 face recognition algorithms provided to NIST since mid-March 2020
- ▷ Assessment of when both the enrollment and verification images are masked (in addition to when only the verification image is masked)
- ▷ Results for red and white colored masks (in addition to light-blue and black)
- ▷ Cumulative results for 152 algorithms evaluated to date (submitted both prior to and after mid-March 2020)

**MOTIVATION**

Traditionally, face recognition systems (in cooperative settings) are presented with mostly non-occluded faces, which include primary facial features such as the eyes, nose, and mouth. However, there are a number of circumstances in which faces are occluded by masks such as in pandemics, medical settings, excessive pollution, or laboratories. Inspired by the COVID-19 pandemic response, the widespread requirement that people wear protective face masks in public places has driven a need to understand how cooperative face recognition technology deals with occluded faces, often with just the periocular area and above visible. An increasing number of research publications have surfaced on the topic of face recognition on people wearing masks along with face-masked research datasets [10]. A number of commercial providers have announced the availability of face recognition algorithms capable of handling face masks, and this report documents performance results for 65 algorithms submitted to NIST after mid-March 2020. This report includes results for all algorithms evaluated to date. At the time of this writing, we are not aware of any large-scale, independent, and publicly reported evaluation on the effects of face mask occlusion on face recognition.

**WHAT WE DID**

The NIST Information Technology Laboratory (ITL) quantified the accuracy of face recognition algorithms on faces occluded by masks applied digitally to a large set of photos that has been used in an FRVT verification benchmark since 2018. These algorithms were submitted to FRVT 1:1 and includes 65 new algorithms provided to NIST since mid-March 2020. While we do not have information on whether or not a particular algorithm was designed with face coverings in mind, the algorithms were submitted with the expectation that NIST would execute them on masked face images. Using the original unmasked images to form a baseline for accuracy, we measured the impact of occlusion by digitally applying a mask to the face and varying mask shape, mask color, and nose coverage.

We ran these algorithms over a large set of photographs collected in U.S. governmental applications that are currently in operation: **application photographs** from a global population of applicants for immigration benefits and **border crossing photographs** of travelers entering the United States. Both datasets were collected for authorized travel or immigration processes.





FNMR(T) "False non-match rate"
FMR(T) "False match rate"

**WHAT WE DID (CONTINUED)**

The application photos (used as reference images) have good compliance with image capture standards. The border crossing photos (used as probe images) are not in good compliance with image capture standards given possible constraints on capture equipment, duration, facilities, and environment. We evaluated the case where the application photos were left unmasked, and synthetic masks were applied to the border crossing photos. This mimics an operational scenario where a person wearing a mask attempts to authenticate against a prior visa or passport photo. We also evaluated when both the application photos and border crossing photos were masked. This mimics, for example, a seamless travel scenario through an airport where a masked face image captured at check-in is enrolled and used during subsequent authentication attempts of the passenger still wearing a face mask. Together these datasets allowed us to process a total of 6.2 million images through a cumulative total of 152 algorithms.

Our use of software to apply masks to face images has the following advantages: it allows very rapid characterization of the effect of masks on face recognition; it allows controlled exploration of factors such as mask size, shape, and color; it affords repeatability, which is key to the fair comparison of algorithms; it scales to very large datasets - in our study, some 6.2 million photographs - which allows fine-grained characterization of false positive rates in addition to false negative rates. Conversely, our use of digital masks presents a number of limitations - please see the *Limitations* section of this executive summary for a more detailed discussion on the limitations of this study.

**WHAT WE FOUND**

The following results represent observations on algorithms provided to NIST both before and after the COVID-19 pandemic to date. We do not have information on whether or not a particular algorithm was designed with face coverings in mind. The results documented capture a snapshot of algorithms submitted to the FRVT 1:1 in face recognition on subjects potentially wearing face masks.

- **False rejection performance**: All algorithms submitted after the pandemic continue to give increased false non-match rates (FNMR) when the probes are masked. While a few pre-pandemic algorithms still remain within the most accurate on masked photos, some developers have submitted algorithms after the pandemic showing significantly improved accuracy and are now among the most accurate in our test. Using border crossing images, without masks, the most accurate algorithms will fail to authenticate about 0.3% of persons while falsely accepting no more than 1 in 100000 impostors (i.e. FNMR$=0.003$ at FMR$=0.00001$). With the highest coverage mask we tested and the most accurate algorithms, this failure rate rises to about 5% (FNMR = 0.05) among all algorithms. This is noteworthy given that around 70% of the face area is occluded by the mask. However, many algorithms submitted since mid-March 2020 remain much less tolerant: some algorithms that are quite competitive with unmasked faces (FNMR $< 0.01$) still fail to authenticate between 10% to 40% of masked images (FNMR $\rightarrow 0.4$).

  *See Figures 6, 7 and Table 5*

  For the case where both the enrollment and verification images are masked, interestingly, many algorithms show a reduction in false non-match rates compared to when only the verification image is masked, at a fixed threshold. While the reduction in FNMR is favorable, we observe much larger false match rates when both images are masked. These findings are discussed in subsequent sections of this executive summary. *See Figure 37*

  In cooperative access control applications, false rejections can traditionally be remedied by users making second attempts. This is effective when users correct pose, expression, or illumination aspects of their presentation. With masked faces, however, a second attempt may not be effective if the failure is a systematic property of the algorithm.

**WHAT WE FOUND (CONTINUED)**

▷ **Evolution of algorithms on face masks**: We observe that a number of algorithms submitted since mid-March 2020 show notable reductions in error rates with face masks over their pre-pandemic predecessors. When comparing error rates for unmasked versus masked faces, the median FNMR across algorithms submitted since mid-March 2020 has been reduced by around 25% from the median pre-pandemic results. The figure below presents examples of developer evolution on both masked and unmasked datasets. For some developers, false rejection rates in their algorithms submitted since mid-March 2020 decreased by as much as a factor of 10 over their pre-pandemic algorithms, which is evidence that some providers are adapting their algorithms to handle face masks. However, in the best cases, when comparing results for unmasked images to masked images, false rejection rates have increased from 0.3%-0.5% (unmasked) to 2.4%-5% (masked). The current performance of face recognition with face masks is comparable to the state-of-the-art on unmasked images in mid-2017 [4].

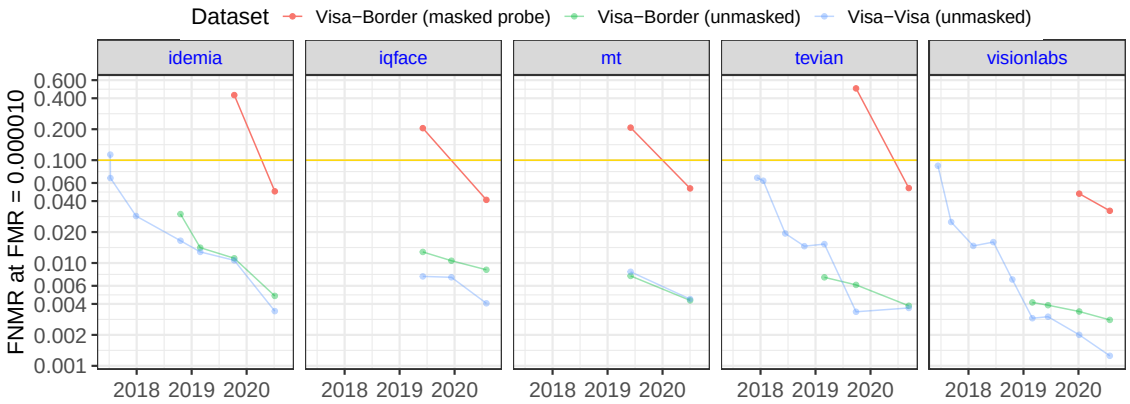


*Figure 1: Examples of developer evolution of accuracy on masked and unmasked datasets.*

*See Figures 6, 5, and 7*

▷ **False acceptance performance**: As most systems are configured with a fixed threshold, it is necessary to report both false negative and false positive rates for each group at that threshold. When comparing a masked probe to an unmasked enrollment photo, in most cases, false match rates (FMR) are reduced by masks. The effect is generally modest with reductions in FMR usually being smaller than a factor of two. This property is valuable in that masked probes do not impart adverse false match security consequences for verification.

However, when both the enrollment and verification images are masked, most algorithms give elevated false match rates, with FMR ranging from 10 to 100 times higher than when only the probe is masked or both images are unmasked, at the same threshold. This behavior applies to most algorithms tested, with the exception of particular algorithms submitted by Idemia (idemia-006) and Pensees (pensees-001). These two algorithms generate approximately constant FMR across any masked/unmasked combination, and similarly, yield approximately constant FNMR across masked-probe and masked-enrollment-and-probe combinations. *See Figure 37*

▷ **Mask-agnostic face recognition**: All 1:1 verification algorithms submitted to the FRVT test since the start of the pandemic are evaluated on both masked and unmasked datasets. The test is designed this way to mimic operational reality: some images will have masks, some will not (especially enrollment samples from a database or ID card). And to the extent that the use of protective masks will exist for some time, our test will continue to evaluate algorithmic capability on verifying all combinations of masked and unmasked faces.





FNMR(T) "False non-match rate"
FMR(T) "False match rate"

**WHAT WE FOUND (CONTINUED)**

At least two developers - Idemia and Pensees - have developed algorithms that work with any combination of masked and unmasked images, favorably generating approximately constant FMR across any masked/unmasked combination.

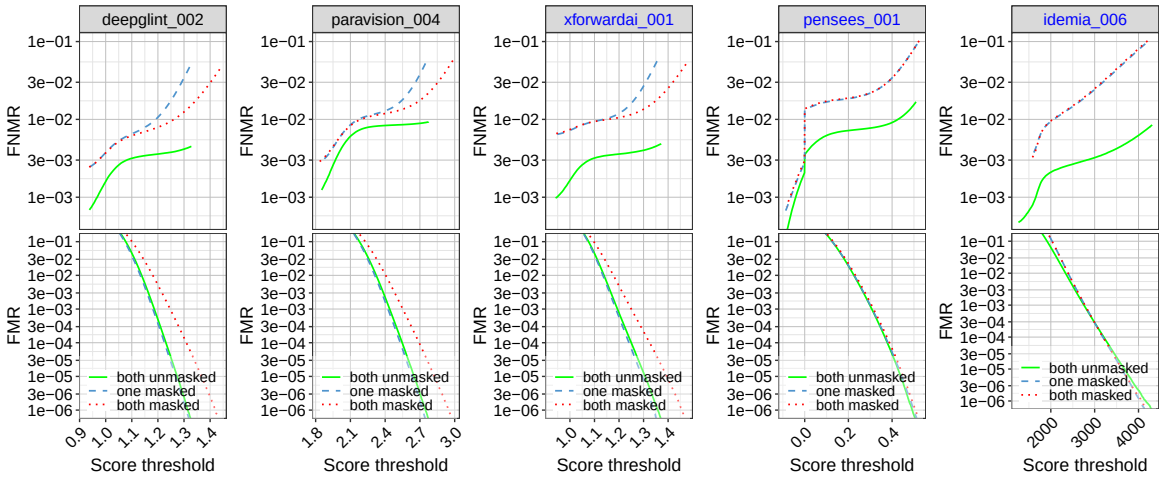


*Figure 2: FNMR and FMR calibration curves on masked/unmasked combinations.*

An example of an integrated approach might be: 1) inclusion of a mask detector 2) on an unmasked image, extract features from both the full face and the periocular region 3) on a detected masked image, extract features from the periocular region 4) at match time, compare full-face templates when both images are unmasked, and periocular templates otherwise.

- **Coverage of the masks**: Masks that occlude more of the face give larger false non-match rates. We surveyed over the extent to which the mask covers the nose, from not at all ("low") to typical ("medium") to near the eyes ("high"). We baselined those with unmasked faces with the result that FNMR increases by factors of around 6, 20, and 30 respectively for the median algorithm submitted since mid-March 2020. However, as noted, algorithms vary considerably in the their tolerance of coverage. Readers should consult tabulated values for specific algorithms.

  *See Table 5 and Figures 9, 11*

  We included the "low" option not because it is a common position for a mask but as an option for authentication applications where it would be tenable to ask the user to pull the mask down to just below the nose for the duration of the authentication attempt.

- **Color of the masks**: We considered white, light-blue, red, and black masks. Many algorithms have higher error rates in black and red masks than light-blue and white masks. The reason for observed accuracy differences between mask color is unknown but is a point for consideration by impacted developers. Mask color also affects the rate at which some algorithms fail to produce a template from an image. *See Figure 24 and Table 9*

- **Shape of the masks**: The shape of the masks matters. Full-face-width masks generally cover more of the face than rounder N95 type masks. Post-pandemic algorithm results show that wide-width masks generally give false negative rates about a factor of 1.5 higher than do rounder type masks. *See Figure 8*

- **Failure to detect and template:** The false negative rates in this report include the effects of both face detection and localization errors, and low-similarity matching errors. We separately include tables detailing how often an algorithm does not make a template from an input image. While many algorithms give low failure-to-template rates, some give high values ranging close to 100%. Conversely, the successful creation of a template does not guarantee proper facial localization. Such localization failures will not be captured as a failure to detect and template event but will impact accuracy rates nonetheless. *See Table 9 and Figure 10*





FNMR(T) "False non-match rate"
FMR(T) "False match rate"

**LIMITATIONS** As a simulation, this study likely doesn't fully capture the effects of masks on face recognition. Particularly the following points should be weighed by readers in the near term. Some of these will be addressed in subsequent work at NIST.

- **Train algorithms:** As with all NIST evaluations, we regard the software as a black box whose parameters (models) remain fixed for the entirety of its use without learning from the test data. We do not train or fine-tune algorithms.
- **Evaluate one-to-many algorithms:** We have only run one-to-one verification algorithms with masks. This elicits data on the effect of masks on the underlying feature extraction and discrimination of algorithms and can therefore be be expected to give first-order indications of the effect on one-to-many identification algorithms.
- **Consider the effect of eye occlusion:** We did not address the effect of eye-glasses or eye-protection. While our dataset includes examples of people wearing glasses, we didn't collect such data nor simulate it with digital addition.
- **Test with images of real masks:** Given time and resource constraints, we didn't collect photos of subjects wearing masks. The possible downsides of this are several. First, our digital masks are tailored to faces; while a few don't fit realistically, mass-produced real masks may not fit all actual persons correctly either. We were not able to pursue an exhaustive simulation of the endless variations in color, design, shape, texture, bands, and ways masks can be worn. Second, because many cameras run with exposure-control, it is possible that a dark mask will cause less light to be reflecting and the camera to increase gain on the sensor causing overexposure of the periocular region. Likewise a white mask could lead to underexposure problems. Third, it is possible that some cameras that include a face detector, may fail to focus or acquire a masked face correctly.
- **Use textured masks:** All masks synthesized by NIST in this study have a uniform color. The consequences of this are that we do not capture the impact of mask texture or pattern on face recognition. The possibility exists for patterned masks to induce higher facial localization errors, which is not captured in our current study. We received a suggestion that such information may serve as a soft biometric, in that a subject that always wears the same textured mask will be more identifiable. We don't intend to encourage algorithm development along this line, because as mass-produced high-efficacy masks become more common, mask diversity may actually drop.
- **Study demographic effects on masked images:** This report estimates overall performance of existing algorithms on recognition of faces occluded by masks. We deferred tabulating accuracy for different demographic groups until more capable mask-enabled algorithms have been submitted to FRVT.
- **Evaluate algorithms on non-cooperative, unconstrained imagery:** This report documents results for matching masked webcam images to unmasked portrait-style photos. While the properties of the two sets of images differ, subjects are operating in cooperative mode and are for the most part, looking at the camera.
- **Consider effects of human examination:** This report does not consider the various ways humans are involved in face recognition systems. For example, analysts can correct face detection or localization errors induced by masks, prior to automated recognition. Likewise, humans are often tasked with adjudication of images following a rejection or other exception from an automated system. Analysis of human capability and role is pertinent to those operations, but is beyond the scope of this study.





FNMR(T) "False non-match rate"
FMR(T) "False match rate"

**IMPLICATIONS AND FUTURE WORK**

**Know Your Algorithm:** Operational implementations usually employ a single face recognition algorithm. Given algorithm-specific sensitivities to masks and other image or subject properties, it is incumbent upon the system owner to know their algorithm. While publicly available test data from NIST and elsewhere can inform owners, it will usually be informative to specifically measure accuracy of the operational algorithm on the operational image data collected with actual masks.

NIST plans on releasing a series of reports, iteratively assessing different aspects and use cases of face masking on recognition performance.





FNMR(T) "False non-match rate"
FMR(T) "False match rate"

## ACKNOWLEDGMENTS

This work was conducted in collaboration with the Department of Homeland Security's Science & Technology Directorate (S&T), Office of Biometric Identity Management (OBIM), and Customs and Border Protection (CBP). Additionally, the authors are grateful to staff in the NIST Biometrics Research Laboratory for infrastructure supporting rapid evaluation of algorithms.

## DISCLAIMER

Specific hardware and software products identified in this report were used in order to perform the evaluations described in this document. In no case does identification of any commercial product, trade name, or vendor, imply recommendation or endorsement by the National Institute of Standards and Technology, nor does it imply that the products and equipment identified are necessarily the best available for the purpose.

## INSTITUTIONAL REVIEW BOARD

The National Institute of Standards and Technology's Research Protections Office reviewed the protocol for this project and determined it is not human subjects research as defined in Department of Commerce Regulations, 15 CFR 27, also known as the Common Rule for the Protection of Human Subjects (45 CFR 46, Subpart A).





FNMR(T) "False non-match rate"
FMR(T) "False match rate"

# Contents



# List of Tables







FNMR(T) "False non-match rate"
FMR(T) "False match rate"

# List of Figures

# 1 Face Mask Effects

## 1.1 Status

NIST has conducted the second out of a series of tests aimed at quantifying face recognition accuracy for people wearing masks. Our initial approach has been to apply masks to faces digitally (i.e., using software to apply a synthetic mask). This allowed us to leverage large datasets that we already have. This report documents results for 1:1 verification algorithms. In our first report [8], we tested "pre-pandemic" algorithms that were already submitted to FRVT 1:1 prior to mid-March 2020. This report augments its predecessor with results for more recent algorithms provided to NIST **after the COVID-19 pandemic**. While we do not have information on whether or not a particular algorithm was designed with face coverings in mind, the algorithms were submitted with the expectation that NIST would execute them on masked face images. In addition to reporting results for when only the verification image is masked, we also document the effects for the case when both enrollment and verification images are masked. This report quantifies the effect of masks on both false negative and false positives match rates and tracks developer evolution of face recognition accuracy with face masks.

The FRVT evaluation is an ongoing test that remains open to new participation. Comments and suggestions should be directed to frvt@nist.gov.

## 1.2 Introduction

The majority of face recognition systems have been deployed in applications where subjects make cooperative presentations to a camera, for example as part of an application for a benefit or ID credential, or as during access control. With very few exceptions such images would not include face masks or other occlusions. However, with the COVID-19 pandemic, we can anticipate a demand to authenticate persons wearing masks, for example in immigration settings, without the need to the subjects to remove those masks. This presents a problem for face recognition, because regions of the face occluded by masks - the mouth and nose - include information useful for both recognition and, potentially, the detection stage that precedes it.

Previous work on face recognition of occluded faces has been directed at situations such as crime scenes where subjects were actively un-cooperative i.e. acting to evade face detection and recognition. Those applications are often characterized by image properties (low resolution, video compression, uncontrolled head orientation) that are known [5] to degrade recognition accuracy.





FNMR(T) "False non-match rate"
FMR(T) "False match rate"

# 2 Image Datasets

## 2.1 Application Images

The images are collected in an attended interview setting using dedicated capture equipment and lighting. The images are of size 300x300 pixels. The images are all high-quality frontal portraits collected in immigration offices and with a white background. As such, potential quality related drivers of high false match rates (such as blur) can be expected to be absent. The images are encoded as ISO/IEC 10918 i.e. JPEG. Over a random sample of 1000 images, the images have compressed file sizes (mean: 42KB, median: 58KB, 25-th percentile: 15KB, and 75-th percentile: 66KB). The implied bit-rates are mostly benign and superior to many e-Passports. When these images are provided as input into the algorithm, they are labeled with the type "ISO".

*Figure 3: Examples of images with properties similar to the enrollment application photos used in this study. The subjects in the photos are all NIST employees.*

## 2.2 Webcam Images

These images are taken with a camera oriented by an attendant toward a cooperating subject. This is done under time constraints, so there are roll, pitch, and yaw angle variations. Also, background illumination is sometimes bright, so the face is under exposed. Sometimes, there is perspective distortion due to close range images. The images are generally in poor conformance with the ISO/IEC 19794-5 Full Frontal image type. The images have mean interocular distance of 38 pixels. The images are all live capture. When these images are provided as input into the algorithm, they are labeled with the type "WILD". Examples of such images are included in Figure 4 and Figure 4 in NIST Interagency Report 8271. Results for verification of these images (unmasked) appear in FRVT Part 1 - Verification both compared against images of the same type, and with those described in section 2.1.

| Description | # |
|---|---|
| Total images | 6 244 865 |
| Application (enrollment) images | 1 019 232 |
| Subjects in application images | 1 019 232 |
| Webcam (verification) images | 5 225 633 |
| Subjects in webcam (verification) images | 2 535 329 |
| Mated comparisons | 3 225 633 |
| Impostor comparisons | 200 000 000 |
| Subjects in mated comparisons | 535 329 |
| Subjects in impostor comparisons | 3 019 232 |

*Table 1: Summary quantities of the dataset used in this evaluation.*





FNMR(T) "False non-match rate"
FMR(T) "False match rate"

## 2.3 Synthetically Masked Images

In this test, synthetically-generated masks were overlaid on top of 1) just the probe image (webcam images described in Section 2.2) or 2) both the enrollment (application photos described in Section 2.1) and probe images. The Dlib [7] C++ toolkit version 19.19 was used to detect and establish key facial points on the face, and with the facial points, solid masks of different shape, height, and color were drawn on the face. The exact Dlib facial points and details used to generate the masks are documented in Appendix A. In the event that Dlib was unable to detect a face in the image, eye coordinates were used to generate a mask leveraging standardized token frontal geometry [1].

Examples of synthetically-masked probe images are presented in Figures 4.





FNMR(T) "False non-match rate"
FMR(T) "False match rate"


*Figure 4: Examples of synthetically-generated face masks used in this study. The original images are from the NIST MEDS-II Dataset [3]. They were collected in operational settings using the same camera and procedure as is used for the border images that form the mainstay of the experiments in this report.*





FNMR(T) "False non-match rate"
FMR(T) "False match rate"

# 3 Metrics

## 3.1 Matching accuracy

Given a vector of N genuine scores, $u$, the false non-match rate (FNMR) is computed as the proportion below some threshold, T:

$$\text{FNMR}(T) = 1 - \frac{1}{N}\sum_{i=1}^{N} H(u_i - T) \tag{1}$$

where $H(x)$ is the unit step function, and $H(0)$ taken to be 1.

Similarly, given a vector of N impostor scores, $v$, the false match rate (FMR) is computed as the proportion above T:

$$\text{FMR}(T) = \frac{1}{N}\sum_{i=1}^{N} H(v_i - T) \tag{2}$$

The threshold, T, can take on any value. We typically generate a set of thresholds from quantiles of the observed impostor scores, $v$, as follows. Given some interesting false match rate range, $[\text{FMR}_L, \text{FMR}_U]$, we form a vector of K thresholds corresponding to FMR measurements evenly spaced on a logarithmic scale

$$T_k = Q(1 - \text{FMR}_k) \tag{3}$$

where $Q$ is the quantile function, and $\text{FMR}_k$ comes from

$$\log_{10}\text{FMR}_k = \log_{10}\text{FMR}_L + \frac{k}{K}\ [\log_{10}\text{FMR}_U - \log_{10}\text{FMR}_L] \tag{4}$$

Detection error tradeoff (DET) characteristics are plots of FNMR(T) vs. FMR(T). These are plotted with $\text{FMR}_U \rightarrow 1$ and $\text{FMR}_L$ as low as is sustained by the number of impostor comparisons, N. This is somewhat higher than the "rule of three" limit $3/N$ [6] because samples are not independent, due to re-use of images.

## 3.2 Failure to Enroll

Failure to enroll (FTE) is the proportion of failed template generation attempts. Failures can occur because the software throws an exception, or because the software electively refuses to process the input image. This would typically occur if a face is not detected. FTE is measured as the number of function calls that give EITHER a non-zero error code OR that give a "small" template. This is defined as one whose size is less than 60 bytes. This second rule is needed because some algorithms incorrectly fail to return a non-zero error code when template generation fails yet do return a valid default data structure.

The effects of FTE are included in the accuracy results of this report by regarding any template comparison involving a failed template to produce a low similarity score. Thus higher FTE results in higher FNMR and lower FMR.

# 4 Algorithms

The FRVT activity is open to participation worldwide, and the test will evaluate submissions on an ongoing basis. There is no charge to participate. The process and format of algorithm submissions to NIST are described in the FRVT 1:1 Verification Application Programming Interface (API) [9] document. Participants provide their submissions in the form of libraries compiled on a specific Linux kernel, which are linked against NIST's test harness to produce executables. NIST provides a validation package to participants to ensure that NIST's execution of submitted libraries produces the expected output on NIST's test machines.





FNMR(T) "False non-match rate"
FMR(T) "False match rate"

This report documents the results of algorithms submitted to FRVT 1:1 for testing both before (prior to mid-March 2020) and after the COVID-19 pandemic. Table 4 lists the algorithms that were tested. Note that algorithms that are expired or retired are not included in this report.

| | Developer | Algorithm | Submission Date |
|---|---|---|---|
| 1 | 3Divi | 3divi-004 | 2019-07-22 |
| 2 | 3Divi | 3divi-005 | 2020-08-28 |
| 3 | ACI Software | acisw-003 | 2020-08-03 |
| 4 | ADVANCE.AI | advance-002 | 2019-12-19 |
| 5 | ASUSTek Computer Inc | asusaics-000 | 2019-10-24 |
| 6 | AYF Technology | ayftech-001 | 2020-07-06 |
| 7 | Acer Incorporated | acer-000 | 2020-01-08 |
| 8 | Acer Incorporated | acer-001 | 2020-06-30 |
| 9 | Ai First | aifirst-001 | 2019-11-21 |
| 10 | AiUnion Technology | aiunionface-000 | 2019-10-22 |
| 11 | Aigen | aigen-001 | 2020-10-06 |
| 12 | Akurat Satu Indonesia | ptakuratsatu-000 | 2020-09-11 |
| 13 | AlphaSSTG | alphaface-002 | 2020-02-20 |
| 14 | Anke Investments | anke-005 | 2019-11-21 |
| 15 | Antheus Technologia | antheus-000 | 2019-12-05 |
| 16 | Antheus Technologia | antheus-001 | 2020-06-25 |
| 17 | Aware | aware-005 | 2020-02-27 |
| 18 | Awidit Systems | awiros-001 | 2019-09-23 |
| 19 | Awidit Systems | awiros-002 | 2020-10-28 |
| 20 | Beihang University-ERCACAT | ercacat-001 | 2020-07-06 |
| 21 | Beijing Alleyes Technology | alleyes-000 | 2020-03-09 |
| 22 | BioID Technologies SA | bioidtechswiss-000 | 2019-11-15 |
| 23 | BioID Technologies SA | bioidtechswiss-001 | 2020-08-28 |
| 24 | Bresee Technology | bresee-000 | 2020-08-07 |
| 25 | CSA IntelliCloud Technology | intellicloudai-001 | 2019-08-13 |
| 26 | CTBC Bank | ctbcbank-000 | 2019-06-28 |
| 27 | Camvi Technologies | camvi-004 | 2019-07-12 |
| 28 | Canon Information Technology (Beijing) | cib-000 | 2019-12-11 |
| 29 | Canon Information Technology (Beijing) | cib-001 | 2020-08-05 |
| 30 | China University of Petroleum | upc-001 | 2019-06-05 |
| 31 | Chinese Univeristy of Hong Kong | cuhkee-001 | 2020-03-18 |
| 32 | Chosun University | chosun-000 | 2020-02-12 |
| 33 | Chosun University | chosun-001 | 2020-07-01 |
| 34 | Chunghwa Telecom | chtface-002 | 2019-12-07 |
| 35 | Chunghwa Telecom | chtface-003 | 2020-06-24 |
| 36 | Cortica | cor-001 | 2020-09-24 |
| 37 | Cybercore | cybercore-000 | 2020-08-26 |
| 38 | Cyberlink Corp | cyberlink-004 | 2020-02-27 |
| 39 | Cyberlink Corp | cyberlink-005 | 2020-07-31 |
| 40 | DSK | dsk-000 | 2019-06-28 |
| 41 | Dahua Technology | dahua-004 | 2019-12-18 |
| 42 | Dahua Technology | dahua-005 | 2020-08-13 |
| 43 | Decatur Industries Inc | decatur-000 | 2020-08-18 |
| 44 | Deepglint | deepglint-002 | 2019-11-15 |
| 45 | DiDi ChuXing Technology | didiglobalface-001 | 2019-10-23 |
| 46 | Expasoft LLC | expasoft-000 | 2020-01-06 |
| 47 | Expasoft LLC | expasoft-001 | 2020-09-03 |
| 48 | FaceSoft | facesoft-000 | 2019-07-10 |
| 49 | Fiberhome Telecommunication Technologies | fiberhome-nanjing-002 | 2020-08-10 |
| 50 | Fujitsu Research and Development Center | fujitsulab-000 | 2020-02-04 |
| 51 | Fujitsu Research and Development Center | fujitsulab-001 | 2020-09-30 |
| 52 | GeoVision Inc | geo-000 | 2020-06-29 |
| 53 | Glory | glory-002 | 2019-11-12 |
| 54 | Gorilla Technology | gorilla-005 | 2020-03-11 |
| 55 | Gorilla Technology | gorilla-006 | 2020-07-31 |
| 56 | Guangzhou Pixel Solutions | pixelall-003 | 2019-10-15 |
| 57 | Guangzhou Pixel Solutions | pixelall-004 | 2020-07-02 |

*Table 2: List of algorithms included in this report. Algorithms in black were submitted prior to mid-March 2020, and algorithms in blue were submitted thereafter.*





FNMR(T) "False non-match rate"
FMR(T) "False match rate"

| | Developer | Algorithm | Submission Date |
|---|---|---|---|
| 58 | Hengrui AI Technology | hr-003 | 2020-09-25 |
| 59 | ID3 Technology | id3-005 | 2020-08-04 |
| 60 | ITMO University | itmo-007 | 2020-01-06 |
| 61 | Idemia | idemia-005 | 2019-10-11 |
| 62 | Idemia | idemia-006 | 2020-07-06 |
| 63 | Imageware Systems | iws-000 | 2020-08-12 |
| 64 | Imagus Technology Pty | imagus-001 | 2019-10-22 |
| 65 | Imperial College London | imperial-002 | 2019-08-28 |
| 66 | Incode Technologies Inc | incode-006 | 2020-02-20 |
| 67 | Incode Technologies Inc | incode-007 | 2020-08-25 |
| 68 | Innef Labs | innefulabs-000 | 2020-09-04 |
| 69 | Innovative Technology | innovativetechnologyltd-002 | 2020-02-26 |
| 70 | Innovatrics | innovatrics-006 | 2019-08-13 |
| 71 | Institute of Information Technologies | iit-002 | 2019-12-04 |
| 72 | Intel Research Group | intelresearch-001 | 2020-01-14 |
| 73 | Intel Research Group | intelresearch-002 | 2020-07-24 |
| 74 | Intellivision | intellivision-002 | 2019-08-23 |
| 75 | Kakao Enterprise | kakao-003 | 2020-02-26 |
| 76 | Kedacom International Pte | kedacom-000 | 2019-06-03 |
| 77 | Kneron Inc | kneron-005 | 2020-02-21 |
| 78 | Kookmin University | kookmin-001 | 2020-09-28 |
| 79 | Lomonosov Moscow State University | intsysmsu-002 | 2020-03-12 |
| 80 | Lookman Electroplast Industries | lookman-004 | 2019-06-03 |
| 81 | Luxand Inc | luxand-000 | 2019-11-07 |
| 82 | MVision | mvision-001 | 2019-11-12 |
| 83 | Momentum Digital | sertis-000 | 2019-10-07 |
| 84 | Momentum Digital | sertis-001 | 2020-07-30 |
| 85 | Moontime Smart Technology | mt-000 | 2019-06-03 |
| 86 | Moontime Smart Technology | mt-002 | 2020-07-02 |
| 87 | N-Tech Lab | ntech-008 | 2020-01-06 |
| 88 | NSENSE Corp | nsensecorp-001 | 2020-10-20 |
| 89 | Netbridge Technology Incoporation | netbridgetech-001 | 2020-01-08 |
| 90 | Netbridge Technology Incoporation | netbridgetech-002 | 2020-08-11 |
| 91 | Neurotechnology | neurotechnology-008 | 2020-01-08 |
| 92 | Neurotechnology | neurotechnology-009 | 2020-07-07 |
| 93 | Nodeflux | nodeflux-002 | 2019-08-13 |
| 94 | NotionTag Technologies Private Limited | notiontag-000 | 2019-06-12 |
| 95 | Oz Forensics LLC | oz-001 | 2020-07-29 |
| 96 | PXL Vision AG | pxl-001 | 2020-06-30 |
| 97 | Panasonic R+D Center Singapore | psl-005 | 2020-07-06 |
| 98 | Paravision (EverAI) | paravision-004 | 2019-12-11 |
| 99 | Pensees Pte | pensees-001 | 2020-08-17 |
| 100 | Rank One Computing | rankone-009 | 2020-06-26 |
| 101 | Rank One Computing | rankone-010 | 2020-11-05 |
| 102 | Remark Holdings | remarkai-002 | 2019-11-21 |
| 103 | Rokid Corporation | rokid-000 | 2019-08-01 |
| 104 | Samsung S1 Corp | s1-001 | 2019-12-06 |
| 105 | Satellite Innovation/Eocortex | eocortex-000 | 2020-08-26 |
| 106 | Scanovate | scanovate-001 | 2019-11-12 |
| 107 | Scanovate | scanovate-002 | 2020-06-26 |
| 108 | Securif AI | securifai-001 | 2020-10-06 |
| 109 | Sensetime Group | sensetime-003 | 2019-06-04 |
| 110 | Shanghai Jiao Tong University | sjtu-002 | 2020-02-12 |
| 111 | Shanghai Jiao Tong University | sjtu-003 | 2020-11-02 |
| 112 | Shanghai Ulucu Electronics Technology | uluface-002 | 2019-07-10 |
| 113 | Shanghai University - Shanghai Film Academy | shu-002 | 2019-12-10 |
| 114 | Shanghai University - Shanghai Film Academy | shu-003 | 2020-06-24 |

*Table 3: List of algorithms included in this report. Algorithms in black were submitted prior to mid-March 2020, and algorithms in blue were submitted thereafter.*





FNMR(T) "False non-match rate"
FMR(T) "False match rate"

| | Developer | Algorithm | Submission Date |
|---|---|---|---|
| 115 | Shenzhen AiMall Tech | aimall-002 | 2020-03-12 |
| 116 | Shenzhen AiMall Tech | aimall-003 | 2020-08-12 |
| 117 | Shenzhen Intellifusion Technologies | intellifusion-002 | 2020-03-18 |
| 118 | Staqu Technologies | staqu-000 | 2020-07-15 |
| 119 | Star Hybrid Limited | starhybrid-001 | 2019-06-19 |
| 120 | Su Zhou NaZhiTianDi intelligent technology | nazhiai-000 | 2020-06-25 |
| 121 | Synology Inc | synology-000 | 2019-10-23 |
| 122 | TUPU Technology | tuputech-000 | 2019-10-11 |
| 123 | Taiwan AI Labs | ailabs-001 | 2019-12-18 |
| 124 | Tech5 SA | tech5-004 | 2020-03-09 |
| 125 | Tech5 SA | tech5-005 | 2020-07-24 |
| 126 | Tencent Deepsea Lab | deepsea-001 | 2019-06-03 |
| 127 | Tevian | tevian-005 | 2019-09-21 |
| 128 | Tevian | tevian-006 | 2020-09-11 |
| 129 | Trueface.ai | trueface-000 | 2019-10-08 |
| 130 | Trueface.ai | trueface-001 | 2020-07-20 |
| 131 | Universidade de Coimbra | visteam-000 | 2020-01-14 |
| 132 | Veridas Digital Authentication Solutions S.L. | veridas-004 | 2020-07-21 |
| 133 | Via Technologies Inc | via-001 | 2020-01-08 |
| 134 | Videmo Intelligente Videoanalyse | videmo-000 | 2019-12-19 |
| 135 | Videonetics Technology Pvt | videonetics-002 | 2019-11-21 |
| 136 | Viettel Group | vts-000 | 2020-11-04 |
| 137 | Vigilant Solutions | vigilantsolutions-007 | 2019-06-27 |
| 138 | Vigilant Solutions | vigilantsolutions-008 | 2020-08-03 |
| 139 | VinAI Research VietNam | vinai-000 | 2020-09-24 |
| 140 | VisionLabs | visionlabs-008 | 2020-01-06 |
| 141 | VisionLabs | visionlabs-009 | 2020-07-27 |
| 142 | Vocord | vocord-008 | 2020-01-031 |
| 143 | Winsense | winsense-001 | 2019-10-16 |
| 144 | X-Laboratory | x-laboratory-001 | 2020-01-21 |
| 145 | Xforward AI Technology | xforwardai-000 | 2020-02-06 |
| 146 | Xforward AI Technology | xforwardai-001 | 2020-09-25 |
| 147 | Xiamen University | xm-000 | 2020-10-19 |
| 148 | YooniK | yoonik-000 | 2020-06-24 |
| 149 | Yuan High-Tech Development | yuan-000 | 2020-06-30 |
| 150 | iQIYI Inc | iqface-000 | 2019-06-04 |
| 151 | iQIYI Inc | iqface-002 | 2020-07-30 |
| 152 | iSAP Solution Corporation | isap-002 | 2020-09-01 |

*Table 4: List of algorithms included in this report. Algorithms in black were submitted prior to mid-March 2020, and algorithms in blue were submitted thereafter.*



FNMR(T) "False non-match rate"
FMR(T) "False match rate"

# 5 Results

This section includes accuracy results for the 152 one-to-one verification algorithms listed in Section 4, of which 65 were submitted to FRVT after mid-March 2020 and are labeled in blue in figures and tables throughout this report. We do not include speed and computational resource requirements - they are given in Table 1 in the FRVT 1:1 report. Missing entries generally mean the algorithm was not run on that particular mask variation due to time and resource constraints. The results, which span many pages, are comprised of:

- **Evolution of algorithm performance with face masks**: Figure 5 shows the evolution of performance with face masks for developers that have submitted algorithms since mid-March 2020.
- **FNMR - summary**: Figure 6 gives a summary of false non-matches rates between pre and post-COVID algorithms with a common type of mask. FNMR values are stated at a fixed threshold calibrated to give FMR = 0.00001 on unmasked images.
- **FNMR - detailed**: Table 5 tabulates false non-match rates by color, shape, and nose coverage. It includes also FNMR without any mask. FNMR values are stated at a fixed threshold calibrated to give FMR = 0.00001 on unmasked images.
- **Mask vs. no mask**: The scatter plot in Figure 7 shows variation across all algorithms of FNMR without masks against FNMR with a common type of mask, broken out by pre and post-COVID algorithms.
- **Mask shape**: The scatter plot in Figure 8 shows for all algorithms the increase in false negative results for wide masks vs. narrower round masks, broken out by pre and post-COVID algorithms.
- **Mask nose coverage**: The scatter plot in Figure 9 shows for all algorithms the increase in false negative rates for masks that substantially cover the nose and those pulled beneath the nose, broken out by pre and post-COVID algorithms.
- **FTE**: Table 9 gives empirical failure-to-template results by color, shape, and nose coverage. The table was produced using 10 000 images of each kind of mask.
- **FTE as contributor to FNMR**: The FNMR results include failure-to-template rates (FTE). Figure 10 shows the proportion of template generation failures, broken out by pre and post-COVID algorithms.
- **DET - impact of mask nose coverage and shape**: This section of figures shows detection error tradeoff characteristics for each algorithm, across different mask nose coverages and shapes.
- **DET - impact of mask color**: This section of figures shows detection error tradeoff characteristics for each algorithm, across mask colors.
- **FNMR and FMR vs. threshold**: This section of figures shows the explicit dependence of false non-match rate and false match rate on threshold.





FNMR(T) "False non-match rate"
FMR(T) "False match rate"

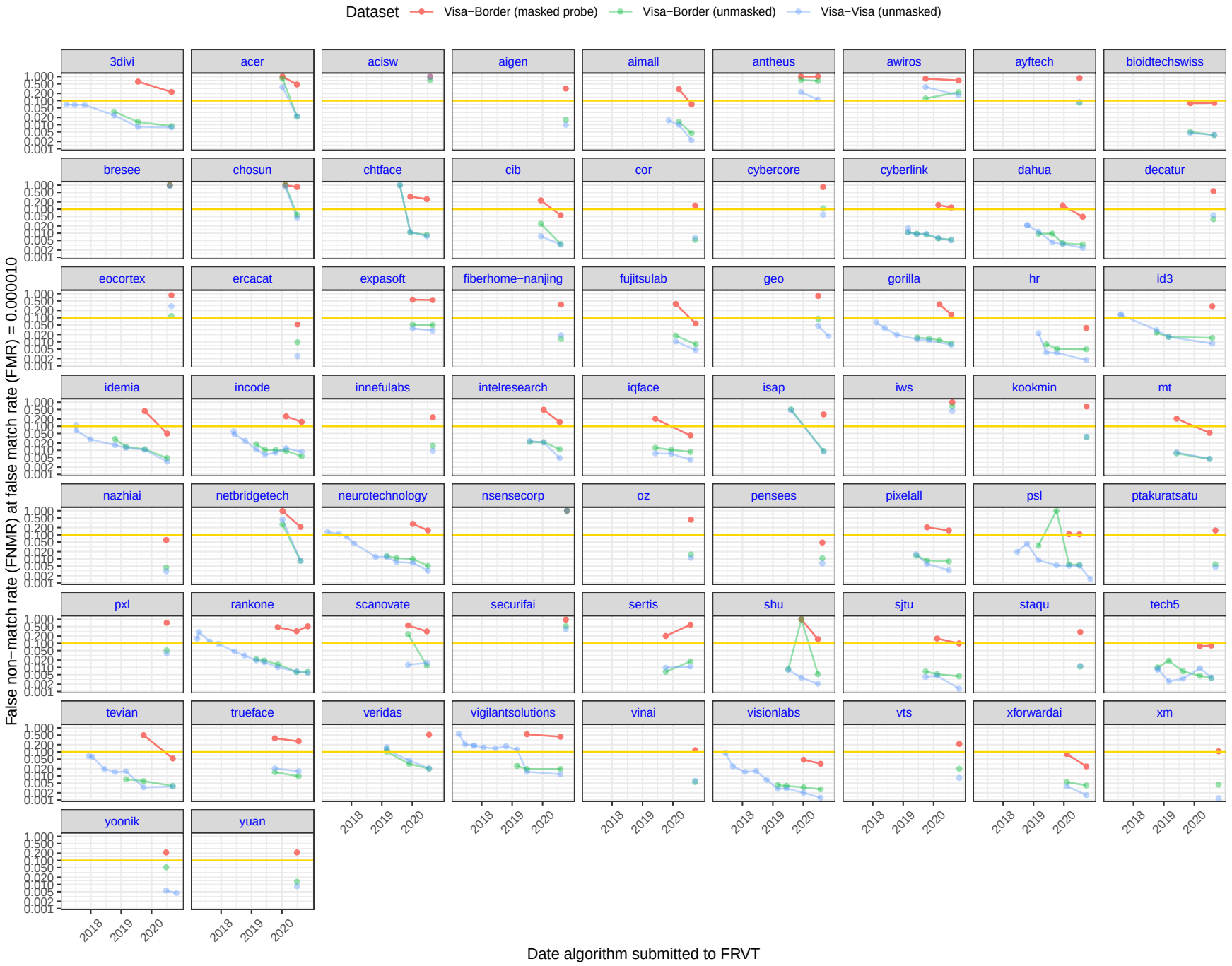


*Figure 5: Evolution of accuracy with face masks for developers that have submitted algorithms since mid-March 2020. Red line represents results on a masked dataset (masked probe), and for reference, the blue and green lines are results for unmasked datasets. FNMR on masked dataset is for medium, wide, lightblue masks. The horizontal gold line shows where FNMR=10%.*





FNMR(T) "False non-match rate"
FMR(T) "False match rate"

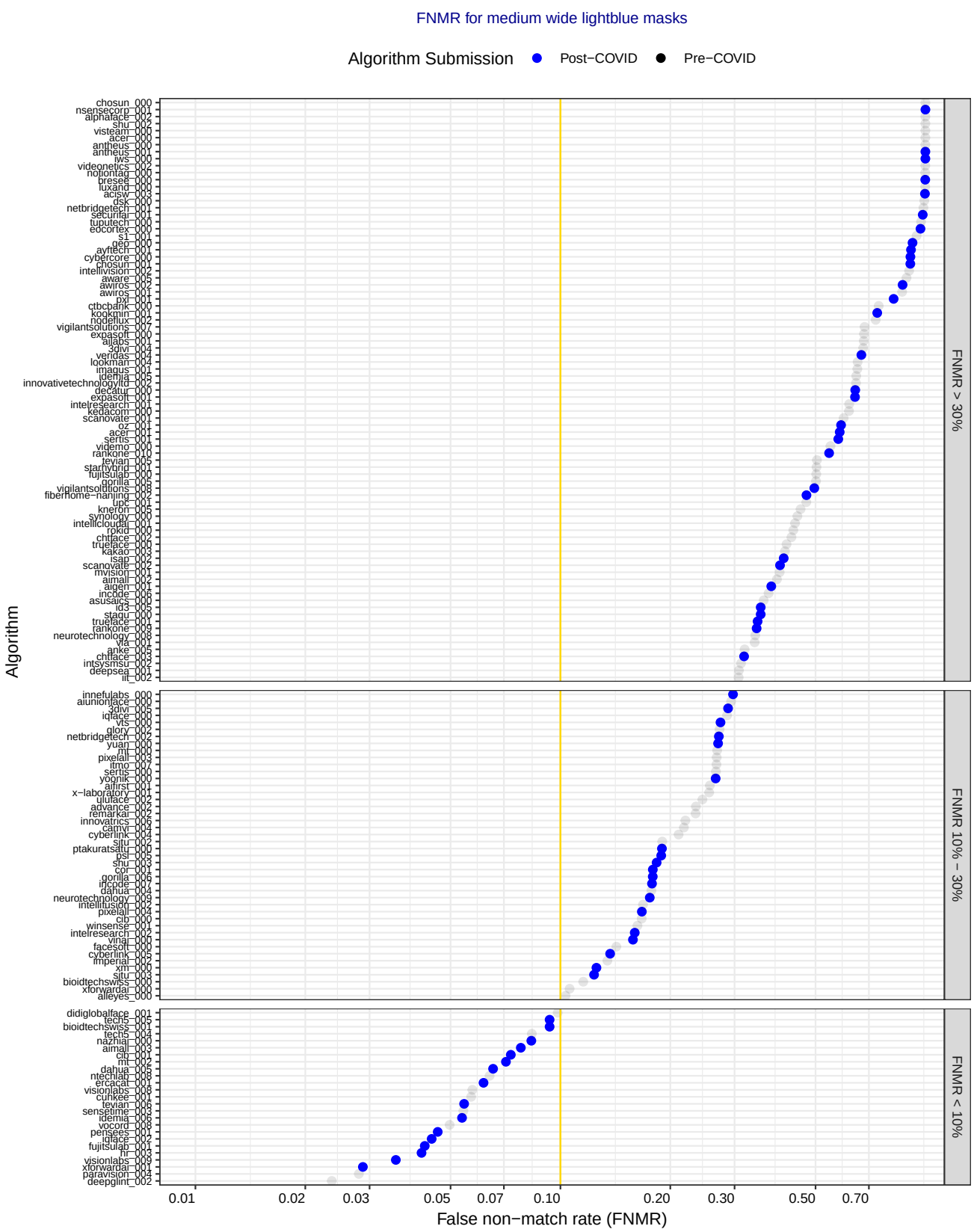


*Figure 6: For each algorithm, each dot shows FNMR @ FMR=0.00001, where the threshold is set for FMR on unmasked probe images. The results are for when the probe is masked, and the enrollment image is unmasked. Gray dots represent results for algorithms submitted prior to mid-March 2020 (pre-COVID), and blue dots represent algorithms submitted thereafter (post-COVID).*





FNMR(T) "False non-match rate"
FMR(T) "False match rate"

| | Algorithm | NOT MASKED | MASK COLOR = LIGHTBLUE | | | | | | COLOR = BLACK | | | COLOR = RED | COLOR = WHITE |
|---|---|---|---|---|---|---|---|---|---|---|---|---|---|
| | Name | | SHAPE = WIDE | | | SHAPE = ROUND | | | SHAPE = WIDE | | | SHAPE = WIDE | SHAPE = WIDE |
| | COVERAGE | | LO | MED | HI | LO | MED | HI | LO | MED | HI | MED | MED |
| 1 | 3divi-004 | 0.0130[87] | 0.4123[99] | 0.6760[117] | - | - | - | - | - | - | - | - | - |
| 2 | 3divi-005 | 0.0088[62] | 0.1006[70] | 0.2895[67] | 0.3670[48] | 0.0783[50] | 0.1918[49] | - | 0.1185[50] | 0.3057[53] | 0.4272[49] | - | - |
| 3 | acer-000 | 0.8432[147] | 0.9995[123] | 0.9999[147] | - | - | - | - | - | - | - | - | - |
| 4 | acer-001 | 0.0219[108] | 0.2587[92] | 0.5835[105] | 0.6719[62] | 0.1536[57] | 0.4325[57] | 0.6831[48] | 0.3132[56] | 0.6304[64] | 0.7143[55] | - | - |
| 5 | acisw-003 | 0.7160[145] | 0.9810[116] | 0.9970[139] | 0.9970[72] | - | - | - | 0.9883[64] | 0.9997[76] | - | - | - |
| 6 | advance-002 | 0.0328[117] | - | 0.2351[52] | - | - | - | - | - | - | - | 0.2333[45] | - |
| 7 | aifirst-001 | 0.0079[54] | 0.0778[56] | 0.2567[55] | - | - | - | - | - | - | - | 0.2624[49] | - |
| 8 | aigen-001 | 0.0159[99] | 0.1268[78] | 0.3790[83] | 0.4432[56] | - | 0.2880[56] | - | 0.1956[54] | 0.4761[59] | 0.6329[54] | 0.3189[51] | 0.3754[39] |
| 9 | ailabs-001 | 0.0243[110] | - | 0.6792[118] | - | - | - | - | - | - | - | - | - |
| 10 | aimall-002 | 0.0133[91] | - | 0.3919[84] | - | - | - | - | - | - | - | - | - |
| 11 | aimall-003 | 0.0045[19] | 0.0188[16] | 0.0781[20] | 0.1325[21] | 0.0175[15] | 0.0524[24] | 0.1021[23] | 0.0223[16] | 0.0913[20] | 0.1577[25] | 0.0738[13] | 0.0800[17] |
| 12 | aiunionface-000 | 0.0094[66] | 0.0917[66] | 0.2935[68] | - | - | - | - | - | - | - | - | - |
| 13 | alleyes-000 | 0.0044[18] | - | 0.1038[26] | - | 0.0181[19] | 0.0542[26] | 0.1050[24] | 0.0262[24] | 0.1287[31] | 0.1991[31] | 0.1066[21] | 0.1098[23] |
| 14 | alphaface-002 | 1.0000[152] | 1.0000[125] | 1.0000[150] | - | - | - | - | - | - | - | - | - |
| 15 | anke-005 | 0.0062[44] | 0.0671[49] | 0.3207[74] | - | - | - | - | - | - | - | - | - |
| 16 | antheus-000 | 0.7319[146] | 0.9994[122] | 0.9999[146] | - | - | - | - | - | - | - | - | - |
| 17 | antheus-001 | 0.6608[142] | 0.9988[121] | 0.9998[145] | 0.9998[73] | 0.9993[65] | 0.9998[67] | 0.9998[54] | 0.9993[66] | 0.9998[77] | 0.9998[64] | - | - |
| 18 | asusaics-000 | 0.0090[64] | - | 0.3616[81] | - | - | - | - | - | - | - | - | - |
| 19 | aware-005 | 0.0308[116] | 0.4962[103] | 0.8876[127] | - | - | - | - | - | - | - | - | - |
| 20 | awiros-001 | 0.1233[133] | 0.6823[110] | 0.8635[125] | - | - | - | - | - | - | - | - | - |
| 21 | awiros-002 | 0.2283[137] | 0.6356[107] | 0.8671[126] | 0.9221[68] | - | - | - | 0.7703[62] | 0.9068[73] | - | 0.8628[57] | 0.8508[42] |
| 22 | ayftech-001 | 0.0828[129] | 0.6740[108] | 0.9132[131] | 0.9333[70] | 0.5865[63] | 0.8519[64] | 0.9538[53] | 0.7540[61] | 0.9048[72] | 0.9705[62] | - | - |
| 23 | bioidtechswiss-000 | 0.0050[24] | 0.0308[23] | 0.1155[28] | 0.1840[30] | 0.0223[24] | 0.0632[28] | 0.1207[28] | 0.0331[27] | 0.1163[27] | 0.1786[27] | 0.1167[23] | 0.1167[25] |
| 24 | bioidtechswiss-001 | 0.0037[6] | 0.0225[21] | 0.0945[24] | 0.1519[25] | 0.0180[18] | 0.0524[25] | 0.1070[26] | 0.0254[21] | 0.0986[23] | 0.1571[23] | 0.0979[19] | 0.0945[22] |
| 25 | bresee-000 | 0.9802[148] | 0.9968[120] | 0.9989[141] | - | - | - | - | 0.9975[65] | - | - | - | - |
| 26 | camvi-004 | 0.0063[45] | 0.0697[51] | 0.2179[50] | - | - | - | - | - | - | - | 0.3337[52] | - |
| 27 | chosun-000 | 1.0000[153] | 1.0000[135] | 1.0000[152] | - | - | - | - | - | - | - | - | - |
| 28 | chosun-001 | 0.0582[128] | 0.5759[104] | 0.9091[129] | 0.9263[69] | 0.5021[62] | 0.8531[65] | 0.9278[51] | 0.5158[58] | 0.9031[71] | 0.9409[60] | - | - |
| 29 | chtface-002 | 0.0108[76] | 0.1423[80] | 0.4303[90] | - | - | - | - | - | - | - | - | - |
| 30 | chtface-003 | 0.0084[56] | 0.1008[71] | 0.3201[73] | - | 0.0774[49] | 0.2393[54] | 0.4387[44] | 0.1232[52] | 0.3309[56] | 0.5044[51] | - | - |
| 31 | cib-000 | 0.0249[111] | 0.0757[54] | 0.1670[37] | - | - | - | - | - | - | - | 0.3825[53] | 0.1859[36] |
| 32 | cib-001 | 0.0036[5] | 0.0149[10] | 0.0731[19] | 0.1095[16] | 0.0125[5] | 0.0336[9] | 0.0690[7] | 0.0175[9] | 0.0731[15] | 0.1137[10] | 0.0863[17] | 0.0779[16] |
| 33 | clova-000 | 0.0087[60] | 0.0881[64] | - | 0.5017[58] | - | - | - | 0.0950[47] | 0.3051[52] | - | - | - |
| 34 | cor-001 | 0.0053[29] | 0.0504[42] | 0.1802[43] | 0.2470[39] | 0.0300[31] | 0.0864[31] | - | 0.0364[31] | 0.1328[32] | 0.1828[28] | 0.1527[29] | - |
| 35 | ctbcbank-000 | 0.0133[89] | 0.1594[87] | 0.7448[123] | - | - | - | - | - | - | - | - | - |
| 36 | cuhkee-001 | 0.0041[13] | 0.0143[9] | 0.0572[13] | 0.0963[13] | 0.0143[9] | 0.0333[8] | 0.0715[8] | 0.0164[8] | 0.0652[10] | 0.1193[11] | - | - |
| 37 | cybercore-000 | 0.1096[131] | - | 0.9097[130] | - | - | - | - | - | - | - | - | - |
| 38 | cyberlink-004 | 0.0061[42] | 0.0538[45] | 0.2115[49] | - | - | - | - | - | - | - | 0.2591[48] | - |
| 39 | cyberlink-005 | 0.0055[30] | 0.0376[32] | 0.1374[32] | 0.1808[29] | 0.0388[42] | 0.1018[35] | 0.2695[39] | 0.0451[38] | 0.1610[37] | 0.3991[46] | 0.4285[55] | 0.1316[26] |
| 40 | dahua-004 | 0.0038[9] | 0.0328[27] | 0.1784[41] | 0.2026[32] | - | - | - | 0.0226[18] | 0.1186[28] | 0.1983[30] | - | - |
| 41 | dahua-005 | 0.0034[4] | 0.0155[11] | 0.0660[17] | 0.1135[19] | 0.0127[7] | 0.0340[10] | 0.0829[13] | 0.0137[6] | 0.0601[8] | 0.1019[8] | 0.0579[6] | 0.0613[10] |
| 42 | decatur-000 | 0.0384[119] | - | 0.6440[111] | - | - | - | - | - | - | - | - | - |
| 43 | deepglint-002 | 0.0039[11] | 0.0077[1] | 0.0237[1] | 0.0455[1] | 0.0078[1] | 0.0141[1] | 0.0292[1] | 0.0083[1] | 0.0254[1] | 0.0513[1] | 0.0234[1] | 0.0248[1] |
| 44 | deepsea-001 | 0.0110[79] | 0.1218[75] | 0.3094[71] | 0.3778[52] | 0.0922[54] | 0.2217[52] | 0.4469[47] | - | - | - | - | - |
| 45 | didiglobalface-001 | 0.0050[25] | - | 0.0986[25] | 0.1517[23] | 0.0255[25] | 0.0515[22] | 0.0979[20] | 0.0291[25] | 0.1033[25] | 0.1558[22] | 0.1241[24] | 0.1655[32] |

*Table 5: This table summarizes False Non-Match Rate (FNMR) on unmasked and masked probe images. FNMR is the proportion of mated comparisons below a threshold set to achieve FMR=1e-05 on unmasked probe images. False Match Rate (FMR) is the proportion of impostor comparisons at or above that threshold. The red superscripts give rank over all algorithms in that column. Missing entries generally mean the algorithm was not run on that particular mask variation due to time and resource constraints. Algorithms with FTE=1.00 were not run at all. Algorithms in black were submitted prior to mid-March 2020, and algorithms in blue were submitted thereafter.*

FNMR(T) "False non-match rate"
FMR(T) "False match rate"

| | Algorithm | NOT MASKED | MASK COLOR = LIGHTBLUE | | | | | | COLOR = BLACK | | | COLOR = RED | COLOR = WHITE |
|---|---|---|---|---|---|---|---|---|---|---|---|---|---|
| | Name | | SHAPE = WIDE | | | SHAPE = ROUND | | | SHAPE = WIDE | | | SHAPE = WIDE | SHAPE = WIDE |
| | COVERAGE | | LO | MED | HI | LO | MED | HI | LO | MED | HI | MED | MED |
| 46 | dsk-000 | 0.1961[134] | 0.9108[113] | 0.9929[138] | - | - | - | - | - | - | - | - | - |
| 47 | eocortex-000 | 0.1187[132] | - | 0.9694[134] | - | - | - | - | - | - | - | - | - |
| 48 | ercacat-001 | 0.0096[69] | 0.0187[15] | 0.0616[15] | 0.0994[14] | 0.0173[14] | 0.0357[11] | 0.0728[10] | 0.0200[13] | 0.0663[12] | 0.1114[9] | 0.0679[12] | 0.0648[12] |
| 49 | expasoft-000 | 0.0519[126] | 0.3186[96] | 0.6796[119] | - | - | - | - | - | - | - | - | - |
| 50 | expasoft-001 | 0.0492[124] | - | 0.6414[110] | - | - | - | - | - | - | - | - | - |
| 51 | facesoft-000 | 0.0057[36] | 0.0397[34] | 0.1428[33] | - | - | - | - | - | 0.1573[36] | - | 0.1446[28] | 0.1428[29] |
| 52 | fiberhome-nanjing-002 | 0.0133[90] | 0.1554[86] | 0.4734[96] | - | - | - | - | 0.1641[53] | - | - | - | - |
| 53 | fujitsulab-000 | 0.0180[103] | - | 0.5052[101] | - | - | - | - | - | - | - | - | - |
| 54 | fujitsulab-001 | 0.0078[53] | 0.0330[28] | 0.0427[6] | 0.0608[4] | 0.0311[32] | 0.0363[12] | 0.0666[5] | 0.0407[34] | 0.0985[21] | 0.1525[21] | 0.0898[18] | 0.0776[15] |
| 55 | geo-000 | 0.0902[130] | 0.5765[105] | 0.9236[132] | - | - | 0.8082[63] | 0.9311[52] | 0.6214[60] | 0.9428[74] | 0.9541[61] | - | - |
| 56 | glory-002 | 0.0109[78] | - | 0.2729[64] | - | - | - | - | - | - | - | - | - |
| 57 | gorilla-005 | 0.0117[83] | 0.1463[82] | 0.5037[99] | - | - | - | - | - | - | - | - | - |
| 58 | gorilla-006 | 0.0085[57] | 0.0495[41] | 0.1805[44] | 0.2883[43] | 0.0385[41] | 0.1134[42] | - | - | 0.2260[46] | 0.3419[43] | 0.1980[40] | - |
| 59 | hr-003 | 0.0049[23] | 0.0133[5] | 0.0419[5] | 0.0613[5] | 0.0122[3] | 0.0247[4] | 0.0475[4] | 0.0142[7] | 0.0527[6] | 0.0914[5] | 0.0542[5] | 0.0476[7] |
| 60 | id3-005 | 0.0145[96] | 0.1181[74] | 0.3540[80] | - | - | - | - | - | - | - | - | - |
| 61 | idemia-005 | 0.0111[81] | 0.2051[90] | 0.6469[113] | 0.6968[64] | 0.1349[56] | 0.4387[58] | - | 0.2786[55] | 0.7402[69] | 0.8119[56] | - | - |
| 62 | idemia-006 | 0.0048[22] | 0.0327[26] | 0.0539[10] | 0.0911[10] | 0.0322[33] | 0.0440[19] | 0.0946[17] | 0.0359[29] | 0.0714[14] | 0.1489[19] | 0.0607[8] | 0.0564[9] |
| 63 | iit-002 | 0.0141[94] | - | 0.3078[70] | - | - | - | - | - | - | - | - | - |
| 64 | imagus-001 | 0.0276[113] | 0.3488[98] | 0.6510[114] | - | - | - | - | - | - | - | - | - |
| 65 | imperial-002 | 0.0055[31] | 0.0320[25] | 0.1350[31] | 0.1972[31] | 0.0258[26] | 0.0775[30] | 0.1556[29] | 0.0359[30] | 0.1510[35] | 0.2302[36] | 0.1533[30] | 0.1432[30] |
| 66 | incode-006 | 0.0095[68] | - | 0.3725[82] | - | - | - | - | - | - | - | - | - |
| 67 | incode-007 | 0.0058[37] | 0.0470[38] | 0.1790[42] | 0.2393[38] | 0.0323[34] | 0.1040[37] | 0.1779[31] | 0.0561[41] | 0.1891[43] | 0.2754[39] | 0.1978[39] | - |
| 68 | innefulabs-000 | 0.0155[98] | - | 0.2971[69] | - | - | - | - | - | - | - | - | - |
| 69 | innovativetechnologyltd-002 | 0.0251[112] | 0.2701[93] | 0.6454[112] | - | - | - | - | - | - | - | - | - |
| 70 | innovatrics-006 | 0.0059[40] | 0.0543[48] | 0.2210[51] | 0.3118[44] | 0.0369[37] | 0.1109[40] | 0.1984[33] | 0.0557[40] | 0.1909[44] | 0.2764[40] | 0.1936[38] | - |
| 71 | intellicloudai-001 | 0.0095[67] | 0.1044[72] | 0.4394[92] | - | - | - | - | - | - | - | - | - |
| 72 | intellifusion-002 | 0.0056[35] | 0.0539[46] | 0.1690[39] | - | - | - | - | - | 0.1822[42] | - | 0.2556[47] | 0.2119[37] |
| 73 | intellivision-002 | 0.0463[123] | 0.5999[106] | 0.9028[128] | - | - | - | - | - | - | - | - | - |
| 74 | intelresearch-001 | 0.0220[109] | 0.2254[91] | 0.6184[108] | - | - | - | - | - | - | - | - | - |
| 75 | intelresearch-002 | 0.0111[80] | 0.0458[36] | 0.1598[35] | 0.2085[33] | 0.0384[40] | 0.1025[36] | 0.2568[38] | 0.0598[42] | 0.1764[41] | 0.2583[38] | 0.1857[36] | 0.1595[31] |
| 76 | intsysmsu-002 | 0.0089[63] | 0.0827[60] | 0.3138[72] | - | - | - | - | - | - | - | - | - |
| 77 | iqface-000 | 0.0128[86] | 0.0885[65] | 0.2867[66] | - | - | - | - | - | - | - | - | - |
| 78 | iqface-002 | 0.0086[58] | 0.0193[17] | 0.0445[7] | 0.0725[7] | 0.0184[21] | 0.0317[6] | 0.0671[6] | 0.0215[15] | 0.0643[9] | 0.0997[7] | 0.0633[10] | 0.0448[5] |
| 79 | isap-002 | 0.0094[65] | - | 0.4090[87] | - | - | - | - | - | - | - | - | - |
| 80 | itmo-007 | 0.0098[72] | 0.0840[61] | 0.2685[60] | - | - | - | - | - | - | - | - | - |
| 81 | iws-000 | 0.6797[143] | 0.9960[118] | 0.9997[144] | - | - | - | - | - | - | - | - | - |
| 82 | kakao-003 | 0.0170[101] | 0.1541[85] | 0.4123[88] | - | - | - | - | - | - | - | - | - |
| 83 | kedacom-000 | 0.0391[120] | 0.3444[97] | 0.6188[109] | 0.6848[63] | 0.2663[59] | 0.5975[60] | - | - | - | - | - | - |
| 84 | kneron-005 | 0.0296[115] | - | 0.4567[94] | - | - | - | - | - | - | - | - | - |
| 85 | kookmin-001 | 0.0357[118] | 0.4479[101] | 0.7378[122] | 0.8497[66] | 0.2933[60] | 0.6006[61] | - | 0.4160[57] | 0.7365[68] | 0.8917[58] | 0.8642[58] | 0.7432[41] |
| 86 | lookman-004 | 0.0398[121] | - | 0.6520[115] | - | - | - | - | - | - | - | - | - |
| 87 | luxand-000 | 0.2167[136] | 0.9732[115] | 0.9988[140] | - | - | - | - | - | - | - | - | - |
| 88 | mt-000 | 0.0075[51] | 0.0768[55] | 0.2700[61] | 0.3736[50] | 0.0482[43] | 0.1746[46] | - | 0.0749[43] | 0.3084[54] | 0.4239[48] | - | - |
| 89 | mt-002 | 0.0043[15] | 0.0215[18] | 0.0713[18] | 0.1114[17] | 0.0162[12] | 0.0404[15] | 0.0777[12] | 0.0225[17] | 0.0877[19] | 0.1399[18] | 0.0804[15] | 0.0757[14] |
| 90 | mvision-001 | 0.0137[92] | - | 0.3987[85] | - | - | - | - | - | - | - | - | - |

*Table 6: This table summarizes False Non-Match Rate (FNMR) on unmasked and masked probe images. FNMR is the proportion of mated comparisons below a threshold set to achieve FMR=1e-05 on unmasked probe images. False Match Rate (FMR) is the proportion of impostor comparisons at or above that threshold. The red superscripts give rank over all algorithms in that column. Missing entries generally mean the algorithm was not run on that particular mask variation due to time and resource constraints. Algorithms with FTE=1.00 were not run at all. Algorithms in black were submitted prior to mid-March 2020, and algorithms in blue were submitted thereafter.*



FNMR(T) "False non-match rate"
FMR(T) "False match rate"

| | Algorithm | NOT MASKED | MASK COLOR = LIGHTBLUE | | | | | | COLOR = BLACK | | | COLOR = RED | COLOR = WHITE |
|---|---|---|---|---|---|---|---|---|---|---|---|---|---|
| | Name | | SHAPE = WIDE | | | SHAPE = ROUND | | | SHAPE = WIDE | | | SHAPE = WIDE | SHAPE = WIDE |
| | COVERAGE | | LO | MED | HI | LO | MED | HI | LO | MED | HI | MED | MED |
| 91 | nazhiai-000 | 0.0043[16] | 0.0184[13] | 0.0835[21] | 0.1318[20] | 0.0156[11] | 0.0463[20] | 0.0947[18] | 0.0177[10] | 0.0764[16] | 0.1271[14] | 0.0792[14] | 0.0854[20] |
| 92 | netbridgetech-001 | 0.2673[139] | 0.8940[112] | 0.9878[137] | - | - | - | - | - | - | - | - | - |
| 93 | netbridgetech-002 | 0.0083[55] | 0.0781[57] | 0.2723[63] | 0.3522[46] | 0.0528[45] | 0.1551[44] | - | 0.0875[46] | 0.2863[51] | 0.4151[47] | - | - |
| 94 | neurotechnology-008 | 0.0100[73] | 0.0794[58] | 0.3450[77] | 0.4460[57] | 0.0818[51] | 0.1834[48] | 0.3127[40] | 0.0953[48] | 0.4893[60] | 0.5472[52] | - | - |
| 95 | neurotechnology-009 | 0.0051[26] | 0.0351[31] | 0.1768[40] | 0.2537[41] | 0.0268[27] | 0.0953[33] | 0.2034[34] | 0.0414[35] | 0.2180[45] | 0.3192[42] | 0.1658[32] | - |
| 96 | nodeflux-002 | 0.0424[122] | 0.4177[100] | 0.7307[121] | - | - | - | - | - | - | - | - | - |
| 97 | notiontag-000 | 0.6814[144] | 0.9966[119] | 0.9992[142] | - | - | - | - | - | - | - | - | - |
| 98 | nsensecorp-001 | 1.0000[151] | 1.0000[126] | 1.0000[151] | 1.0000[74] | - | - | - | 1.0000[67] | 1.0000[78] | - | 1.0000[60] | 1.0000[44] |
| 99 | ntechlab-008 | 0.0033[2] | 0.0179[12] | 0.0642[16] | 0.1126[18] | 0.0137[8] | 0.0413[18] | 0.0953[19] | 0.0208[14] | 0.0842[18] | 0.1348[17] | 0.0645[11] | 0.0840[19] |
| 100 | oz-001 | 0.0152[97] | 0.1969[89] | 0.5887[106] | - | - | - | - | - | - | - | - | - |
| 101 | paravision-004 | 0.0088[61] | 0.0124[4] | 0.0281[2] | 0.0476[2] | 0.0125[6] | 0.0181[3] | 0.0313[2] | 0.0135[4] | 0.0327[3] | 0.0581[3] | 0.0332[3] | 0.0313[3] |
| 102 | pensees-001 | 0.0106[75] | 0.0309[24] | 0.0461[8] | 0.0921[12] | 0.0326[36] | 0.0413[17] | 0.0893[15] | 0.0333[28] | 0.0579[7] | 0.1217[12] | 0.1338[26] | 0.0462[6] |
| 103 | pixelall-003 | 0.0086[59] | 0.0746[52] | 0.2680[58] | - | - | - | - | - | - | - | - | - |
| 104 | pixelall-004 | 0.0078[52] | 0.0524[44] | 0.1676[38] | 0.2141[35] | 0.0495[44] | 0.1131[41] | 0.2254[37] | 0.0849[45] | 0.2461[47] | 0.3158[41] | 0.3148[50] | 0.1791[34] |
| 105 | psl-005 | 0.0056[34] | 0.0433[35] | 0.1904[47] | 0.2576[42] | 0.0292[30] | 0.1054[39] | 0.2210[36] | 0.0433[37] | 0.1681[39] | 0.2223[34] | 0.1851[35] | - |
| 106 | ptakuratsatu-000 | 0.0059[41] | 0.0542[47] | 0.1897[46] | 0.2485[40] | 0.0380[39] | 0.1047[38] | - | 0.0502[39] | 0.1652[38] | 0.2360[37] | 0.2003[41] | - |
| 107 | pxl-001 | 0.0511[125] | 0.4879[102] | 0.8183[124] | 0.8754[67] | 0.3675[61] | 0.7276[62] | 0.9182[50] | 0.5416[59] | 0.8047[70] | 0.8718[57] | - | - |
| 108 | rankone-009 | 0.0065[46] | 0.0951[67] | 0.3450[76] | 0.3709[49] | 0.1004[55] | 0.2244[53] | 0.4467[46] | - | 0.5624[61] | 0.9343[59] | - | - |
| 109 | rankone-010 | 0.0065[47] | 0.1514[84] | 0.5452[102] | 0.3915[53] | - | - | - | - | 0.7196[67] | - | 0.5811[56] | 0.5719[40] |
| 110 | remarkai-002 | 0.0073[49] | 0.0685[50] | 0.2352[53] | - | - | - | - | - | - | - | 0.2406[46] | - |
| 111 | rokid-000 | 0.0117[82] | 0.1448[81] | 0.4346[91] | - | - | - | - | - | - | - | - | - |
| 112 | s1-001 | 0.0277[114] | 0.6776[109] | 0.9459[133] | - | - | - | - | - | - | - | - | - |
| 113 | scanovate-001 | 0.2403[138] | - | 0.5973[107] | - | - | - | - | - | - | - | - | - |
| 114 | scanovate-002 | 0.0119[84] | 0.1304[79] | 0.4006[86] | 0.5142[59] | 0.0757[48] | 0.2206[51] | 0.3622[42] | 0.1215[51] | 0.3172[55] | 0.4633[50] | - | - |
| 115 | securifai-001 | 0.5185[140] | 0.9381[114] | 0.9835[136] | 0.9880[71] | 0.9146[64] | 0.9788[66] | - | 0.9352[63] | 0.9853[75] | 0.9949[63] | 0.9867[59] | 0.9829[43] |
| 116 | sensetime-003 | 0.0045[21] | 0.0185[14] | 0.0544[11] | 0.0912[11] | 0.0221[23] | 0.0365[13] | 0.0739[11] | 0.0232[20] | 0.0654[11] | 0.1230[13] | - | - |
| 117 | sertis-000 | 0.0066[48] | 0.0751[53] | 0.2685[59] | - | - | - | - | - | - | - | - | - |
| 118 | sertis-001 | 0.0179[102] | - | 0.5774[104] | 0.6655[61] | - | - | - | - | 0.5632[62] | - | - | - |
| 119 | shu-002 | 1.0000[150] | - | 1.0000[149] | - | - | - | - | - | - | - | - | - |
| 120 | shu-003 | 0.0053[28] | 0.0465[37] | 0.1839[45] | 0.2148[36] | 0.0379[38] | 0.1148[43] | 0.2196[35] | 0.0422[36] | 0.1702[40] | 0.2210[33] | 0.1901[37] | - |
| 121 | sjtu-002 | 0.0052[27] | 0.0475[40] | 0.1912[48] | - | - | - | - | - | - | - | 0.2090[42] | - |
| 122 | sjtu-003 | 0.0043[14] | 0.0340[30] | 0.1239[29] | 0.1609[26] | - | - | - | - | 0.1008[24] | - | 0.1333[25] | 0.1323[27] |
| 123 | staqu-000 | 0.0108[77] | 0.1251[77] | 0.3537[79] | 0.4429[55] | 0.0913[53] | 0.2434[55] | 0.4447[45] | - | 0.3862[58] | 0.6319[53] | - | - |
| 124 | starhybrid-001 | 0.0104[74] | 0.1923[88] | 0.5033[98] | - | - | - | - | - | - | - | - | - |
| 125 | synology-000 | 0.0123[85] | - | 0.4459[93] | - | - | - | - | - | - | - | - | - |
| 126 | tech5-004 | 0.0045[20] | 0.0218[19] | 0.0839[22] | 0.1389[22] | 0.0172[13] | 0.0464[21] | 0.0905[16] | 0.0228[19] | 0.0818[17] | 0.1288[16] | 0.0826[16] | 0.0830[18] |
| 127 | tech5-005 | 0.0037[7] | 0.0224[20] | 0.0941[23] | 0.1518[24] | 0.0180[17] | 0.0524[23] | 0.1066[25] | 0.0254[22] | 0.0986[22] | 0.1571[24] | 0.0979[20] | 0.0945[21] |
| 128 | tevian-005 | 0.0061[43] | 0.0961[68] | 0.5044[100] | - | - | - | - | - | 0.6178[63] | - | - | - |
| 129 | tevian-006 | 0.0038[10] | 0.0140[7] | 0.0547[12] | 0.0894[9] | 0.0184[20] | 0.0325[7] | 0.1013[22] | 0.0183[11] | 0.1281[30] | 0.1507[20] | 0.1437[27] | 0.0659[13] |
| 130 | trueface-000 | 0.0143[95] | 0.1512[83] | 0.4164[89] | - | - | - | - | - | - | - | - | - |
| 131 | trueface-001 | 0.0097[71] | 0.0978[69] | 0.3483[78] | 0.4310[54] | 0.0710[47] | 0.2064[50] | 0.3846[43] | - | 0.3752[57] | - | - | - |
| 132 | tuputech-000 | 0.2014[135] | 0.8743[111] | 0.9731[135] | - | - | - | - | - | - | - | - | - |
| 133 | uluface-002 | 0.0073[50] | 0.0796[59] | 0.2450[54] | - | - | - | - | - | - | - | 0.3939[54] | - |
| 134 | upc-001 | 0.0167[100] | - | 0.4723[95] | - | - | - | - | - | - | - | - | - |
| 135 | veridas-004 | 0.0202[107] | 0.2783[94] | 0.6697[116] | 0.7334[65] | 0.1941[58] | 0.5025[59] | 0.6906[49] | - | 0.6592[66] | - | - | - |

*Table 7: This table summarizes False Non-Match Rate (FNMR) on unmasked and masked probe images. FNMR is the proportion of mated comparisons below a threshold set to achieve FMR=1e-05 on unmasked probe images. False Match Rate (FMR) is the proportion of impostor comparisons at or above that threshold. The red superscripts give rank over all algorithms in that column. Missing entries generally mean the algorithm was not run on that particular mask variation due to time and resource constraints. Algorithms with FTE=1.00 were not run at all. Algorithms in black were submitted prior to mid-March 2020, and algorithms in blue were submitted thereafter.*



FNMR(T) "False non-match rate"
FMR(T) "False match rate"

| | Algorithm | NOT MASKED | MASK COLOR = LIGHTBLUE | | | | | | COLOR = BLACK | | | COLOR = RED | COLOR = WHITE |
|---|---|---|---|---|---|---|---|---|---|---|---|---|---|
| | Name | | SHAPE = WIDE | | | SHAPE = ROUND | | | SHAPE = WIDE | | | SHAPE = WIDE | SHAPE = WIDE |
| | COVERAGE | | LO | MED | HI | LO | MED | HI | LO | MED | HI | MED | MED |
| 136 | via-001 | 0.0097[70] | 0.1234[76] | 0.3406[75] | - | - | - | - | - | - | - | - | - |
| 137 | videmo-000 | 0.0140[93] | - | 0.5509[103] | - | - | - | - | - | - | - | - | - |
| 138 | videonetics-002 | 0.6032[141] | 0.9941[117] | 0.9996[143] | - | - | - | - | - | - | - | - | - |
| 139 | vigilantsolutions-007 | 0.0194[104] | 0.2849[95] | 0.6839[120] | - | - | - | - | - | - | - | - | - |
| 140 | vigilantsolutions-008 | 0.0195[105] | - | 0.4970[97] | 0.5521[60] | - | - | - | - | 0.6365[65] | - | - | - |
| 141 | vinai-000 | 0.0056[33] | 0.0388[33] | 0.1587[34] | 0.2130[34] | 0.0286[29] | 0.0965[34] | - | 0.0364[32] | 0.1487[34] | 0.2024[32] | 0.1691[33] | 0.1710[33] |
| 142 | visionlabs-008 | 0.0034[3] | 0.0139[6] | 0.0579[14] | 0.1014[15] | 0.0154[10] | 0.0412[16] | 0.1004[21] | 0.0187[12] | 0.0664[13] | 0.1284[15] | 0.0614[9] | 0.0618[11] |
| 143 | visionlabs-009 | 0.0028[1] | 0.0095[3] | 0.0355[4] | 0.0667[6] | 0.0123[4] | 0.0307[5] | 0.0719[9] | 0.0123[3] | 0.0423[4] | 0.0943[6] | 0.0399[4] | 0.0395[4] |
| 144 | visteam-000 | 0.9960[149] | 1.0000[124] | 1.0000[148] | - | - | - | - | - | - | - | - | - |
| 145 | vocord-008 | 0.0038[8] | 0.0140[8] | 0.0500[9] | 0.0762[8] | 0.0176[16] | 0.0393[14] | 0.0892[14] | 0.0135[5] | 0.0459[5] | 0.0771[4] | 0.0607[7] | 0.0482[8] |
| 146 | vts-000 | 0.0199[106] | 0.0870[62] | 0.2755[65] | 0.3566[47] | - | - | - | - | 0.2584[50] | - | 0.2249[43] | 0.2976[38] |
| 147 | winsense-001 | 0.0058[38] | 0.0473[39] | 0.1626[36] | 0.2244[37] | 0.0325[35] | 0.0946[32] | 0.1853[32] | 0.0406[33] | 0.1471[33] | 0.2231[35] | 0.1622[31] | 0.1843[35] |
| 148 | x-laboratory-001 | 0.0058[39] | 0.0517[43] | 0.2569[56] | - | - | - | - | - | - | - | 0.2333[44] | - |
| 149 | xforwardai-000 | 0.0056[32] | 0.0235[22] | 0.1064[27] | 0.1615[27] | 0.0197[22] | 0.0606[27] | 0.1156[27] | 0.0255[23] | 0.1091[26] | 0.1608[26] | 0.1108[22] | 0.1101[24] |
| 150 | xforwardai-001 | 0.0041[12] | 0.0087[2] | 0.0289[3] | 0.0536[3] | 0.0087[2] | 0.0180[2] | 0.0377[3] | 0.0090[2] | 0.0303[2] | 0.0544[2] | 0.0313[2] | 0.0294[2] |
| 151 | xm-000 | 0.0044[17] | 0.0334[29] | 0.1255[30] | 0.1682[28] | 0.0275[28] | 0.0774[29] | 0.1648[30] | 0.0324[26] | 0.1274[29] | 0.1839[29] | 0.1706[34] | 0.1381[28] |
| 152 | yoonik-000 | 0.0520[127] | 0.1056[73] | 0.2675[57] | 0.3773[51] | 0.0895[52] | 0.1823[47] | 0.3214[41] | 0.1027[49] | 0.2582[49] | 0.3628[44] | - | - |
| 153 | yuan-000 | 0.0130[88] | 0.0871[63] | 0.2704[62] | 0.3516[45] | 0.0654[46] | 0.1661[45] | - | 0.0805[44] | 0.2492[48] | 0.3645[45] | - | - |

*Table 8: This table summarizes False Non-Match Rate (FNMR) on unmasked and masked probe images. FNMR is the proportion of mated comparisons below a threshold set to achieve FMR=1e-05 on unmasked probe images. False Match Rate (FMR) is the proportion of impostor comparisons at or above that threshold. The red superscripts give rank over all algorithms in that column. Missing entries generally mean the algorithm was not run on that particular mask variation due to time and resource constraints. Algorithms with FTE=1.00 were not run at all. Algorithms in black were submitted prior to mid-March 2020, and algorithms in blue were submitted thereafter.*

2020/11/30 08:35:54



FNMR(T) "False non-match rate"
FMR(T) "False match rate"

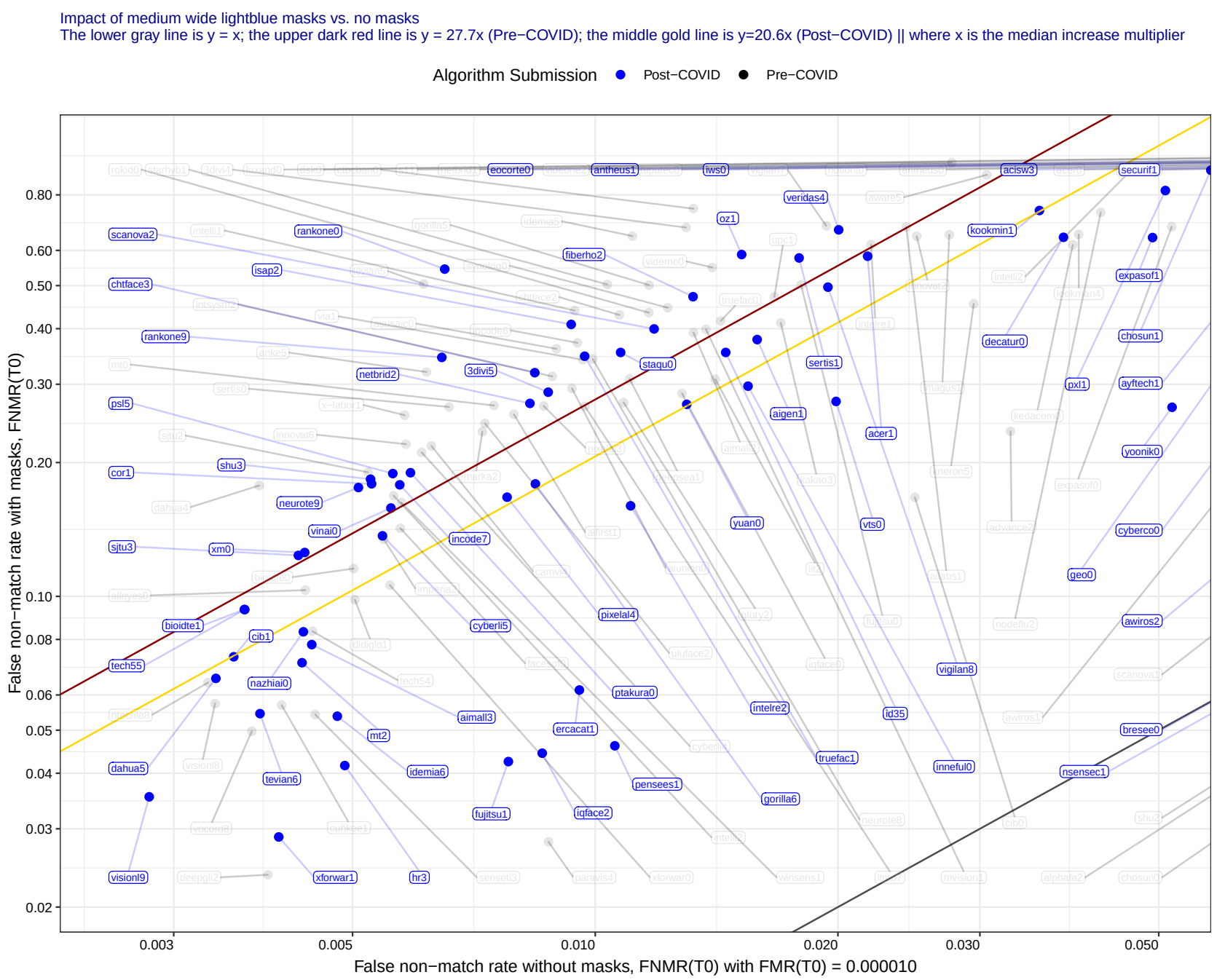


*Figure 7: At a fixed threshold, a plot of FNMR with and without masks. The displacement of the dark red line relative to the black "parity" line shows a large increase in FNMR with masks for pre-COVID algorithms. The reduction in distance (relative to the black line) observed in the gold line indicates a reduction in median FNMR with masks for post-COVID algorithms. The value in the title is the median increase multiplier.*





FNMR(T) "False non-match rate"
FMR(T) "False match rate"

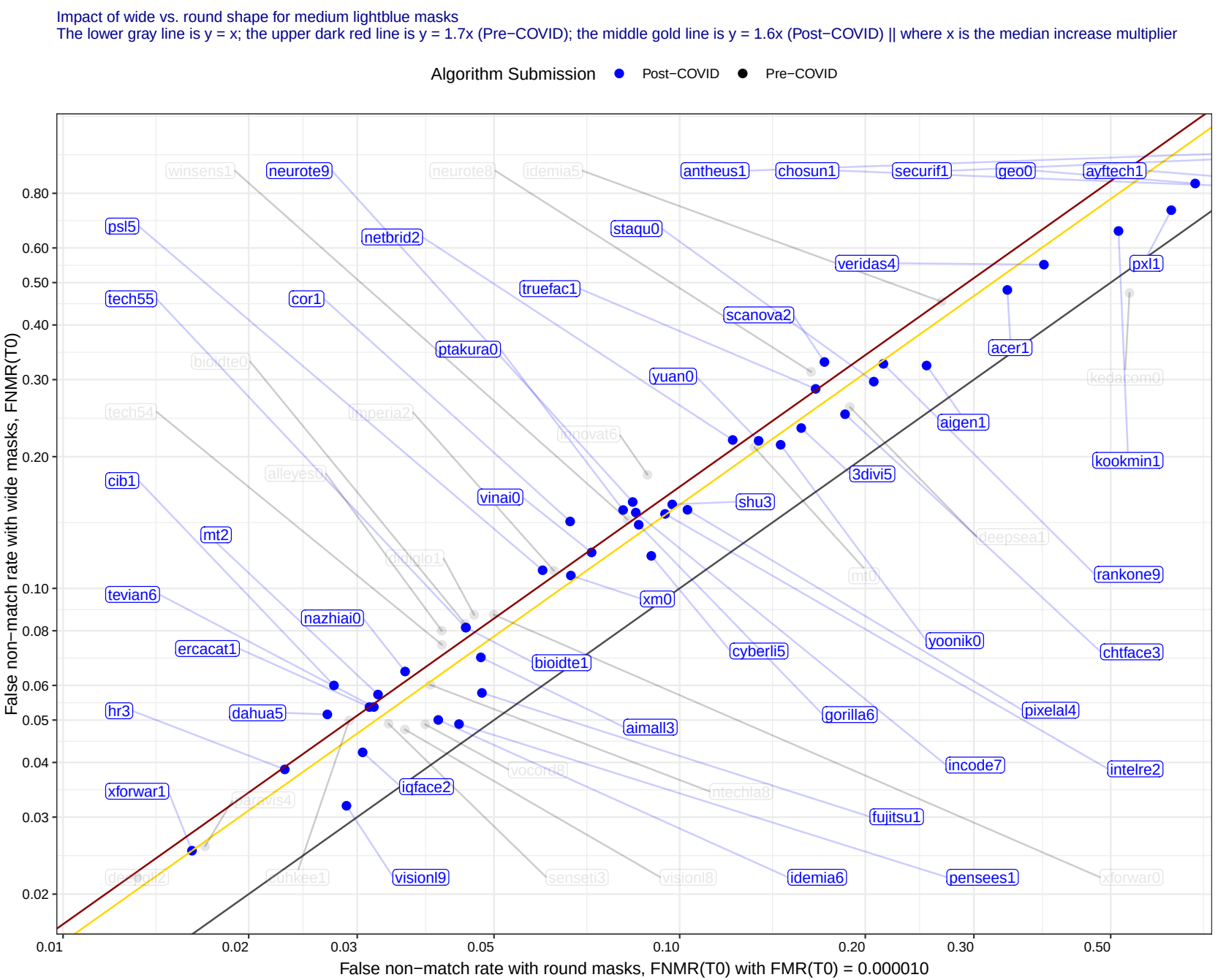


*Figure 8: At a fixed threshold, a plot of FNMR with round versus wide masks. The displacement of the dark red (pre-COVID algorithms) and gold (post-COVID algorithms) lines relative to the black "parity" line shows a modest increase in FNMR with wide masks, with median post-COVID results showing nominal FNMR reductions. The value in the title is the median increase multiplier.*

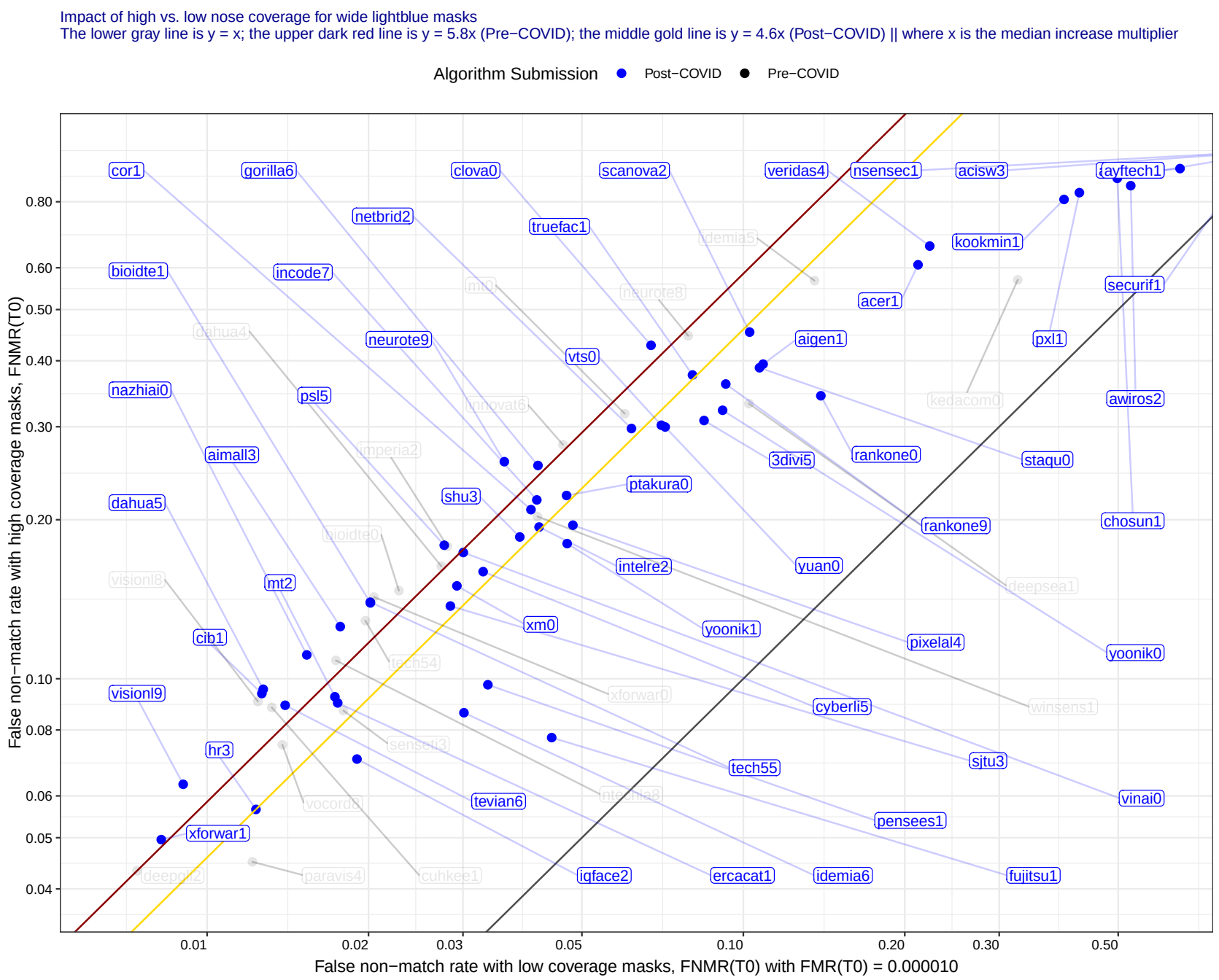


*Figure 9: At a fixed threshold, a plot of FNMR with low versus high masks. The displacement of the dark red (pre-COVID algorithms) and gold (post-COVID algorithms) lines relative to the black "parity" lines shows a considerable increase in FNMR with high vs. low nose coverage masks, with median post-COVID results showing modest FNMR reductions. The value in the title is the median increase multiplier.*





FNMR(T) "False non-match rate"
FMR(T) "False match rate"

| | Algorithm Name | COLOR = WHITE SHAPE = WIDE | | | COLOR = LIGHTBLUE SHAPE = WIDE | | | COLOR = LIGHTBLUE SHAPE = ROUND | | | COLOR = RED SHAPE = WIDE | | | COLOR = BLACK SHAPE = WIDE | | |
|---|---|---|---|---|---|---|---|---|---|---|---|---|---|---|---|---|
| | COVERAGE | LO | MED | HI | LO | MED | HI | LO | MED | HI | LO | MED | HI | LO | MED | HI |
| 1 | 3divi-004 | 0.514 | 0.659 | 0.627 | 0.420 | 0.599 | 0.603 | 0.378 | 0.663 | 0.769 | 0.290 | 0.691 | 0.864 | 0.653 | 0.920 | 0.939 |
| 2 | 3divi-005 | 0.003 | 0.012 | 0.029 | 0.002 | 0.013 | 0.030 | 0.007 | 0.011 | 0.026 | 0.005 | 0.040 | 0.077 | 0.002 | 0.006 | 0.012 |
| 3 | acer-000 | 0.048 | 0.105 | 0.139 | 0.035 | 0.080 | 0.114 | 0.052 | 0.078 | 0.137 | 0.168 | 0.321 | 0.445 | 0.107 | 0.197 | 0.270 |
| 4 | acer-001 | 0.020 | 0.048 | 0.091 | 0.019 | 0.051 | 0.096 | 0.025 | 0.034 | 0.060 | 0.025 | 0.080 | 0.147 | 0.026 | 0.088 | 0.157 |
| 5 | acisw-003 | 0.000 | 0.000 | 0.000 | 0.000 | 0.000 | 0.000 | 0.000 | 0.000 | 0.000 | 0.000 | 0.000 | 0.000 | 0.000 | 0.000 | 0.000 |
| 6 | advance-002 | 0.019 | 0.046 | 0.096 | 0.020 | 0.045 | 0.096 | 0.026 | 0.037 | 0.085 | 0.028 | 0.088 | 0.174 | 0.034 | 0.104 | 0.200 |
| 7 | aifirst-001 | 0.000 | 0.000 | 0.000 | 0.000 | 0.000 | 0.000 | 0.000 | 0.000 | 0.000 | 0.000 | 0.000 | 0.000 | 0.000 | 0.000 | 0.000 |
| 8 | aigen-001 | 0.000 | 0.000 | 0.000 | 0.000 | 0.000 | 0.000 | 0.000 | 0.000 | 0.000 | 0.000 | 0.000 | 0.000 | 0.000 | 0.000 | 0.000 |
| 9 | ailabs-001 | 0.071 | 0.208 | 0.248 | 0.061 | 0.194 | 0.233 | 0.102 | 0.177 | 0.314 | 0.096 | 0.319 | 0.389 | 0.116 | 0.310 | 0.465 |
| 10 | aimall-002 | 0.073 | 0.129 | 0.225 | 0.095 | 0.152 | 0.260 | 0.107 | 0.159 | 0.236 | 0.086 | 0.122 | 0.230 | 0.049 | 0.071 | 0.154 |
| 11 | aimall-003 | 0.011 | 0.038 | 0.097 | 0.014 | 0.047 | 0.113 | 0.020 | 0.041 | 0.085 | 0.013 | 0.039 | 0.103 | 0.012 | 0.033 | 0.081 |
| 12 | aiunionface-000 | 0.000 | 0.000 | 0.000 | 0.000 | 0.000 | 0.000 | 0.000 | 0.000 | 0.000 | 0.000 | 0.000 | 0.000 | 0.000 | 0.000 | 0.000 |
| 13 | alleyes-000 | 0.006 | 0.023 | 0.062 | 0.006 | 0.020 | 0.056 | 0.007 | 0.012 | 0.028 | 0.007 | 0.035 | 0.088 | 0.010 | 0.043 | 0.104 |
| 14 | alphaface-002 | 0.025 | 0.056 | 0.099 | 0.024 | 0.054 | 0.095 | 0.033 | 0.044 | 0.072 | 0.041 | 0.104 | 0.174 | 0.027 | 0.071 | 0.132 |
| 15 | anke-005 | 0.009 | 0.028 | 0.066 | 0.011 | 0.030 | 0.069 | 0.012 | 0.018 | 0.041 | 0.013 | 0.036 | 0.079 | 0.009 | 0.056 | 0.091 |
| 16 | antheus-000 | 0.000 | 0.000 | 0.000 | 0.000 | 0.000 | 0.000 | 0.000 | 0.000 | 0.000 | 0.000 | 0.000 | 0.000 | 0.000 | 0.000 | 0.000 |
| 17 | antheus-001 | 0.000 | 0.000 | 0.000 | 0.000 | 0.000 | 0.000 | 0.000 | 0.000 | 0.000 | 0.000 | 0.000 | 0.000 | 0.000 | 0.000 | 0.000 |
| 18 | asusaics-000 | 0.000 | 0.000 | 0.000 | 0.000 | 0.000 | 0.000 | 0.000 | 0.000 | 0.000 | 0.000 | 0.000 | 0.000 | 0.000 | 0.000 | 0.000 |
| 19 | aware-005 | 0.053 | 0.151 | 0.218 | 0.039 | 0.129 | 0.211 | 0.046 | 0.089 | 0.244 | 0.095 | 0.380 | 0.516 | 0.091 | 0.236 | 0.449 |
| 20 | awiros-001 | 0.195 | 0.370 | 0.450 | 0.162 | 0.298 | 0.379 | 0.161 | 0.258 | 0.355 | 0.388 | 0.650 | 0.772 | 0.198 | 0.415 | 0.642 |
| 21 | awiros-002 | 0.101 | 0.212 | 0.215 | 0.103 | 0.202 | 0.220 | 0.187 | 0.261 | 0.356 | 0.071 | 0.272 | 0.296 | 0.232 | 0.405 | 0.455 |
| 22 | ayftech-001 | 0.237 | 0.610 | 0.587 | 0.251 | 0.615 | 0.609 | 0.301 | 0.553 | 0.728 | 0.105 | 0.405 | 0.626 | 0.193 | 0.596 | 0.758 |
| 23 | bioidtechswiss-000 | 0.005 | 0.022 | 0.061 | 0.006 | 0.028 | 0.070 | 0.010 | 0.021 | 0.046 | 0.006 | 0.025 | 0.068 | 0.006 | 0.021 | 0.058 |
| 24 | bioidtechswiss-001 | 0.004 | 0.014 | 0.044 | 0.004 | 0.017 | 0.046 | 0.006 | 0.011 | 0.026 | 0.005 | 0.020 | 0.051 | 0.007 | 0.022 | 0.056 |
| 25 | bresee-000 | 0.005 | 0.022 | 0.049 | 0.005 | 0.020 | 0.049 | 0.009 | 0.014 | 0.034 | 0.010 | 0.051 | 0.108 | 0.008 | 0.041 | 0.097 |
| 26 | camvi-004 | 0.000 | 0.000 | 0.000 | 0.000 | 0.000 | 0.000 | 0.000 | 0.000 | 0.000 | 0.000 | 0.000 | 0.000 | 0.000 | 0.000 | 0.000 |
| 27 | chosun-000 | 0.000 | 0.000 | 0.000 | 0.000 | 0.000 | 0.000 | 0.000 | 0.000 | 0.000 | 0.000 | 0.000 | 0.000 | 0.000 | 0.000 | 0.000 |
| 28 | chosun-001 | 0.000 | 0.000 | 0.000 | 0.000 | 0.000 | 0.000 | 0.000 | 0.000 | 0.000 | 0.000 | 0.000 | 0.000 | 0.000 | 0.000 | 0.000 |
| 29 | chtface-002 | 0.033 | 0.100 | 0.154 | 0.026 | 0.081 | 0.126 | 0.031 | 0.056 | 0.107 | 0.110 | 0.321 | 0.480 | 0.042 | 0.144 | 0.270 |
| 30 | chtface-003 | 0.022 | 0.075 | 0.125 | 0.018 | 0.059 | 0.099 | 0.023 | 0.039 | 0.077 | 0.080 | 0.259 | 0.418 | 0.030 | 0.108 | 0.224 |
| 31 | cib-000 | 0.000 | 0.000 | 0.000 | 0.000 | 0.000 | 0.000 | 0.000 | 0.000 | 0.000 | 0.000 | 0.000 | 0.000 | 0.000 | 0.000 | 0.000 |
| 32 | cib-001 | 0.000 | 0.000 | 0.000 | 0.000 | 0.000 | 0.000 | 0.000 | 0.000 | 0.000 | 0.000 | 0.000 | 0.000 | 0.000 | 0.000 | 0.000 |
| 33 | clova-000 | 0.035 | 0.089 | 0.149 | 0.033 | 0.081 | 0.136 | 0.039 | 0.059 | 0.128 | 0.071 | 0.245 | 0.361 | 0.049 | 0.146 | 0.252 |
| 34 | cor-001 | 0.002 | 0.010 | 0.031 | 0.003 | 0.013 | 0.035 | 0.004 | 0.008 | 0.020 | 0.004 | 0.013 | 0.032 | 0.004 | 0.011 | 0.031 |
| 35 | ctbcbank-000 | 0.179 | 0.794 | 0.803 | 0.171 | 0.786 | 0.865 | 0.205 | 0.620 | 0.915 | 0.433 | 0.857 | 0.913 | 0.189 | 0.806 | 0.895 |
| 36 | cuhkee-001 | 0.009 | 0.029 | 0.069 | 0.009 | 0.031 | 0.074 | 0.014 | 0.025 | 0.057 | 0.012 | 0.048 | 0.115 | 0.013 | 0.048 | 0.140 |
| 37 | cybercore-000 | 0.194 | 0.376 | 0.371 | 0.222 | 0.447 | 0.453 | 0.267 | 0.461 | 0.751 | 0.191 | 0.432 | 0.554 | 0.367 | 0.678 | 0.805 |
| 38 | cyberlink-004 | 0.014 | 0.042 | 0.096 | 0.013 | 0.039 | 0.091 | 0.018 | 0.029 | 0.063 | 0.020 | 0.096 | 0.177 | 0.018 | 0.064 | 0.136 |
| 39 | cyberlink-005 | 0.012 | 0.035 | 0.080 | 0.011 | 0.029 | 0.067 | 0.014 | 0.021 | 0.043 | 0.016 | 0.072 | 0.147 | 0.015 | 0.049 | 0.114 |
| 40 | dahua-004 | 0.033 | 0.150 | 0.087 | 0.027 | 0.126 | 0.094 | 0.047 | 0.121 | 0.190 | 0.012 | 0.071 | 0.187 | 0.011 | 0.057 | 0.183 |
| 41 | dahua-005 | 0.000 | 0.000 | 0.000 | 0.000 | 0.000 | 0.000 | 0.000 | 0.000 | 0.000 | 0.000 | 0.000 | 0.000 | 0.000 | 0.000 | 0.000 |
| 42 | decatur-000 | 0.014 | 0.036 | 0.074 | 0.014 | 0.033 | 0.069 | 0.018 | 0.028 | 0.058 | 0.032 | 0.065 | 0.135 | 0.033 | 0.069 | 0.135 |
| 43 | deepglint-002 | 0.002 | 0.009 | 0.028 | 0.002 | 0.012 | 0.031 | 0.004 | 0.006 | 0.017 | 0.003 | 0.014 | 0.035 | 0.003 | 0.010 | 0.024 |
| 44 | deepsea-001 | 0.000 | 0.000 | 0.000 | 0.000 | 0.000 | 0.000 | 0.000 | 0.000 | 0.000 | 0.000 | 0.000 | 0.000 | 0.000 | 0.000 | 0.000 |
| 45 | didiglobalface-001 | 0.025 | 0.056 | 0.099 | 0.024 | 0.054 | 0.095 | 0.033 | 0.044 | 0.072 | 0.041 | 0.104 | 0.174 | 0.027 | 0.071 | 0.132 |

*Table 9: This table summarizes Failure to Enroll (FTE) rates surveyed over 10 000 images of each mask variant. FTE is the proportion of failed template generation attempts. Failures can occur because the software throws an exception, or because the software electively refuses to process the input image as would occur if the algorithms does not detect a face or determines that the face has insufficient information. FTE is measured as the number of function calls that give EITHER a non-zero error code OR that give a "small" template containing fewer than 60 bytes. This second rule is needed because some algorithms incorrectly fail to return a non-zero error code when template generation fails but do produce a skeletal template. The effects of FTE are included in the accuracy results of this report by regarding any template comparison involving a failed template to produce a low similarity score. Thus higher FTE results in higher FNMR and lower FMR. Algorithms in black were submitted prior to mid-March 2020, and algorithms in blue were submitted thereafter.*



FNMR(T) "False non-match rate"
FMR(T) "False match rate"

| | Algorithm Name | COLOR = WHITE SHAPE = WIDE | | | COLOR = LIGHTBLUE SHAPE = WIDE | | | COLOR = LIGHTBLUE SHAPE = ROUND | | | COLOR = RED SHAPE = WIDE | | | COLOR = BLACK SHAPE = WIDE | | |
|---|---|---|---|---|---|---|---|---|---|---|---|---|---|---|---|---|
| | COVERAGE | LO | MED | HI | LO | MED | HI | LO | MED | HI | LO | MED | HI | LO | MED | HI |
| 46 | dsk-000 | 0.000 | 0.000 | 0.000 | 0.000 | 0.000 | 0.000 | 0.000 | 0.000 | 0.000 | 0.000 | 0.000 | 0.000 | 0.000 | 0.000 | 0.000 |
| 47 | eocortex-000 | 0.692 | 0.862 | 0.861 | 0.653 | 0.841 | 0.860 | 0.647 | 0.887 | 0.904 | 0.800 | 0.960 | 0.990 | 0.814 | 0.950 | 0.990 |
| 48 | ercacat-001 | 0.002 | 0.007 | 0.014 | 0.002 | 0.006 | 0.013 | 0.002 | 0.002 | 0.006 | 0.002 | 0.008 | 0.016 | 0.003 | 0.009 | 0.017 |
| 49 | expasoft-000 | 0.000 | 0.000 | 0.000 | 0.000 | 0.000 | 0.000 | 0.000 | 0.000 | 0.000 | 0.000 | 0.000 | 0.000 | 0.000 | 0.000 | 0.000 |
| 50 | expasoft-001 | 0.000 | 0.000 | 0.000 | 0.000 | 0.000 | 0.000 | 0.000 | 0.000 | 0.000 | 0.000 | 0.000 | 0.000 | 0.000 | 0.000 | 0.000 |
| 51 | f8-001 | 1.000 | 1.000 | 1.000 | 1.000 | 1.000 | 1.000 | 1.000 | 1.000 | 1.000 | 1.000 | 1.000 | 1.000 | 1.000 | 1.000 | 1.000 |
| 52 | facesoft-000 | 0.000 | 0.000 | 0.000 | 0.000 | 0.000 | 0.000 | 0.000 | 0.000 | 0.000 | 0.000 | 0.000 | 0.000 | 0.000 | 0.000 | 0.000 |
| 53 | fujitsulab-000 | 0.006 | 0.013 | 0.018 | 0.006 | 0.013 | 0.019 | 0.008 | 0.011 | 0.018 | 0.024 | 0.059 | 0.066 | 0.014 | 0.033 | 0.045 |
| 54 | fujitsulab-001 | 0.008 | 0.014 | 0.032 | 0.006 | 0.011 | 0.020 | 0.005 | 0.005 | 0.008 | 0.014 | 0.038 | 0.108 | 0.012 | 0.025 | 0.066 |
| 55 | geo-000 | 0.000 | 0.000 | 0.000 | 0.000 | 0.000 | 0.000 | 0.000 | 0.000 | 0.000 | 0.000 | 0.000 | 0.000 | 0.000 | 0.000 | 0.000 |
| 56 | glory-002 | 0.059 | 0.106 | 0.128 | 0.056 | 0.101 | 0.124 | 0.053 | 0.074 | 0.126 | 0.062 | 0.148 | 0.239 | 0.054 | 0.154 | 0.279 |
| 57 | gorilla-005 | 0.006 | 0.018 | 0.040 | 0.007 | 0.018 | 0.038 | 0.009 | 0.012 | 0.024 | - | - | - | 0.012 | 0.037 | 0.071 |
| 58 | gorilla-006 | 0.003 | 0.008 | 0.014 | 0.003 | 0.008 | 0.013 | 0.002 | 0.003 | 0.005 | 0.005 | 0.013 | 0.034 | 0.005 | 0.014 | 0.031 |
| 59 | hr-002 | 1.000 | 1.000 | 1.000 | 1.000 | 1.000 | 1.000 | 1.000 | 1.000 | 1.000 | 1.000 | 1.000 | 1.000 | 1.000 | 1.000 | 1.000 |
| 60 | hr-003 | 0.003 | 0.008 | 0.013 | 0.003 | 0.009 | 0.012 | 0.006 | 0.008 | 0.014 | 0.005 | 0.011 | 0.022 | 0.005 | 0.009 | 0.017 |
| 61 | id3-005 | 0.143 | 0.256 | 0.304 | 0.169 | 0.364 | 0.424 | 0.196 | 0.287 | 0.539 | 0.192 | 0.395 | 0.527 | 0.216 | 0.389 | 0.557 |
| 62 | idemia-005 | 0.002 | 0.008 | 0.028 | 0.002 | 0.007 | 0.023 | 0.002 | 0.004 | 0.015 | 0.002 | 0.015 | 0.037 | 0.002 | 0.010 | 0.029 |
| 63 | idemia-006 | 0.002 | 0.008 | 0.028 | 0.002 | 0.007 | 0.023 | 0.002 | 0.004 | 0.015 | 0.002 | 0.013 | 0.035 | 0.002 | 0.010 | 0.029 |
| 64 | iit-002 | 0.012 | 0.036 | 0.074 | 0.013 | 0.043 | 0.091 | 0.015 | 0.027 | 0.072 | 0.016 | 0.060 | 0.137 | 0.015 | 0.087 | 0.185 |
| 65 | imagus-001 | 0.016 | 0.040 | 0.074 | 0.014 | 0.037 | 0.066 | 0.023 | 0.029 | 0.056 | 0.023 | 0.084 | 0.135 | 0.021 | 0.085 | 0.149 |
| 66 | imperial-002 | 0.000 | 0.000 | 0.000 | 0.000 | 0.000 | 0.000 | 0.000 | 0.000 | 0.000 | 0.000 | 0.000 | 0.000 | 0.000 | 0.000 | 0.000 |
| 67 | incode-006 | 0.002 | 0.008 | 0.020 | 0.002 | 0.008 | 0.018 | 0.002 | 0.003 | 0.007 | 0.002 | 0.010 | 0.028 | 0.002 | 0.012 | 0.031 |
| 68 | incode-007 | 0.003 | 0.013 | 0.034 | 0.003 | 0.013 | 0.031 | 0.003 | 0.006 | 0.014 | 0.004 | 0.016 | 0.045 | 0.004 | 0.020 | 0.060 |
| 69 | innefulabs-000 | 0.007 | 0.024 | 0.064 | 0.009 | 0.028 | 0.069 | 0.014 | 0.027 | 0.053 | 0.008 | 0.025 | 0.060 | 0.009 | 0.025 | 0.064 |
| 70 | innovativetechnologyltd-002 | 0.082 | 0.176 | 0.232 | 0.074 | 0.172 | 0.233 | 0.091 | 0.131 | 0.265 | 0.132 | 0.269 | 0.391 | 0.149 | 0.362 | 0.516 |
| 71 | innovatrics-006 | 0.002 | 0.017 | 0.051 | 0.003 | 0.018 | 0.054 | 0.005 | 0.012 | 0.035 | 0.007 | 0.045 | 0.103 | 0.005 | 0.037 | 0.087 |
| 72 | innovatrics-007 | 0.001 | 0.005 | 0.015 | 0.002 | 0.005 | 0.017 | 0.003 | 0.003 | 0.007 | 0.003 | 0.012 | 0.038 | 0.002 | 0.009 | 0.026 |
| 73 | intellicloudai-001 | 0.000 | 0.000 | 0.000 | 0.000 | 0.000 | 0.000 | 0.000 | 0.000 | 0.000 | 0.000 | 0.000 | 0.000 | 0.000 | 0.000 | 0.000 |
| 74 | intellifusion-002 | 0.000 | 0.001 | 0.004 | 0.000 | 0.000 | 0.001 | 0.000 | 0.000 | 0.002 | 0.001 | 0.035 | 0.112 | 0.000 | 0.001 | 0.004 |
| 75 | intellivision-002 | 0.073 | 0.213 | 0.267 | 0.068 | 0.210 | 0.261 | 0.143 | 0.204 | 0.340 | 0.308 | 0.517 | 0.618 | 0.137 | 0.396 | 0.469 |
| 76 | intelresearch-001 | 0.088 | 0.212 | 0.242 | 0.086 | 0.213 | 0.257 | 0.132 | 0.191 | 0.316 | 0.052 | 0.176 | 0.265 | 0.068 | 0.230 | 0.358 |
| 77 | intelresearch-002 | 0.006 | 0.016 | 0.031 | 0.007 | 0.017 | 0.032 | 0.008 | 0.011 | 0.025 | 0.008 | 0.021 | 0.046 | 0.008 | 0.023 | 0.052 |
| 78 | intsysmsu-002 | 0.008 | 0.055 | 0.117 | 0.007 | 0.047 | 0.110 | 0.015 | 0.033 | 0.100 | 0.010 | 0.078 | 0.191 | 0.036 | 0.105 | 0.231 |
| 79 | iqface-000 | 0.000 | 0.000 | 0.000 | 0.000 | 0.000 | 0.000 | 0.000 | 0.000 | 0.000 | 0.000 | 0.000 | 0.000 | 0.000 | 0.000 | 0.000 |
| 80 | iqface-002 | 0.000 | 0.000 | 0.000 | 0.000 | 0.000 | 0.000 | 0.000 | 0.000 | 0.000 | 0.000 | 0.000 | 0.000 | 0.000 | 0.000 | 0.000 |
| 81 | isap-001 | 1.000 | 1.000 | 1.000 | 1.000 | 1.000 | 1.000 | 1.000 | 1.000 | 1.000 | 1.000 | 1.000 | 1.000 | 1.000 | 1.000 | 1.000 |
| 82 | isap-002 | 0.000 | 0.000 | 0.000 | 0.000 | 0.000 | 0.000 | 0.000 | 0.000 | 0.000 | 0.000 | 0.000 | 0.000 | 0.000 | 0.000 | 0.000 |
| 83 | itmo-007 | 0.008 | 0.034 | 0.086 | 0.009 | 0.046 | 0.106 | 0.017 | 0.034 | 0.071 | 0.009 | 0.039 | 0.102 | 0.011 | 0.034 | 0.082 |
| 84 | iws-000 | 0.489 | 0.829 | 0.795 | 0.476 | 0.827 | 0.804 | 0.627 | 0.800 | 0.937 | 0.387 | 0.873 | 0.895 | 0.512 | 0.961 | 0.984 |
| 85 | kakao-003 | 0.000 | 0.000 | 0.000 | 0.000 | 0.000 | 0.000 | 0.000 | 0.000 | 0.000 | 0.000 | 0.000 | 0.000 | 0.000 | 0.000 | 0.000 |
| 86 | kedacom-000 | 0.000 | 0.000 | 0.000 | 0.000 | 0.000 | 0.000 | 0.000 | 0.000 | 0.000 | 0.000 | 0.000 | 0.000 | 0.000 | 0.000 | 0.000 |
| 87 | kneron-005 | 0.063 | 0.184 | 0.206 | 0.058 | 0.166 | 0.212 | 0.094 | 0.146 | 0.276 | 0.080 | 0.292 | 0.309 | 0.101 | 0.440 | 0.505 |
| 88 | kookmin-001 | 0.000 | 0.000 | 0.000 | 0.000 | 0.000 | 0.000 | 0.000 | 0.000 | 0.000 | 0.000 | 0.000 | 0.000 | 0.000 | 0.000 | 0.000 |
| 89 | lookman-004 | 0.000 | 0.000 | 0.000 | 0.000 | 0.000 | 0.000 | 0.000 | 0.000 | 0.000 | 0.000 | 0.000 | 0.000 | 0.000 | 0.000 | 0.000 |
| 90 | luxand-000 | 0.000 | 0.000 | 0.000 | 0.000 | 0.000 | 0.000 | 0.000 | 0.000 | 0.000 | 0.000 | 0.000 | 0.000 | 0.000 | 0.000 | 0.000 |

*Table 10: This table summarizes Failure to Enroll (FTE) rates surveyed over 10 000 images of each mask variant. FTE is the proportion of failed template generation attempts. Failures can occur because the software throws an exception, or because the software electively refuses to process the input image as would occur if the algorithms does not detect a face or determines that the face has insufficient information. FTE is measured as the number of function calls that give EITHER a non-zero error code OR that give a "small" template containing fewer than 60 bytes. This second rule is needed because some algorithms incorrectly fail to return a non-zero error code when template generation fails but do produce a skeletal template. The effects of FTE are included in the accuracy results of this report by regarding any template comparison involving a failed template to produce a low similarity score. Thus higher FTE results in higher FNMR and lower FMR. Algorithms in black were submitted prior to mid-March 2020, and algorithms in blue were submitted thereafter.*



FNMR(T) "False non-match rate"
FMR(T) "False match rate"

| | Algorithm Name | COLOR = WHITE SHAPE = WIDE | | | COLOR = LIGHTBLUE SHAPE = WIDE | | | COLOR = LIGHTBLUE SHAPE = ROUND | | | COLOR = RED SHAPE = WIDE | | | COLOR = BLACK SHAPE = WIDE | | |
|---|---|---|---|---|---|---|---|---|---|---|---|---|---|---|---|---|
| | COVERAGE | LO | MED | HI | LO | MED | HI | LO | MED | HI | LO | MED | HI | LO | MED | HI |
| 91 | mobai-000 | 0.186 | 0.306 | 0.323 | 0.200 | 0.299 | 0.329 | 0.204 | 0.275 | 0.386 | 0.403 | 0.643 | 0.755 | 0.219 | 0.397 | 0.527 |
| 92 | mt-000 | 0.005 | 0.021 | 0.061 | 0.006 | 0.024 | 0.063 | 0.011 | 0.021 | 0.045 | 0.006 | 0.024 | 0.058 | 0.007 | 0.023 | 0.059 |
| 93 | mt-002 | 0.001 | 0.004 | 0.007 | 0.001 | 0.004 | 0.006 | 0.001 | 0.001 | 0.003 | 0.001 | 0.005 | 0.013 | 0.002 | 0.005 | 0.009 |
| 94 | mvision-001 | 0.000 | 0.000 | 0.000 | 0.000 | 0.000 | 0.000 | 0.000 | 0.000 | 0.000 | 0.000 | 0.000 | 0.000 | 0.000 | 0.000 | 0.000 |
| 95 | nazhiai-000 | 0.000 | 0.000 | 0.000 | 0.000 | 0.000 | 0.000 | 0.000 | 0.000 | 0.000 | 0.000 | 0.000 | 0.000 | 0.000 | 0.000 | 0.000 |
| 96 | netbridgetech-001 | 0.000 | 0.000 | 0.000 | 0.000 | 0.000 | 0.000 | 0.000 | 0.000 | 0.000 | 0.000 | 0.000 | 0.000 | 0.000 | 0.000 | 0.000 |
| 97 | netbridgetech-002 | 0.000 | 0.000 | 0.000 | 0.000 | 0.000 | 0.000 | 0.000 | 0.000 | 0.000 | 0.000 | 0.000 | 0.000 | 0.000 | 0.000 | 0.000 |
| 98 | neurotechnology-008 | 0.008 | 0.029 | 0.035 | 0.007 | 0.025 | 0.032 | 0.007 | 0.010 | 0.020 | 0.007 | 0.047 | 0.041 | 0.019 | 0.107 | 0.082 |
| 99 | neurotechnology-009 | 0.006 | 0.018 | 0.026 | 0.005 | 0.015 | 0.023 | 0.004 | 0.005 | 0.014 | 0.009 | 0.030 | 0.043 | 0.015 | 0.100 | 0.086 |
| 100 | nodeflux-002 | 0.402 | 0.598 | 0.538 | 0.440 | 0.671 | 0.628 | 0.482 | 0.681 | 0.877 | 0.393 | 0.672 | 0.772 | 0.602 | 0.835 | 0.915 |
| 101 | notiontag-000 | 0.000 | 0.000 | 0.000 | 0.000 | 0.000 | 0.000 | 0.000 | 0.000 | 0.000 | 0.000 | 0.000 | 0.000 | 0.000 | 0.000 | 0.000 |
| 102 | nsensecorp-001 | 0.074 | 0.139 | 0.196 | 0.089 | 0.174 | 0.241 | 0.073 | 0.119 | 0.264 | 0.073 | 0.137 | 0.204 | 0.083 | 0.219 | 0.291 |
| 103 | ntechlab-008 | 0.064 | 0.126 | 0.196 | 0.053 | 0.011 | 0.183 | 0.003 | 0.095 | 0.018 | 0.003 | 0.016 | 0.043 | 0.003 | 0.016 | 0.042 |
| 104 | oz-001 | 0.010 | 0.030 | 0.057 | 0.010 | 0.034 | 0.066 | 0.024 | 0.031 | 0.063 | 0.036 | 0.164 | 0.209 | 0.007 | 0.027 | 0.040 |
| 105 | paravision-004 | 0.002 | 0.011 | 0.027 | 0.002 | 0.010 | 0.024 | 0.003 | 0.004 | 0.009 | 0.003 | 0.019 | 0.056 | 0.003 | 0.016 | 0.043 |
| 106 | pensees-001 | 0.000 | 0.000 | 0.000 | 0.000 | 0.000 | 0.000 | 0.000 | 0.000 | 0.000 | 0.000 | 0.000 | 0.000 | 0.000 | 0.000 | 0.000 |
| 107 | pixelall-003 | 0.000 | 0.000 | 0.000 | 0.000 | 0.000 | 0.000 | 0.000 | 0.000 | 0.000 | 0.000 | 0.000 | 0.000 | 0.000 | 0.000 | 0.000 |
| 108 | pixelall-004 | 0.000 | 0.000 | 0.000 | 0.000 | 0.000 | 0.000 | 0.000 | 0.000 | 0.000 | 0.000 | 0.000 | 0.000 | 0.000 | 0.000 | 0.000 |
| 109 | psl-005 | 0.004 | 0.015 | 0.038 | 0.003 | 0.014 | 0.036 | 0.006 | 0.011 | 0.029 | 0.006 | 0.025 | 0.061 | 0.008 | 0.020 | 0.047 |
| 110 | ptakuratsatu-000 | 0.001 | 0.005 | 0.015 | 0.002 | 0.005 | 0.017 | 0.003 | 0.003 | 0.007 | 0.003 | 0.012 | 0.038 | 0.002 | 0.009 | 0.026 |
| 111 | pxl-001 | 0.096 | 0.268 | 0.329 | 0.082 | 0.208 | 0.273 | 0.090 | 0.161 | 0.294 | 0.272 | 0.579 | 0.712 | 0.116 | 0.302 | 0.500 |
| 112 | rankone-009 | 0.000 | 0.000 | 0.000 | 0.000 | 0.000 | 0.000 | 0.000 | 0.000 | 0.000 | 0.000 | 0.000 | 0.001 | 0.000 | 0.000 | 0.001 |
| 113 | rankone-010 | 0.000 | 0.000 | 0.000 | 0.000 | 0.000 | 0.000 | 0.000 | 0.000 | 0.000 | 0.000 | 0.000 | 0.000 | 0.000 | 0.000 | 0.000 |
| 114 | remarkai-002 | 0.000 | 0.000 | 0.000 | 0.000 | 0.000 | 0.000 | 0.000 | 0.000 | 0.000 | 0.000 | 0.000 | 0.000 | 0.000 | 0.000 | 0.000 |
| 115 | rokid-000 | 0.194 | 0.372 | 0.370 | 0.220 | 0.444 | 0.450 | 0.265 | 0.457 | 0.749 | 0.191 | 0.431 | 0.553 | 0.367 | 0.677 | 0.806 |
| 116 | s1-001 | 0.647 | 0.943 | 0.911 | 0.617 | 0.930 | 0.915 | 0.616 | 0.919 | 0.954 | 0.613 | 0.957 | 0.960 | 0.646 | 0.962 | 0.962 |
| 117 | scanovate-001 | 0.544 | 0.601 | 0.596 | 0.515 | 0.553 | 0.579 | 0.513 | 0.565 | 0.664 | 0.766 | 0.914 | 0.960 | 0.554 | 0.676 | 0.806 |
| 118 | scanovate-002 | 0.008 | 0.019 | 0.046 | 0.008 | 0.018 | 0.045 | 0.008 | 0.012 | 0.027 | 0.010 | 0.025 | 0.079 | 0.012 | 0.036 | 0.101 |
| 119 | securifai-001 | 0.000 | 0.000 | 0.000 | 0.000 | 0.000 | 0.000 | 0.000 | 0.000 | 0.000 | 0.000 | 0.000 | 0.000 | 0.000 | 0.000 | 0.000 |
| 120 | sensetime-003 | 0.009 | 0.029 | 0.069 | 0.009 | 0.031 | 0.074 | 0.014 | 0.025 | 0.057 | 0.012 | 0.048 | 0.115 | 0.013 | 0.048 | 0.140 |
| 121 | sertis-000 | 0.002 | 0.012 | 0.034 | 0.002 | 0.012 | 0.032 | 0.003 | 0.005 | 0.013 | 0.003 | 0.016 | 0.047 | 0.005 | 0.020 | 0.052 |
| 122 | sertis-001 | 0.002 | 0.006 | 0.017 | 0.002 | 0.006 | 0.014 | 0.001 | 0.002 | 0.005 | 0.002 | 0.007 | 0.017 | 0.003 | 0.009 | 0.020 |
| 123 | shu-002 | 0.011 | 0.031 | 0.080 | 0.009 | 0.026 | 0.083 | 0.023 | 0.037 | 0.103 | 0.026 | 0.126 | 0.227 | 0.016 | 0.056 | 0.167 |
| 124 | shu-003 | 0.003 | 0.006 | 0.013 | 0.002 | 0.004 | 0.008 | 0.003 | 0.005 | 0.009 | 0.008 | 0.031 | 0.070 | 0.004 | 0.014 | 0.040 |
| 125 | sjtu-002 | 0.011 | 0.031 | 0.080 | 0.009 | 0.026 | 0.083 | 0.023 | 0.037 | 0.103 | 0.026 | 0.126 | 0.227 | 0.016 | 0.056 | 0.167 |
| 126 | sjtu-003 | 0.002 | 0.004 | 0.009 | 0.002 | 0.003 | 0.006 | 0.002 | 0.003 | 0.006 | 0.005 | 0.022 | 0.049 | 0.003 | 0.009 | 0.028 |
| 127 | staqu-000 | 0.000 | 0.000 | 0.000 | 0.000 | 0.000 | 0.000 | 0.000 | 0.000 | 0.000 | 0.000 | 0.000 | 0.000 | 0.000 | 0.000 | 0.000 |
| 128 | starhybrid-001 | 0.192 | 0.468 | 0.461 | 0.149 | 0.406 | 0.483 | 0.137 | 0.321 | 0.487 | 0.478 | 0.761 | 0.781 | 0.133 | 0.372 | 0.565 |
| 129 | synesis-006 | 0.001 | 0.003 | 0.007 | 0.001 | 0.003 | 0.007 | 0.001 | 0.001 | 0.003 | 0.001 | 0.005 | 0.011 | 0.001 | 0.004 | 0.008 |
| 130 | synesis-007 | 0.007 | 0.021 | 0.047 | 0.008 | 0.028 | 0.056 | 0.013 | 0.025 | 0.056 | 0.007 | 0.046 | 0.114 | 0.018 | 0.124 | 0.134 |
| 131 | synology-000 | 0.000 | 0.000 | 0.000 | 0.000 | 0.000 | 0.000 | 0.000 | 0.000 | 0.000 | 0.000 | 0.000 | 0.000 | 0.000 | 0.000 | 0.000 |
| 132 | synology-002 | 0.000 | 0.000 | 0.000 | 0.000 | 0.000 | 0.000 | 0.000 | 0.000 | 0.000 | 0.000 | 0.000 | 0.000 | 0.000 | 0.000 | 0.000 |
| 133 | tech5-004 | 0.005 | 0.022 | 0.061 | 0.006 | 0.028 | 0.070 | 0.010 | 0.021 | 0.046 | 0.006 | 0.025 | 0.068 | 0.006 | 0.021 | 0.058 |
| 134 | tech5-005 | 0.004 | 0.015 | 0.044 | 0.004 | 0.017 | 0.046 | 0.006 | 0.012 | 0.026 | 0.005 | 0.020 | 0.051 | 0.007 | 0.022 | 0.057 |
| 135 | tevian-005 | 0.125 | 0.463 | 0.370 | 0.148 | 0.650 | 0.557 | 0.208 | 0.359 | 0.705 | 0.086 | 0.667 | 0.679 | 0.131 | 0.786 | 0.787 |

*Table 11: This table summarizes Failure to Enroll (FTE) rates surveyed over 10 000 images of each mask variant. FTE is the proportion of failed template generation attempts. Failures can occur because the software throws an exception, or because the software electively refuses to process the input image as would occur if the algorithms does not detect a face or determines that the face has insufficient information. FTE is measured as the number of function calls that give EITHER a non-zero error code OR that give a "small" template containing fewer than 60 bytes. This second rule is needed because some algorithms incorrectly fail to return a non-zero error code when template generation fails but do produce a skeletal template. The effects of FTE are included in the accuracy results of this report by regarding any template comparison involving a failed template to produce a low similarity score. Thus higher FTE results in higher FNMR and lower FMR. Algorithms in black were submitted prior to mid-March 2020, and algorithms in blue were submitted thereafter.*



FNMR(T) "False non-match rate"
FMR(T) "False match rate"

| | Algorithm | COLOR = WHITE | | | COLOR = LIGHTBLUE | | | | | | COLOR = RED | | | COLOR = BLACK | | |
|---|---|---|---|---|---|---|---|---|---|---|---|---|---|---|---|---|
| | Name | SHAPE = WIDE | | | SHAPE = WIDE | | | SHAPE = ROUND | | | SHAPE = WIDE | | | SHAPE = WIDE | | |
| | COVERAGE | LO | MED | HI | LO | MED | HI | LO | MED | HI | LO | MED | HI | LO | MED | HI |
| 136 | tevian-006 | 0.012 | 0.089 | 0.160 | 0.010 | 0.066 | 0.124 | 0.028 | 0.041 | 0.146 | 0.034 | 0.266 | 0.408 | 0.016 | 0.256 | 0.307 |
| 137 | trueface-000 | 0.000 | 0.000 | 0.000 | 0.000 | 0.000 | 0.000 | 0.000 | 0.000 | 0.000 | 0.000 | 0.000 | 0.000 | 0.000 | 0.000 | 0.000 |
| 138 | trueface-001 | 0.078 | 0.163 | 0.217 | 0.071 | 0.153 | 0.217 | 0.084 | 0.119 | 0.268 | - | - | - | 0.147 | 0.317 | 0.474 |
| 139 | tuputech-000 | 0.517 | 0.679 | 0.684 | 0.626 | 0.758 | 0.765 | 0.502 | 0.619 | 0.714 | 0.652 | 0.893 | 0.926 | 0.661 | 0.904 | 0.933 |
| 140 | uluface-002 | 0.000 | 0.000 | 0.000 | 0.000 | 0.000 | 0.000 | 0.000 | 0.000 | 0.000 | 0.000 | 0.000 | 0.000 | 0.000 | 0.000 | 0.000 |
| 141 | upc-001 | 0.002 | 0.005 | 0.012 | 0.002 | 0.005 | 0.012 | 0.002 | 0.002 | 0.005 | 0.002 | 0.010 | 0.027 | 0.003 | 0.007 | 0.018 |
| 142 | veridas-003 | 1.000 | 1.000 | 1.000 | 1.000 | 1.000 | 1.000 | 1.000 | 1.000 | 1.000 | 1.000 | 1.000 | 1.000 | 1.000 | 1.000 | 1.000 |
| 143 | veridas-004 | 0.047 | 0.139 | 0.202 | 0.041 | 0.112 | 0.164 | 0.048 | 0.085 | 0.154 | 0.106 | 0.401 | 0.568 | 0.054 | 0.213 | 0.383 |
| 144 | via-001 | 0.000 | 0.000 | 0.000 | 0.000 | 0.000 | 0.000 | 0.000 | 0.000 | 0.000 | 0.000 | 0.000 | 0.000 | 0.000 | 0.000 | 0.000 |
| 145 | videmo-000 | 0.019 | 0.067 | 0.125 | 0.018 | 0.051 | 0.106 | 0.023 | 0.040 | 0.089 | 0.122 | 0.352 | 0.368 | 0.027 | 0.100 | 0.296 |
| 146 | videonetics-002 | 0.338 | 0.581 | 0.557 | 0.330 | 0.569 | 0.542 | 0.378 | 0.559 | 0.785 | 0.344 | 0.693 | 0.735 | 0.396 | 0.702 | 0.848 |
| 147 | vigilantsolutions-007 | 0.062 | 0.168 | 0.220 | 0.052 | 0.137 | 0.193 | 0.069 | 0.126 | 0.206 | 0.098 | 0.408 | 0.634 | 0.072 | 0.273 | 0.493 |
| 148 | vigilantsolutions-008 | 0.062 | 0.168 | 0.218 | 0.051 | 0.136 | 0.189 | 0.068 | 0.124 | 0.202 | 0.096 | 0.407 | 0.633 | 0.072 | 0.268 | 0.492 |
| 149 | vinai-000 | 0.000 | 0.000 | 0.000 | 0.000 | 0.000 | 0.000 | 0.000 | 0.000 | 0.000 | 0.000 | 0.000 | 0.000 | 0.000 | 0.000 | 0.000 |
| 150 | visionlabs-008 | 0.013 | 0.035 | 0.083 | 0.012 | 0.031 | 0.072 | 0.019 | 0.038 | 0.097 | 0.016 | 0.040 | 0.096 | 0.024 | 0.061 | 0.124 |
| 151 | visionlabs-009 | 0.011 | 0.037 | 0.082 | 0.010 | 0.035 | 0.076 | 0.018 | 0.042 | 0.097 | 0.016 | 0.052 | 0.120 | 0.024 | 0.065 | 0.150 |
| 152 | visteam-000 | 0.058 | 0.150 | 0.210 | 0.048 | 0.118 | 0.176 | 0.052 | 0.092 | 0.156 | 0.160 | 0.372 | 0.506 | 0.074 | 0.202 | 0.369 |
| 153 | vocord-008 | 0.013 | 0.046 | 0.087 | 0.011 | 0.052 | 0.089 | 0.031 | 0.059 | 0.111 | 0.013 | 0.079 | 0.127 | 0.009 | 0.050 | 0.093 |
| 154 | vts-000 | 0.011 | 0.029 | 0.072 | 0.012 | 0.028 | 0.074 | 0.015 | 0.020 | 0.048 | 0.014 | 0.043 | 0.129 | 0.016 | 0.051 | 0.149 |
| 155 | winsense-001 | 0.000 | 0.000 | 0.000 | 0.000 | 0.000 | 0.000 | 0.000 | 0.000 | 0.000 | 0.000 | 0.000 | 0.000 | 0.000 | 0.000 | 0.000 |
| 156 | xforwardai-000 | 0.000 | 0.000 | 0.000 | 0.000 | 0.000 | 0.000 | 0.000 | 0.000 | 0.000 | 0.000 | 0.000 | 0.000 | 0.000 | 0.000 | 0.000 |
| 157 | xforwardai-001 | 0.006 | 0.025 | 0.069 | 0.007 | 0.031 | 0.079 | 0.011 | 0.021 | 0.052 | 0.007 | 0.030 | 0.079 | 0.007 | 0.022 | 0.060 |
| 158 | xm-000 | 0.003 | 0.006 | 0.013 | 0.002 | 0.004 | 0.008 | 0.003 | 0.004 | 0.009 | 0.008 | 0.031 | 0.070 | 0.005 | 0.013 | 0.038 |
| 159 | yoonik-000 | 0.029 | 0.061 | 0.138 | 0.027 | 0.060 | 0.142 | 0.037 | 0.049 | 0.124 | 0.040 | 0.094 | 0.219 | 0.039 | 0.099 | 0.257 |
| 160 | yoonik-001 | 0.015 | 0.052 | 0.110 | 0.017 | 0.055 | 0.113 | 0.024 | 0.035 | 0.072 | 0.031 | 0.093 | 0.170 | 0.026 | 0.086 | 0.175 |
| 161 | yuan-000 | 0.000 | 0.000 | 0.000 | 0.000 | 0.000 | 0.000 | 0.000 | 0.000 | 0.000 | 0.000 | 0.000 | 0.000 | 0.000 | 0.000 | 0.000 |

*Table 12: This table summarizes Failure to Enroll (FTE) rates surveyed over 10 000 images of each mask variant. FTE is the proportion of failed template generation attempts. Failures can occur because the software throws an exception, or because the software electively refuses to process the input image as would occur if the algorithms does not detect a face or determines that the face has insufficient information. FTE is measured as the number of function calls that give EITHER a non-zero error code OR that give a "small" template containing fewer than 60 bytes. This second rule is needed because some algorithms incorrectly fail to return a non-zero error code when template generation fails but do produce a skeletal template. The effects of FTE are included in the accuracy results of this report by regarding any template comparison involving a failed template to produce a low similarity score. Thus higher FTE results in higher FNMR and lower FMR. Algorithms in black were submitted prior to mid-March 2020, and algorithms in blue were submitted thereafter.*

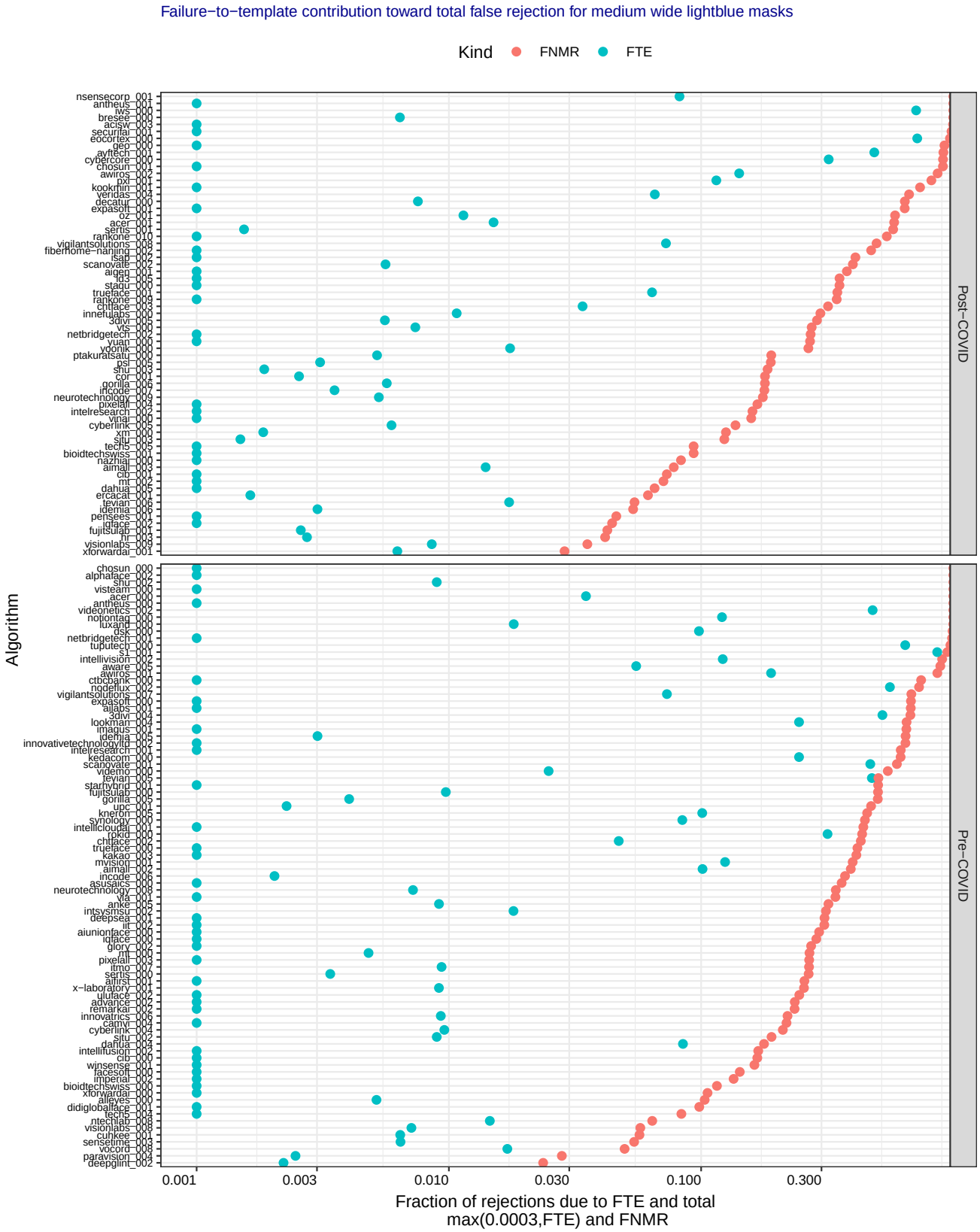


*Figure 10: For each algorithm the rightmost dot shows FNMR @ FMR=0.00001 (as reported throughout this report). The left most dot shows the failure-to-template (FTE) rate over the masked verification set of 5.2M images. The gap between the two dots is attributable to low similarity score. Some FTE rates are zero - rates below 0.001 are shown as 0.001.*





FNMR(T) "False non-match rate"
FMR(T) "False match rate"

The following plots are detection error tradeoff (DET) characteristics for each algorithm, across different mask nose coverages and shapes.



FNMR(T) "False non-match rate"
FMR(T) "False match rate"

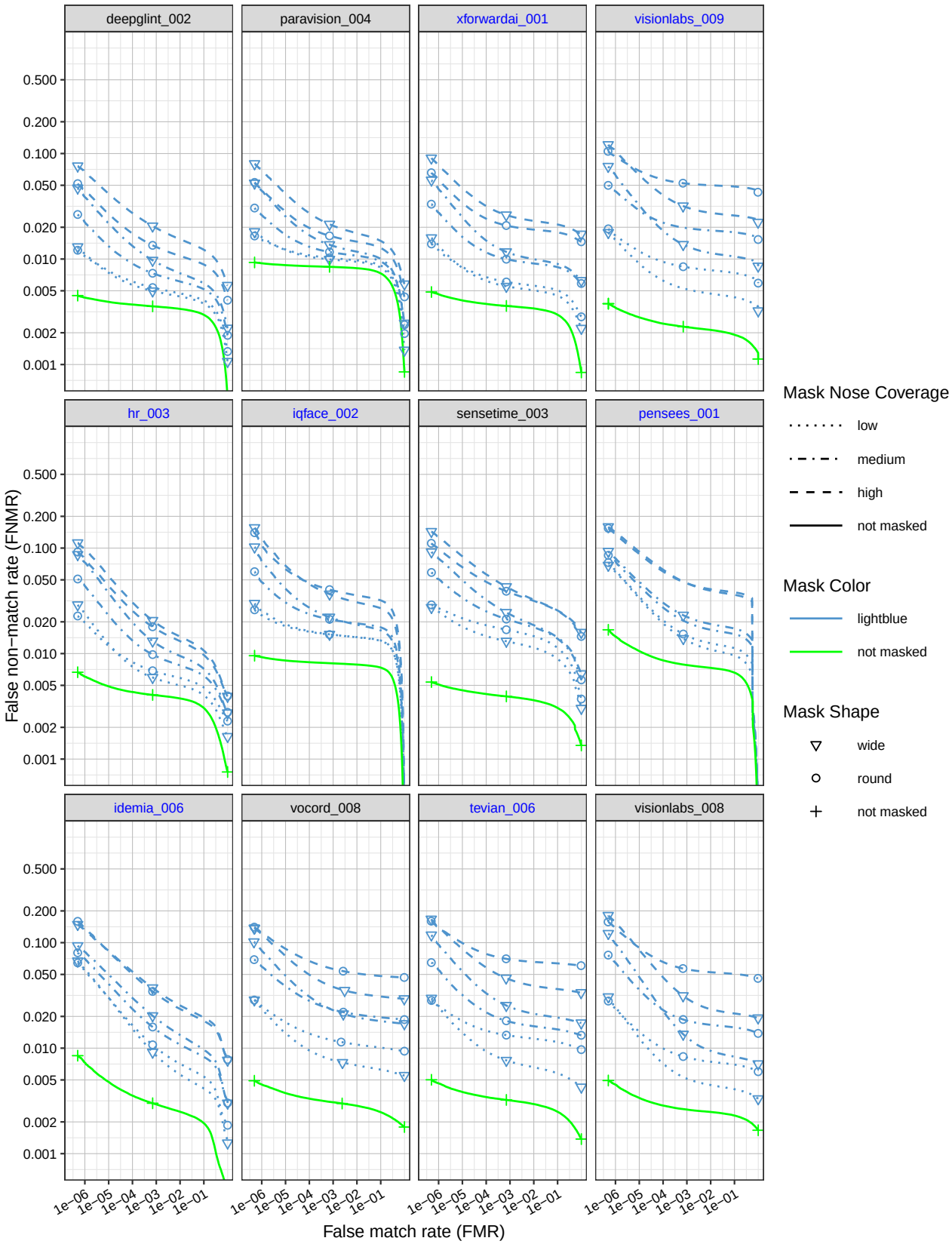


*Figure 11: DET curves showing error rates on unmasked and masked probe images, broken out by mask shape and nose coverage. Algorithms in black were submitted prior to mid-March 2020, and algorithms in blue were submitted thereafter.*



FNMR(T) "False non-match rate"
FMR(T) "False match rate"

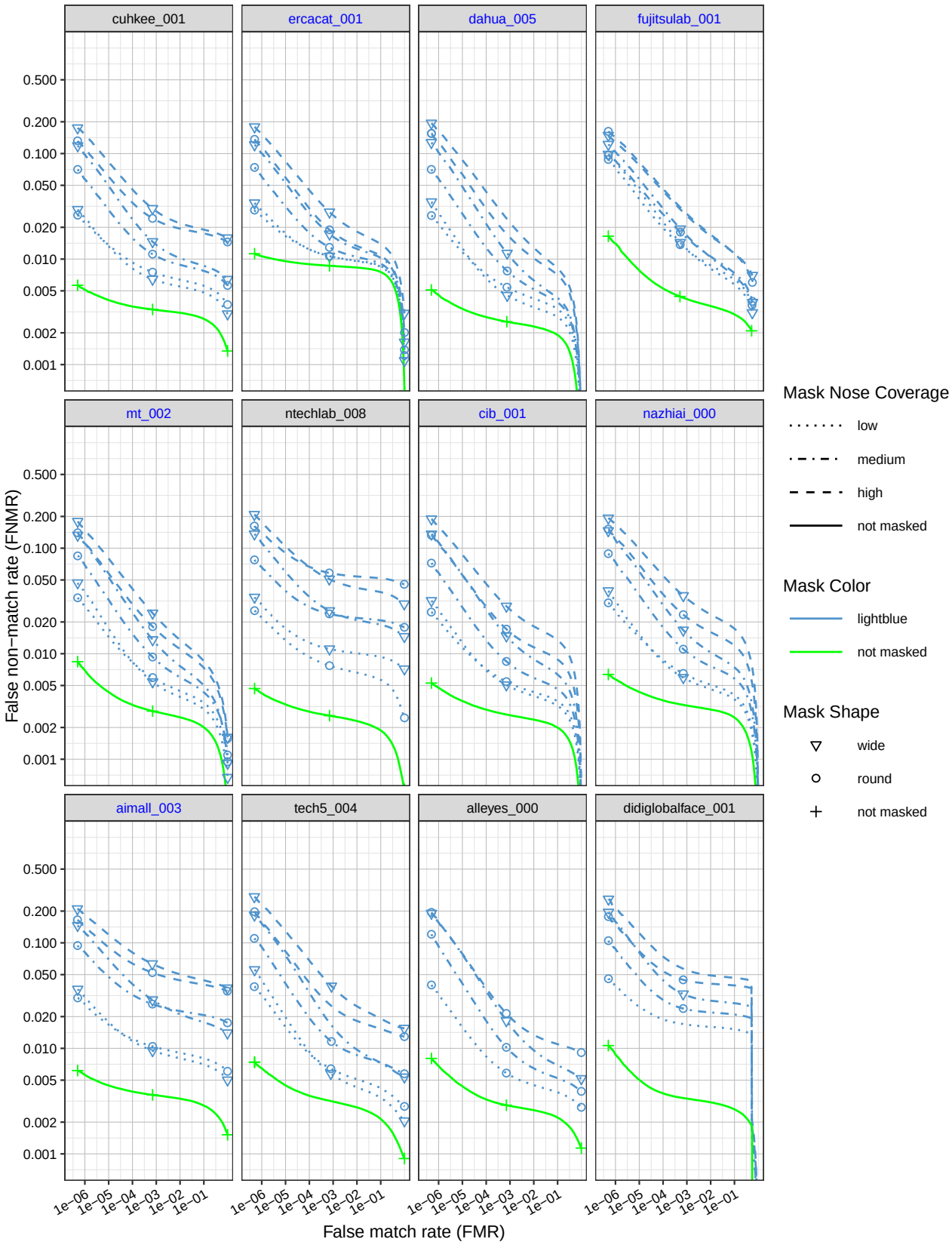


*Figure 12: DET curves showing error rates on unmasked and masked probe images, broken out by mask shape and nose coverage. Algorithms in black were submitted prior to mid-March 2020, and algorithms in blue were submitted thereafter.*





FNMR(T) "False non-match rate"
FMR(T) "False match rate"

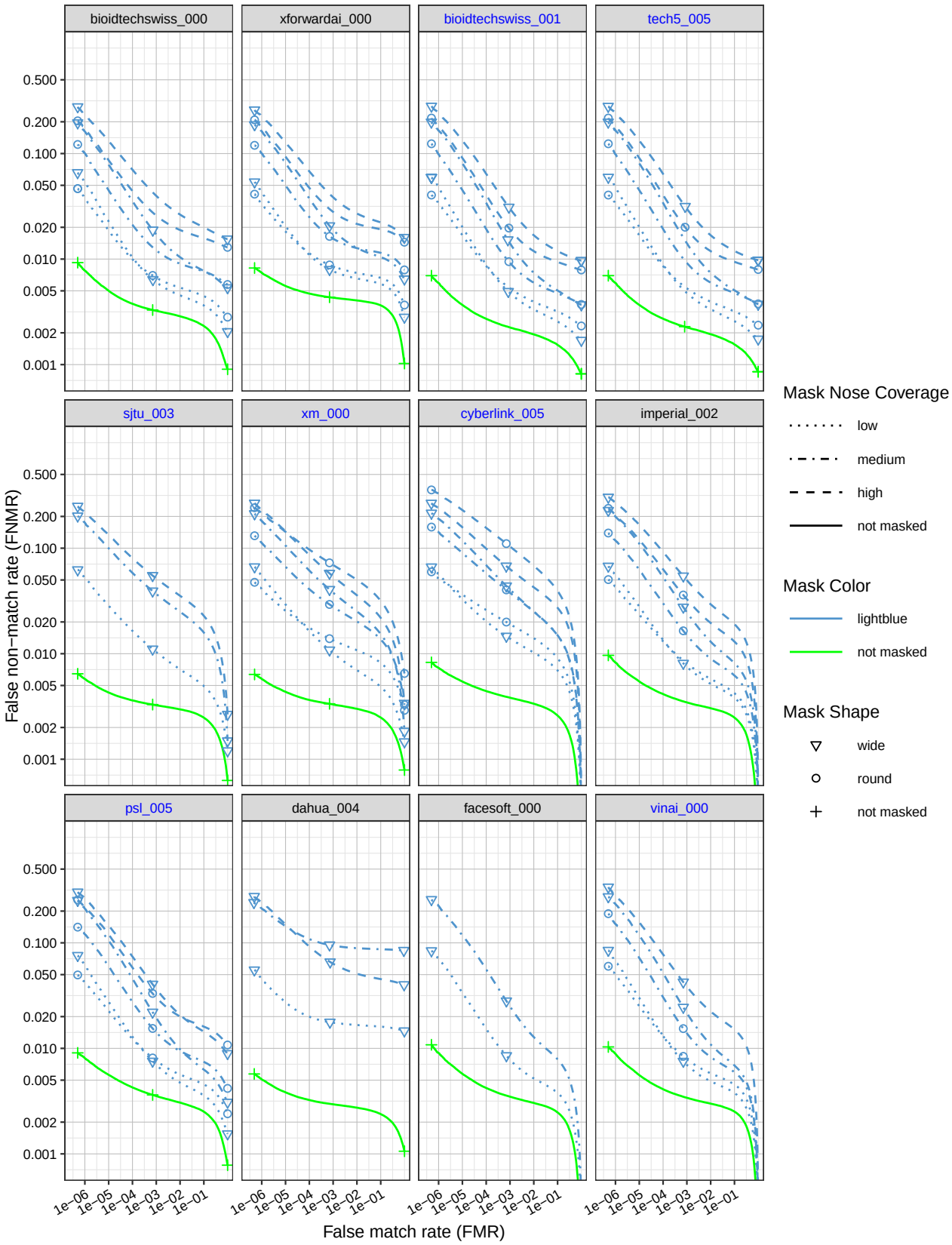


*Figure 13: DET curves showing error rates on unmasked and masked probe images, broken out by mask shape and nose coverage. Algorithms in black were submitted prior to mid-March 2020, and algorithms in blue were submitted thereafter.*



FNMR(T) "False non-match rate"
FMR(T) "False match rate"

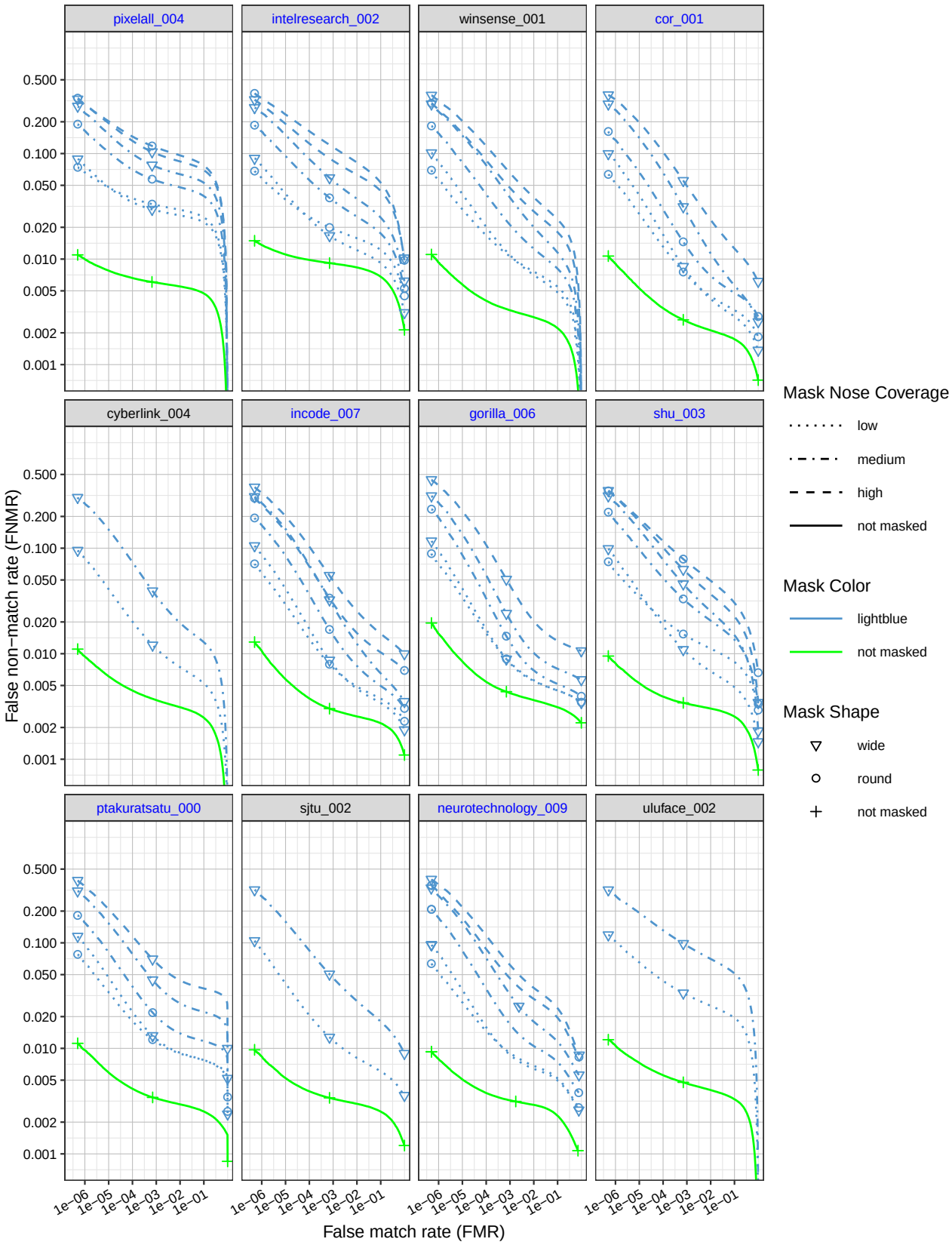


*Figure 14: DET curves showing error rates on unmasked and masked probe images, broken out by mask shape and nose coverage. Algorithms in black were submitted prior to mid-March 2020, and algorithms in blue were submitted thereafter.*



FNMR(T) "False non-match rate"
FMR(T) "False match rate"

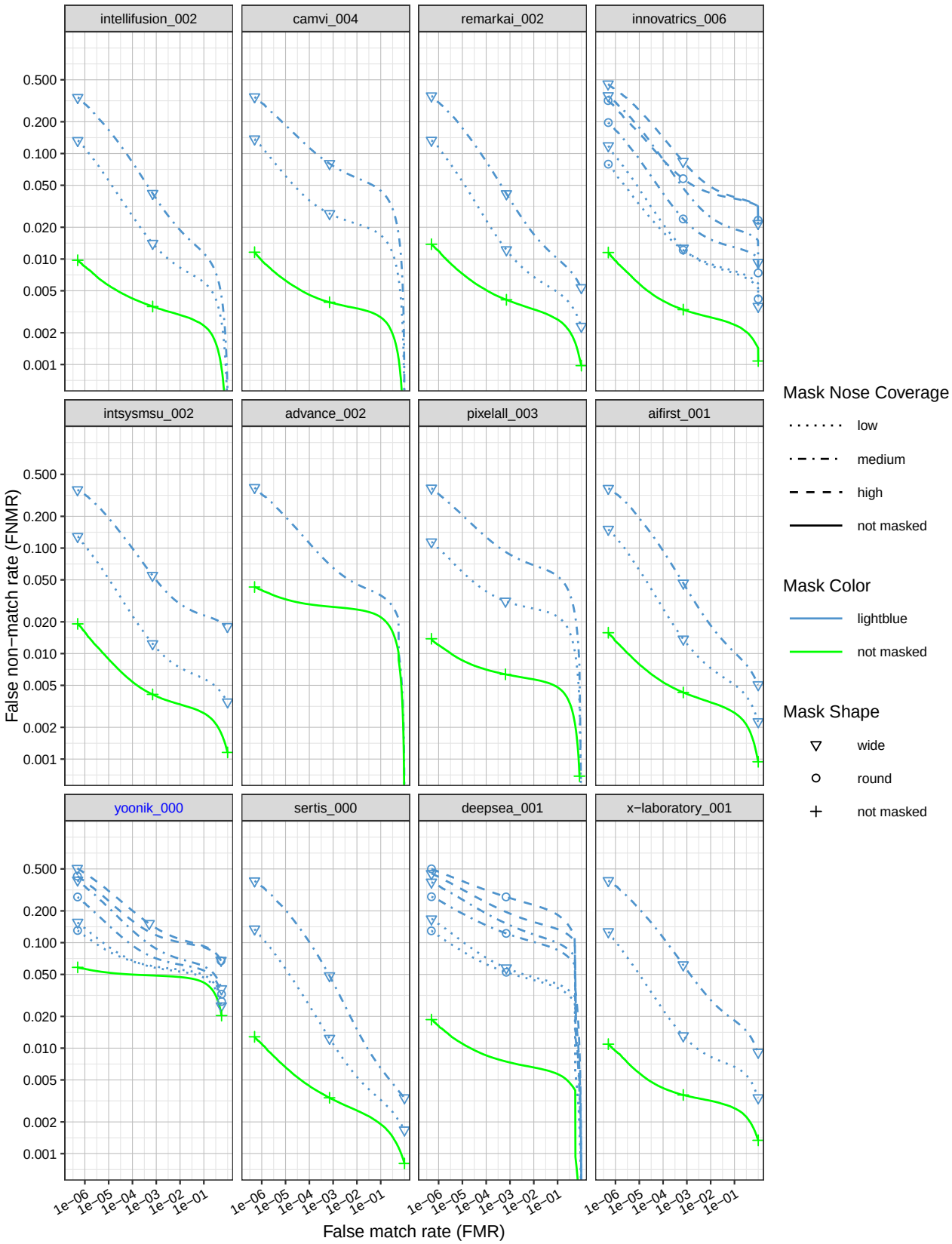


*Figure 15: DET curves showing error rates on unmasked and masked probe images, broken out by mask shape and nose coverage. Algorithms in black were submitted prior to mid-March 2020, and algorithms in blue were submitted thereafter.*



FNMR(T) "False non-match rate"
FMR(T) "False match rate"

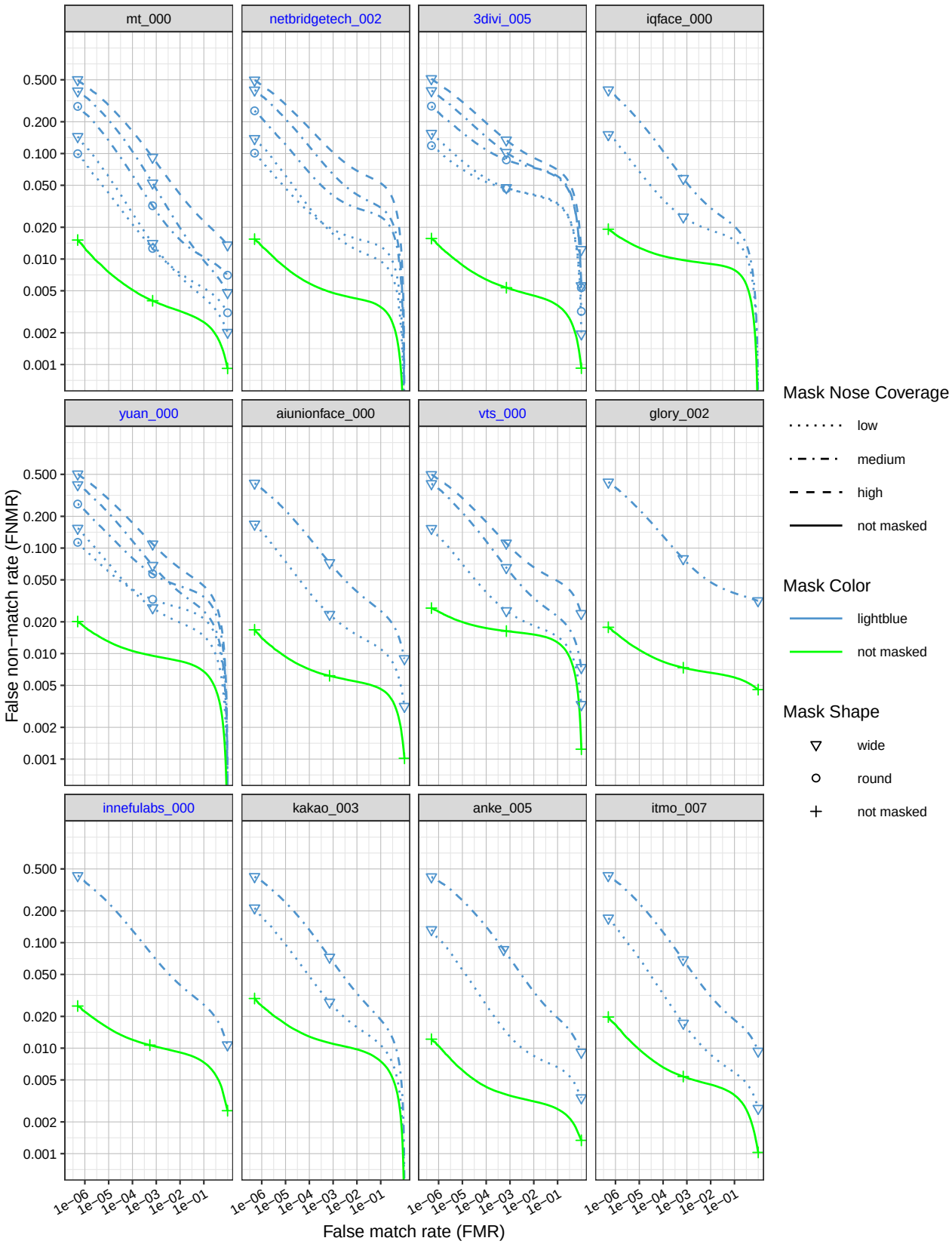


*Figure 16: DET curves showing error rates on unmasked and masked probe images, broken out by mask shape and nose coverage. Algorithms in black were submitted prior to mid-March 2020, and algorithms in blue were submitted thereafter.*



FNMR(T) "False non-match rate"
FMR(T) "False match rate"

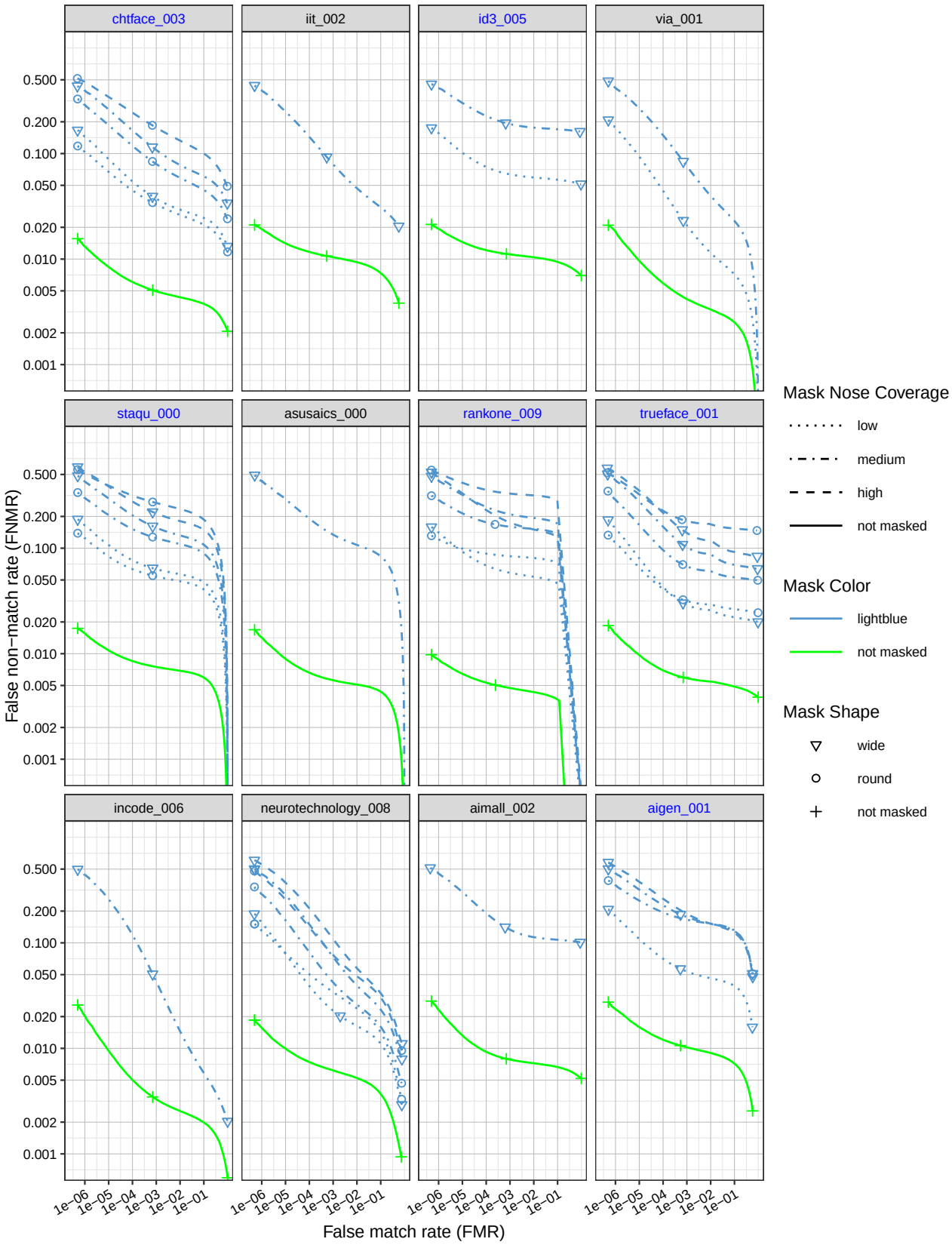


*Figure 17: DET curves showing error rates on unmasked and masked probe images, broken out by mask shape and nose coverage. Algorithms in black were submitted prior to mid-March 2020, and algorithms in blue were submitted thereafter.*



FNMR(T) "False non-match rate"
FMR(T) "False match rate"

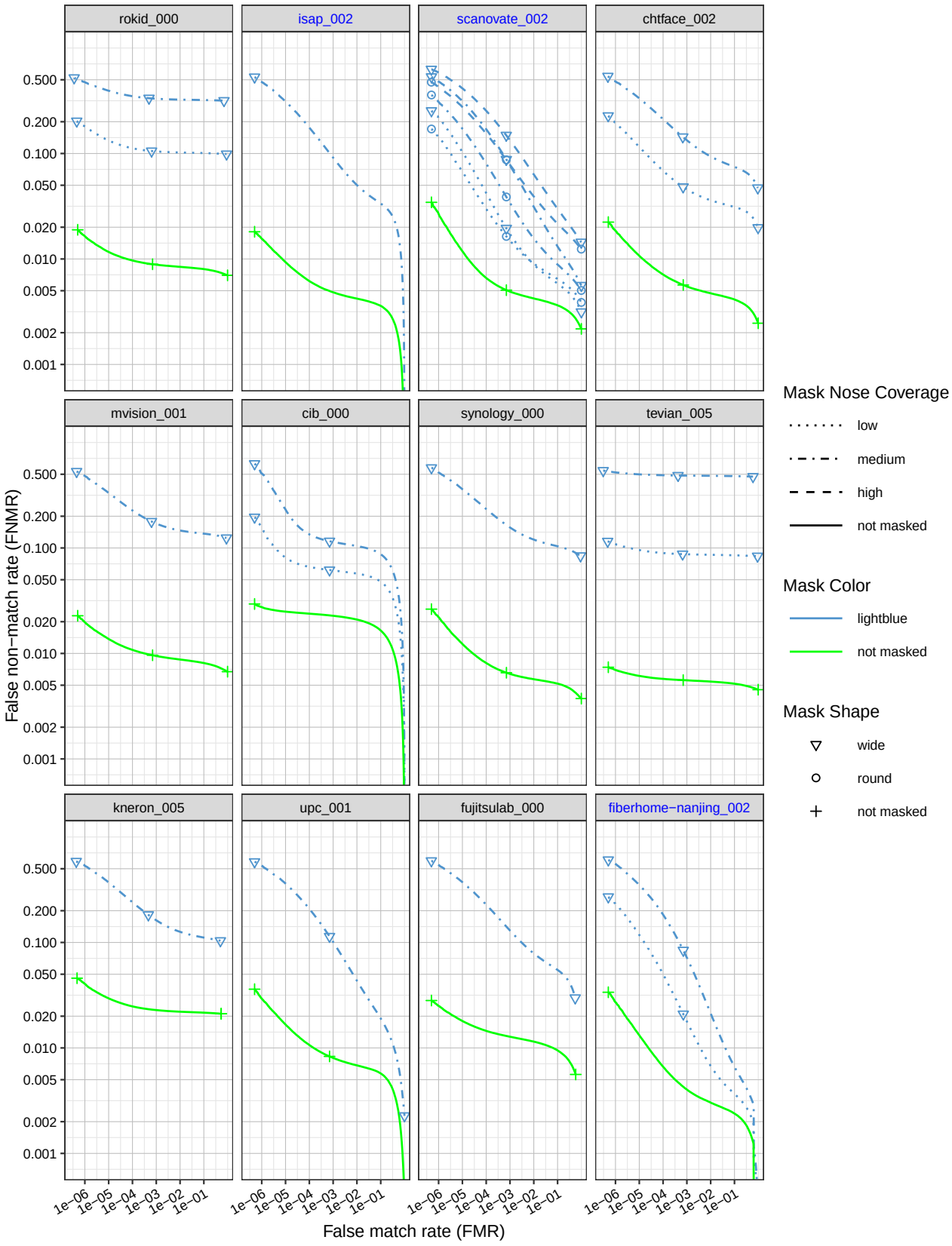


*Figure 18: DET curves showing error rates on unmasked and masked probe images, broken out by mask shape and nose coverage. Algorithms in black were submitted prior to mid-March 2020, and algorithms in blue were submitted thereafter.*



FNMR(T) "False non-match rate"
FMR(T) "False match rate"

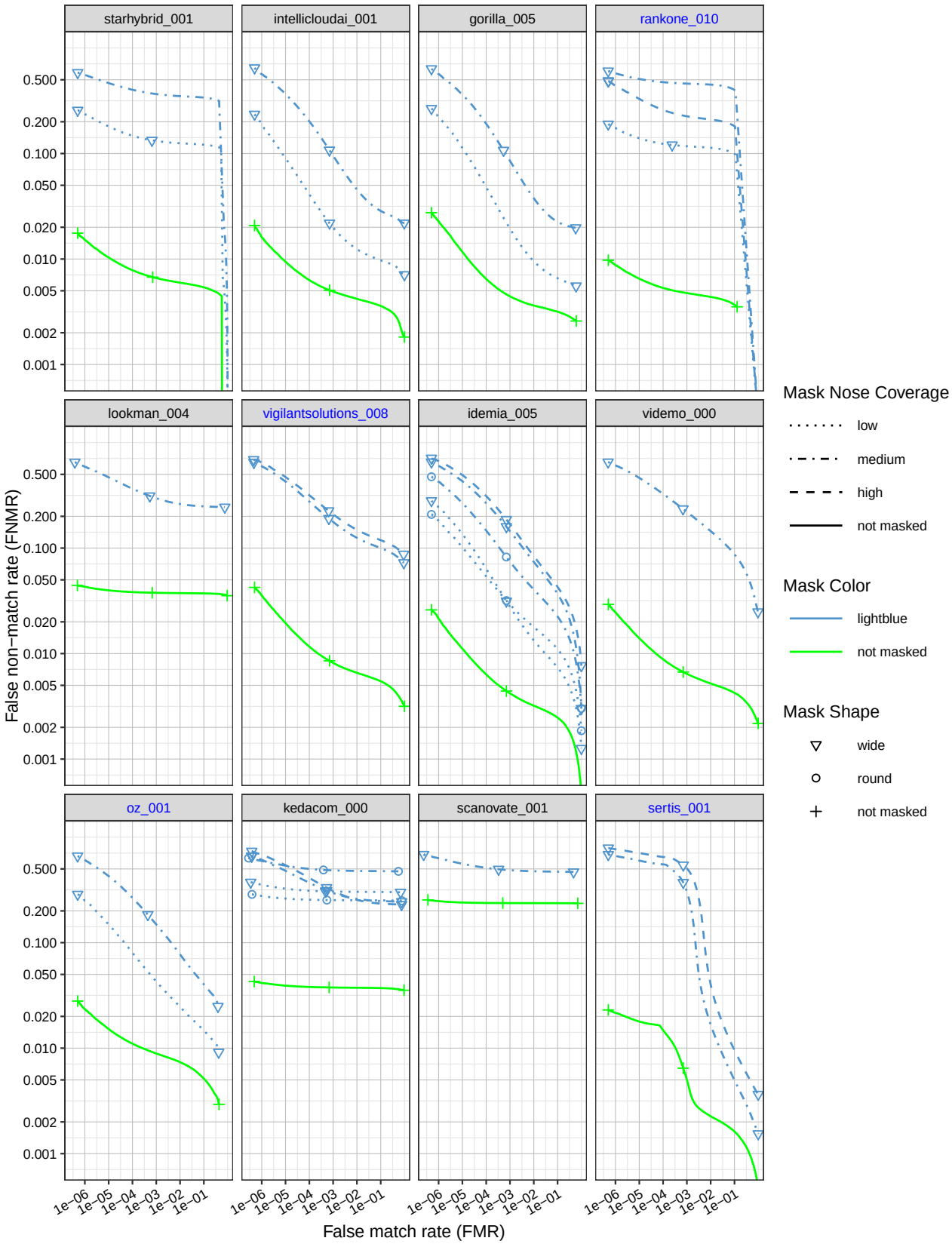


*Figure 19: DET curves showing error rates on unmasked and masked probe images, broken out by mask shape and nose coverage. Algorithms in black were submitted prior to mid-March 2020, and algorithms in blue were submitted thereafter.*



FNMR(T) "False non-match rate"
FMR(T) "False match rate"

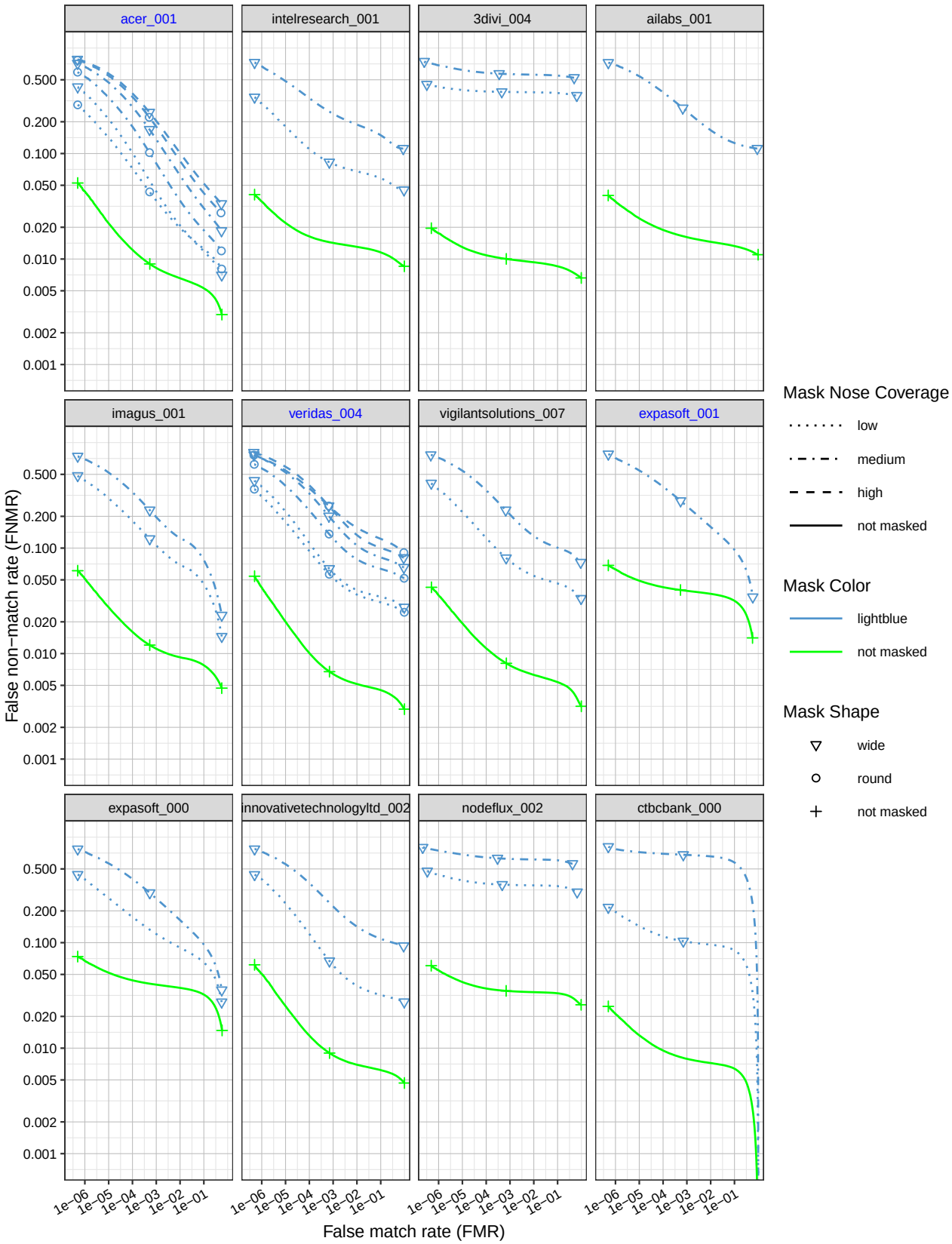


*Figure 20: DET curves showing error rates on unmasked and masked probe images, broken out by mask shape and nose coverage. Algorithms in black were submitted prior to mid-March 2020, and algorithms in blue were submitted thereafter.*



FNMR(T) "False non-match rate"
FMR(T) "False match rate"

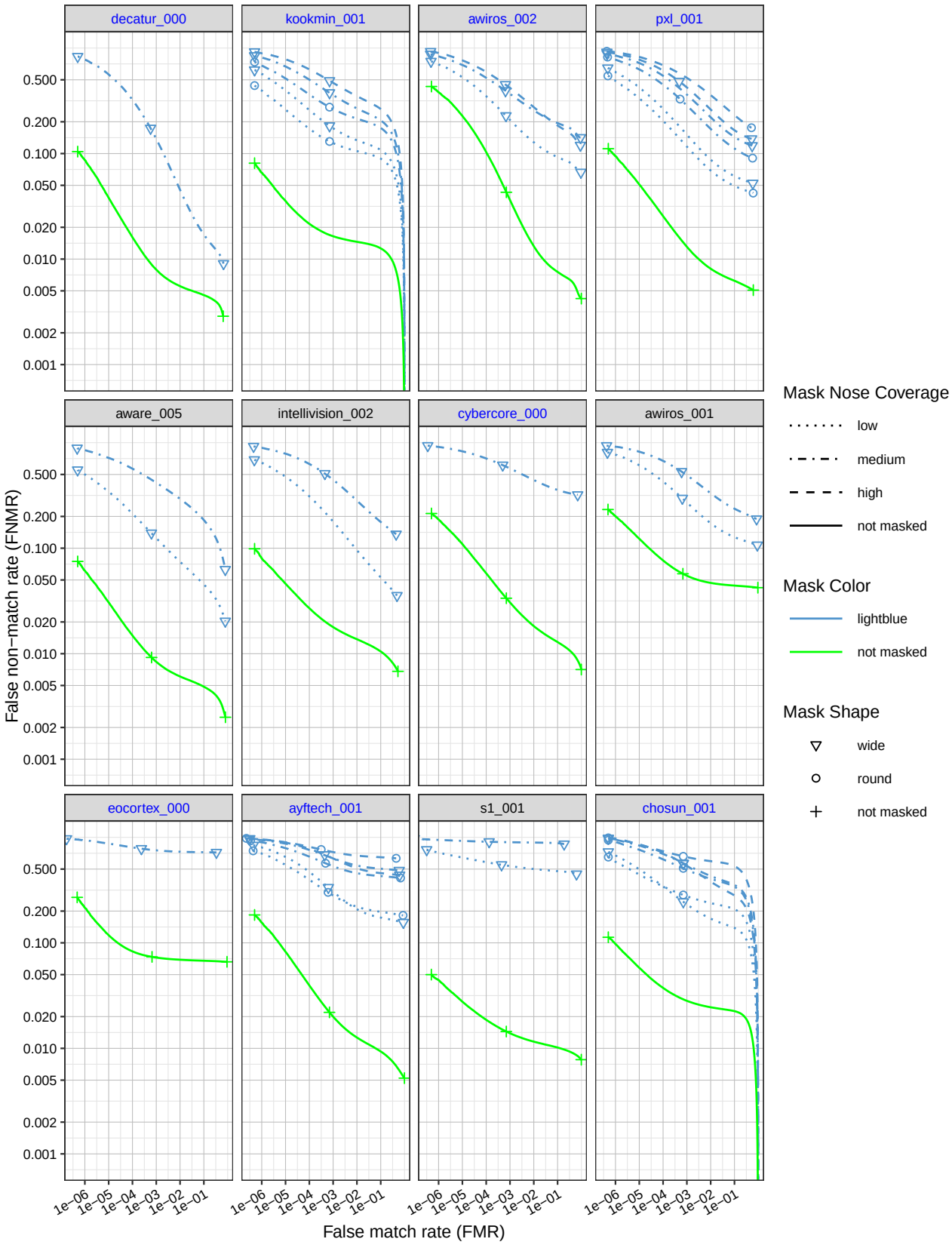


*Figure 21: DET curves showing error rates on unmasked and masked probe images, broken out by mask shape and nose coverage. Algorithms in black were submitted prior to mid-March 2020, and algorithms in blue were submitted thereafter.*



FNMR(T) "False non-match rate"
FMR(T) "False match rate"

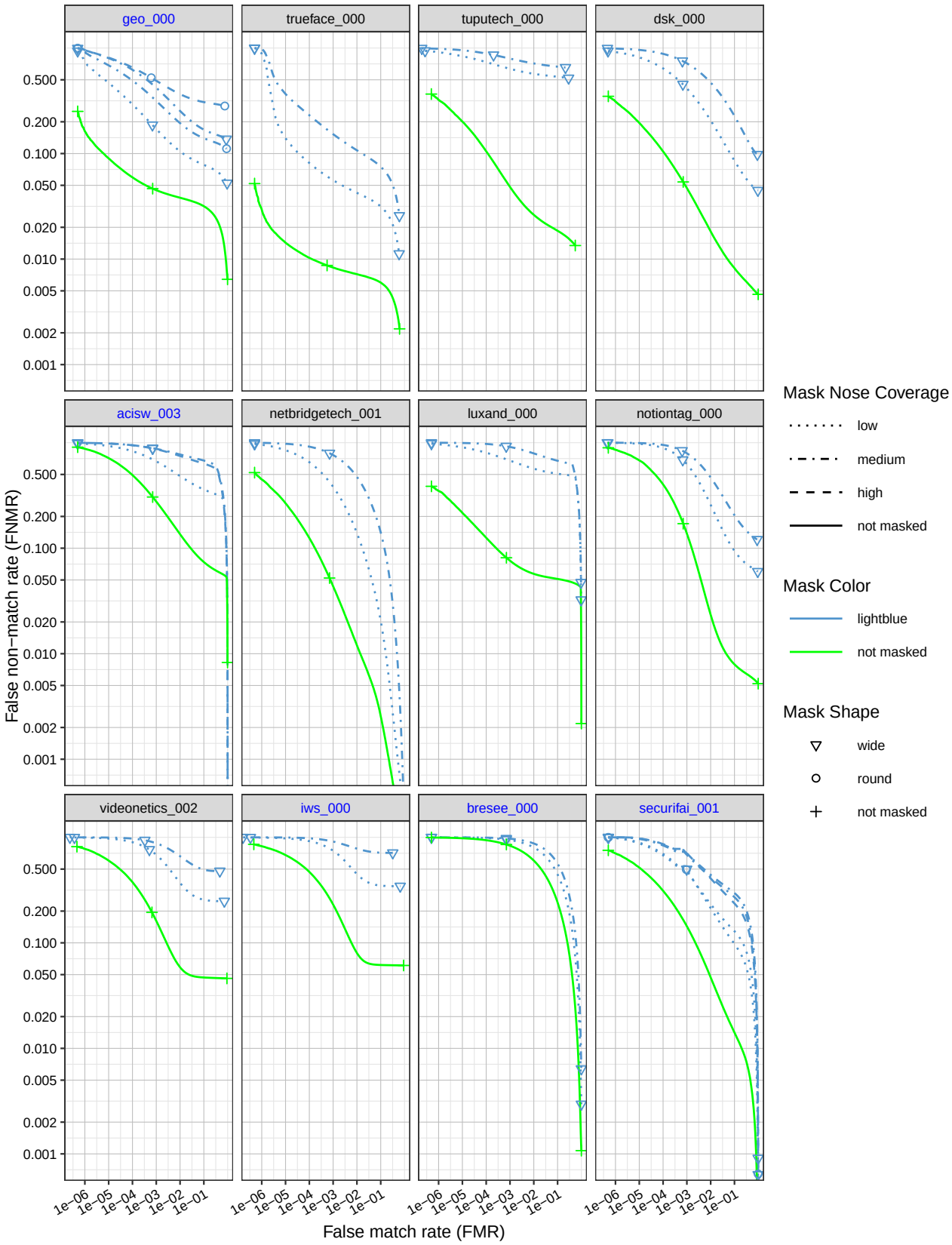


*Figure 22: DET curves showing error rates on unmasked and masked probe images, broken out by mask shape and nose coverage. Algorithms in black were submitted prior to mid-March 2020, and algorithms in blue were submitted thereafter.*



FNMR(T) "False non-match rate"
FMR(T) "False match rate"

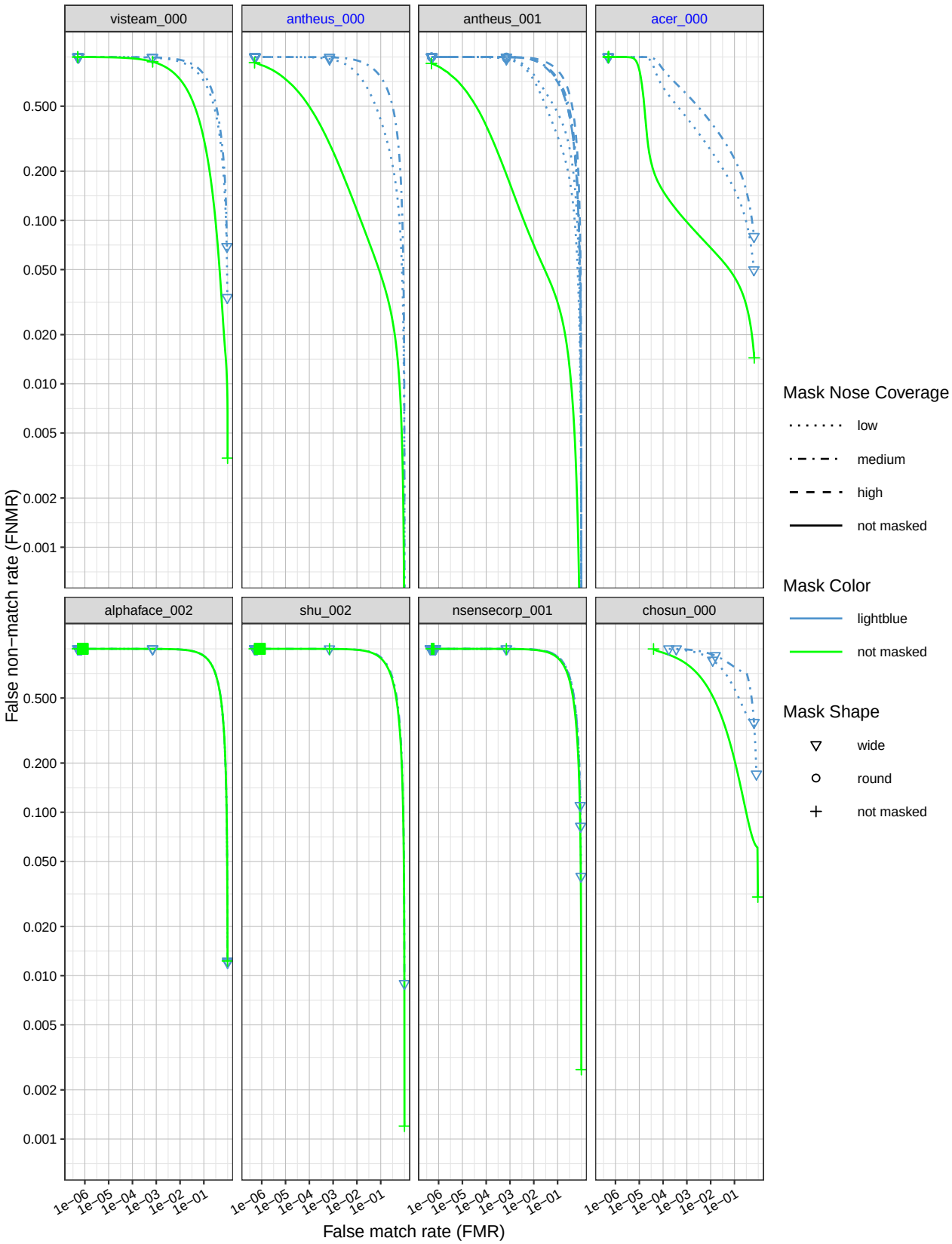


*Figure 23: DET curves showing error rates on unmasked and masked probe images, broken out by mask shape and nose coverage. Algorithms in black were submitted prior to mid-March 2020, and algorithms in blue were submitted thereafter.*



FNMR(T) "False non-match rate"
FMR(T) "False match rate"

The following plots are detection error tradeoff (DET) characteristics for each algorithm, across different mask colors.



FNMR(T) "False non-match rate"
FMR(T) "False match rate"

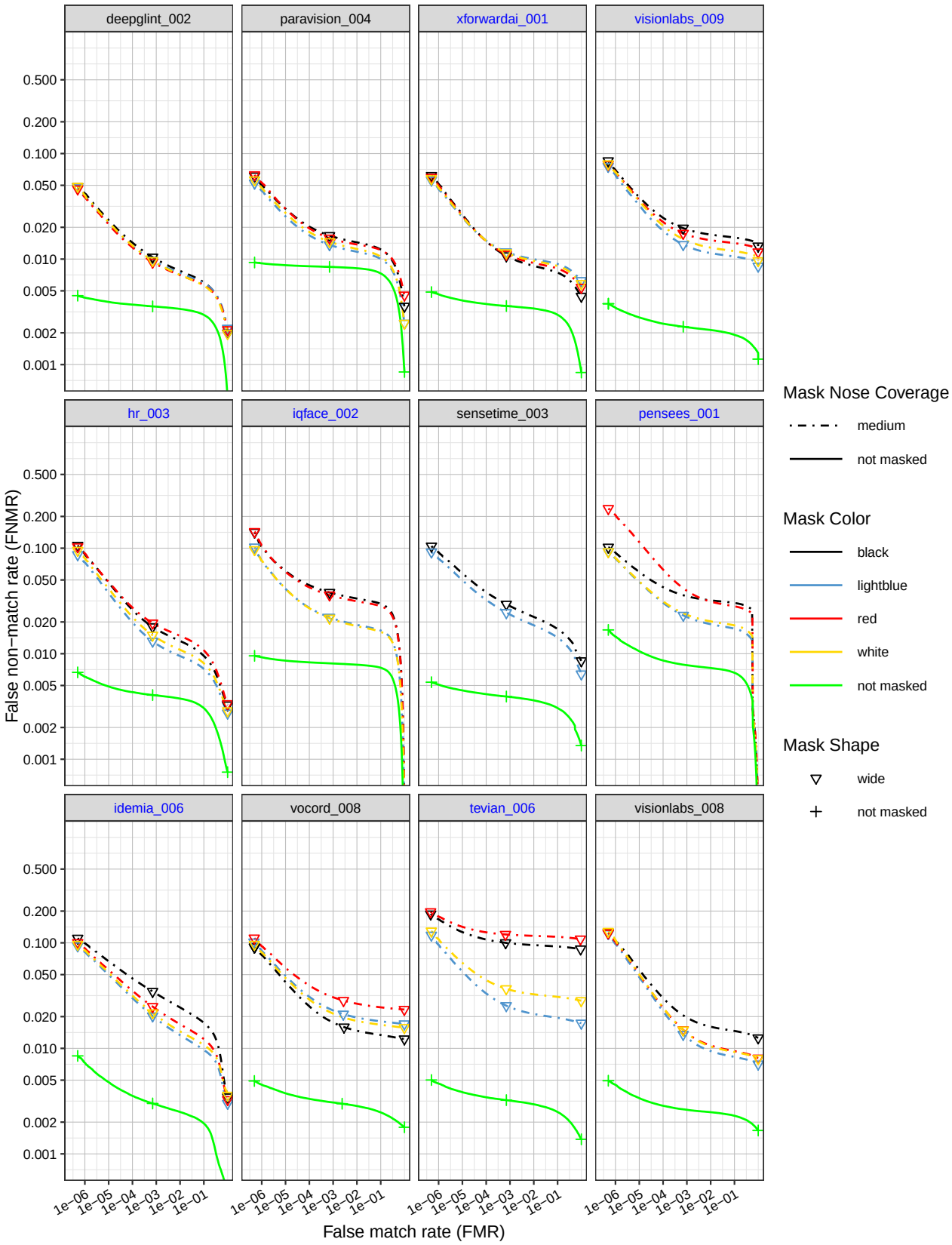


*Figure 24: DET curves showing error rates on unmasked and masked probe images, broken out by mask color. Algorithms in black were submitted prior to mid-March 2020, and algorithms in blue were submitted thereafter.*



FNMR(T) "False non-match rate"
FMR(T) "False match rate"

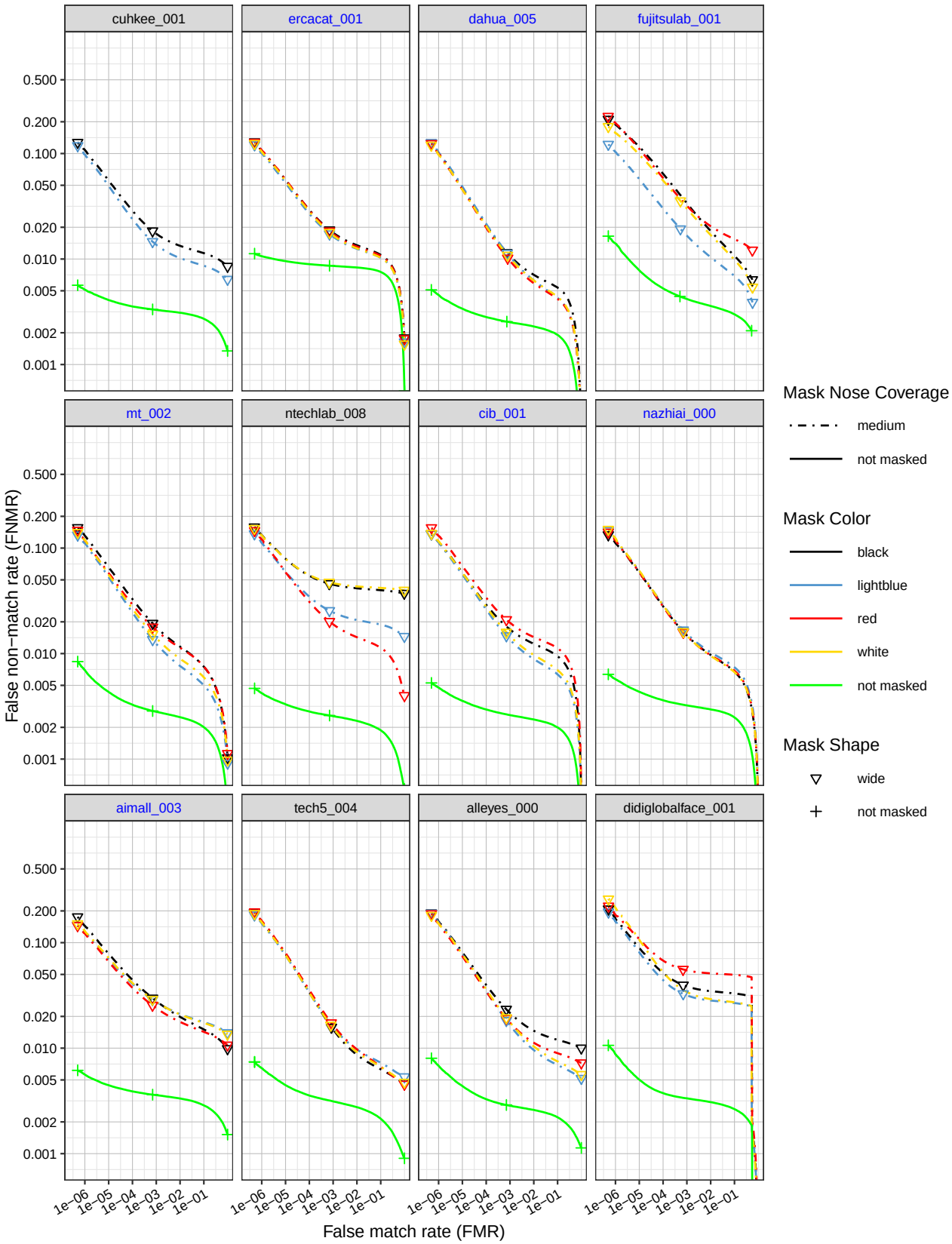


*Figure 25: DET curves showing error rates on unmasked and masked probe images, broken out by mask color. Algorithms in black were submitted prior to mid-March 2020, and algorithms in blue were submitted thereafter.*



FNMR(T) "False non-match rate"
FMR(T) "False match rate"

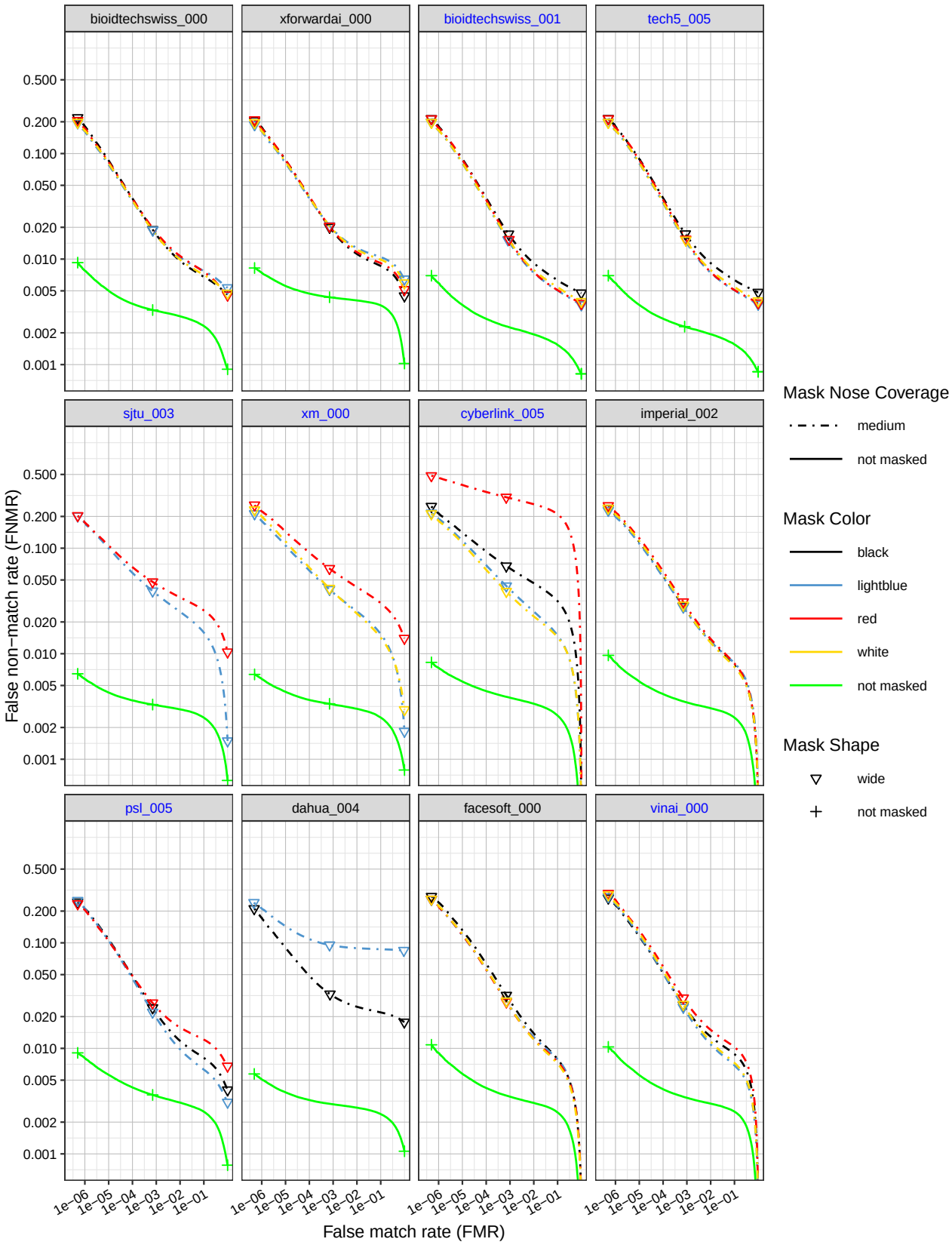


*Figure 26: DET curves showing error rates on unmasked and masked probe images, broken out by mask color. Algorithms in black were submitted prior to mid-March 2020, and algorithms in blue were submitted thereafter.*



FNMR(T) "False non-match rate"
FMR(T) "False match rate"

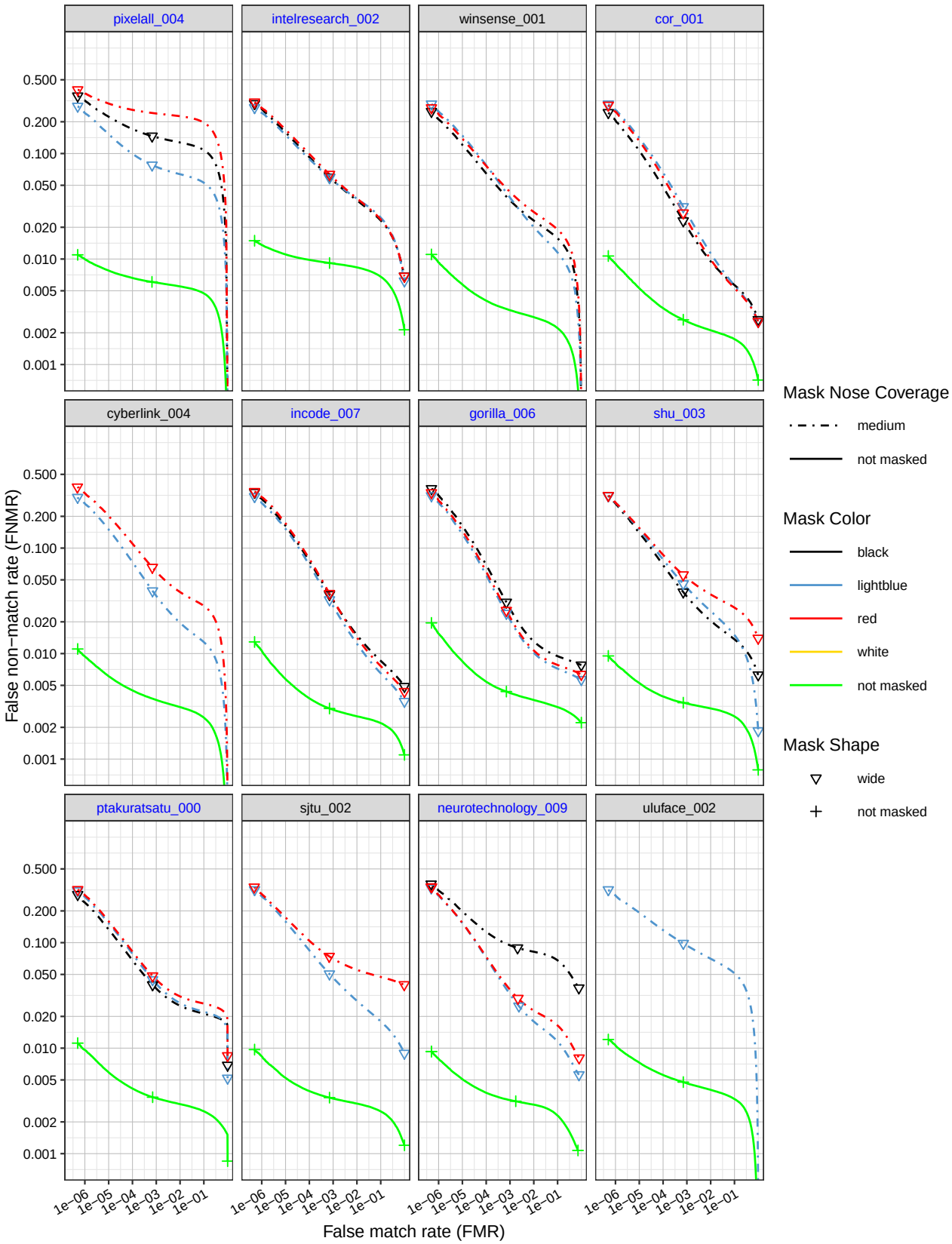


*Figure 27: DET curves showing error rates on unmasked and masked probe images, broken out by mask color. Algorithms in black were submitted prior to mid-March 2020, and algorithms in blue were submitted thereafter.*



FNMR(T) "False non-match rate"
FMR(T) "False match rate"

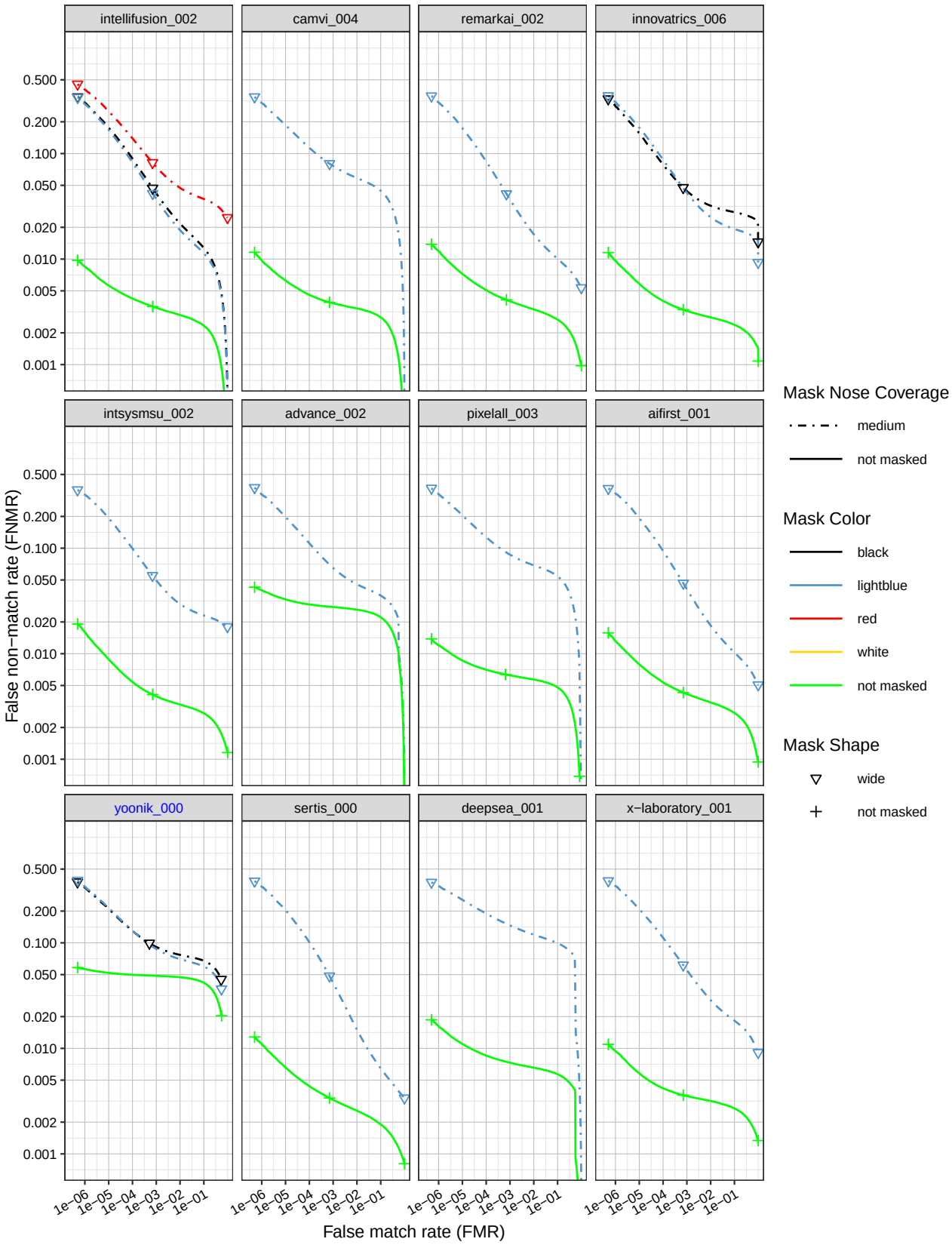


*Figure 28: DET curves showing error rates on unmasked and masked probe images, broken out by mask color. Algorithms in black were submitted prior to mid-March 2020, and algorithms in blue were submitted thereafter.*



FNMR(T) "False non-match rate"
FMR(T) "False match rate"

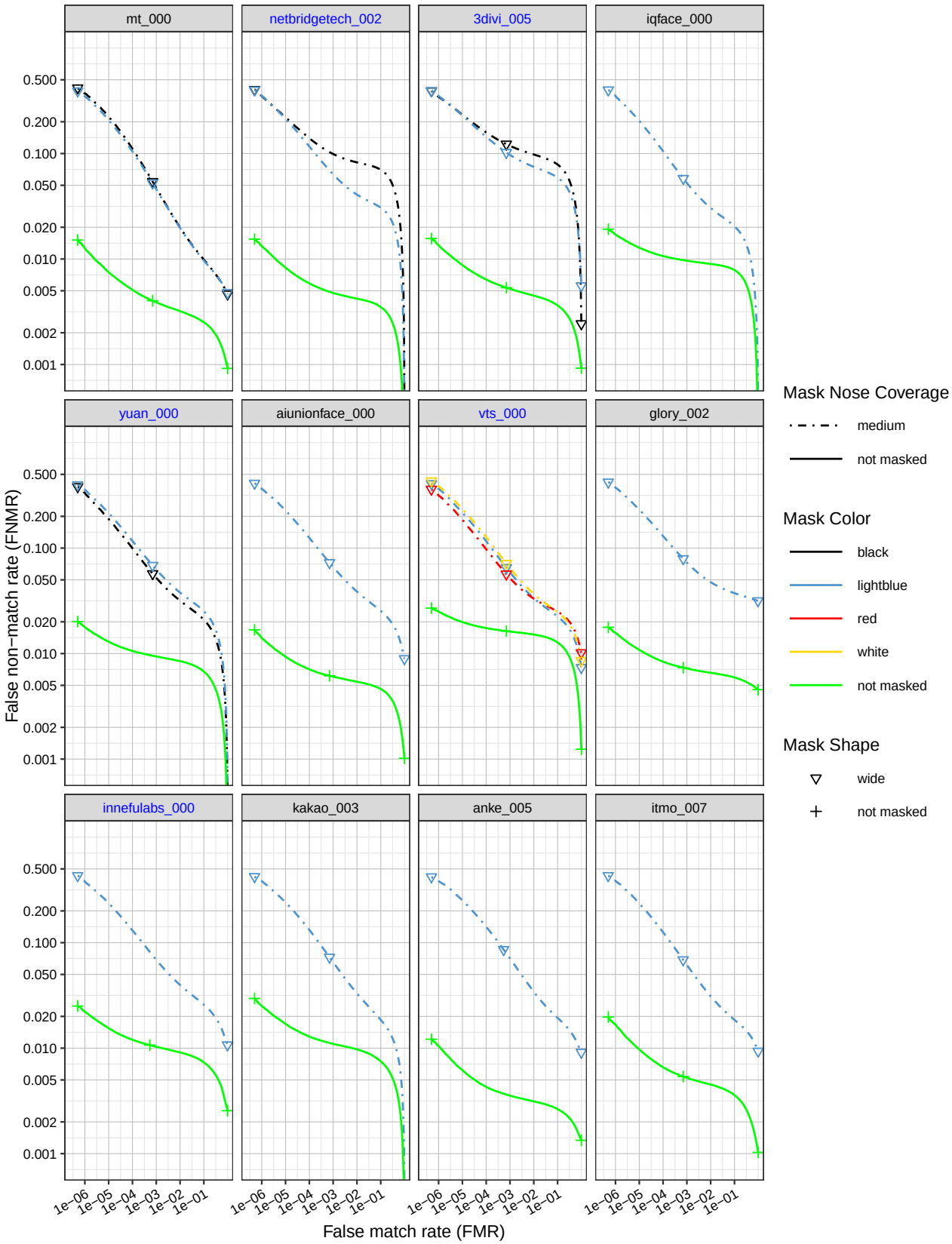


*Figure 29: DET curves showing error rates on unmasked and masked probe images, broken out by mask color. Algorithms in black were submitted prior to mid-March 2020, and algorithms in blue were submitted thereafter.*



FNMR(T) "False non-match rate"
FMR(T) "False match rate"

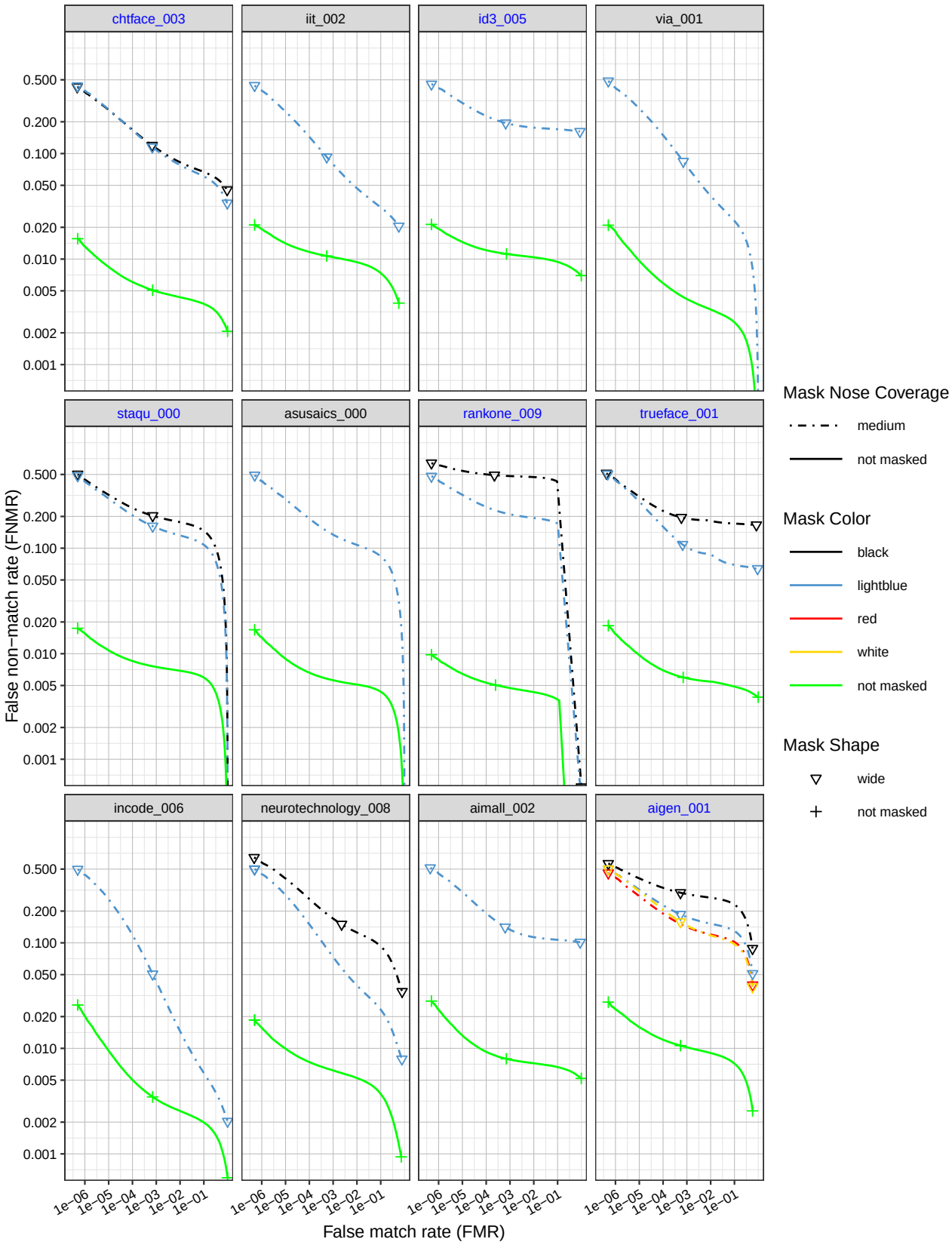


*Figure 30: DET curves showing error rates on unmasked and masked probe images, broken out by mask color. Algorithms in black were submitted prior to mid-March 2020, and algorithms in blue were submitted thereafter.*



FNMR(T) "False non-match rate"
FMR(T) "False match rate"

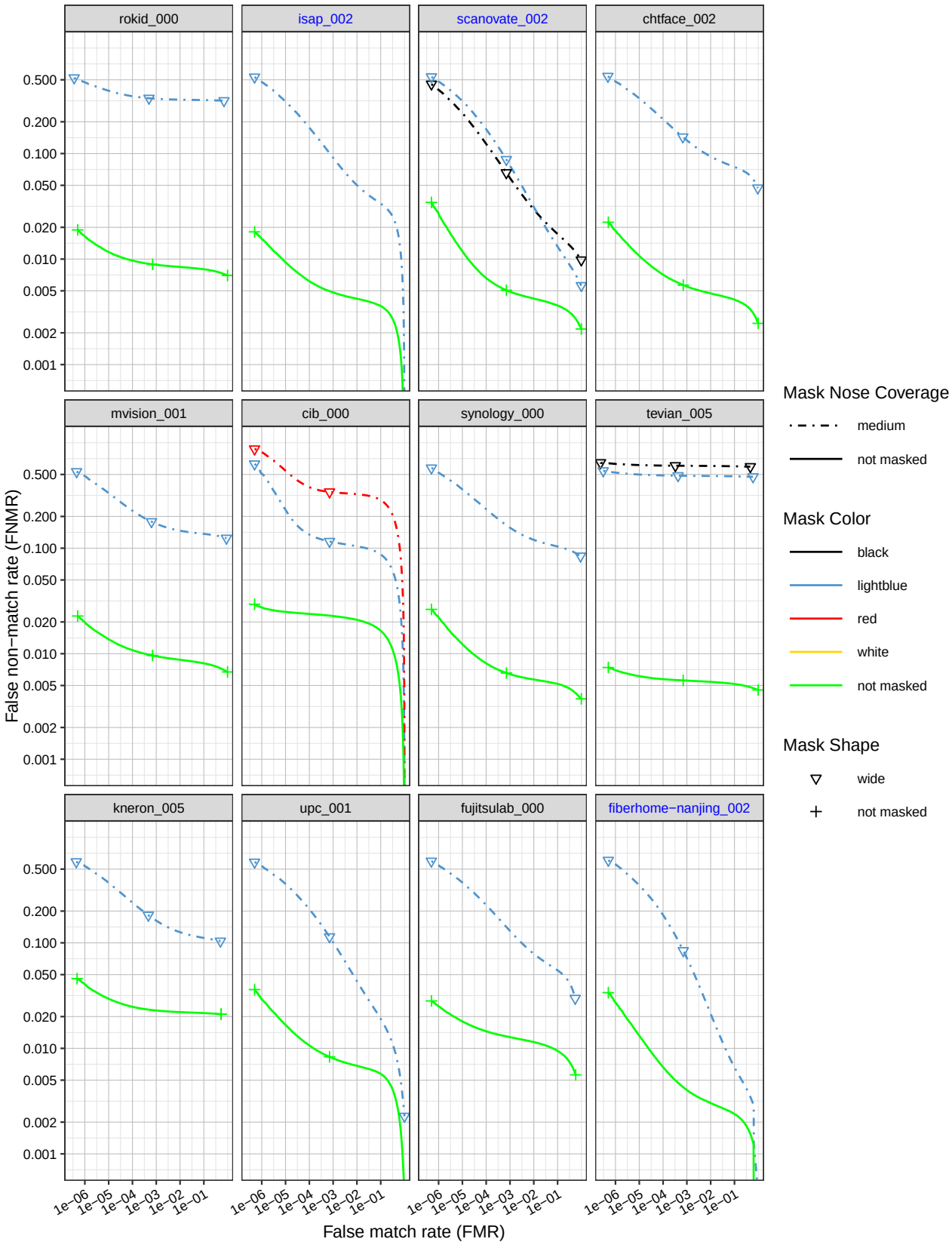


*Figure 31: DET curves showing error rates on unmasked and masked probe images, broken out by mask color. Algorithms in black were submitted prior to mid-March 2020, and algorithms in blue were submitted thereafter.*



FNMR(T) "False non-match rate"
FMR(T) "False match rate"

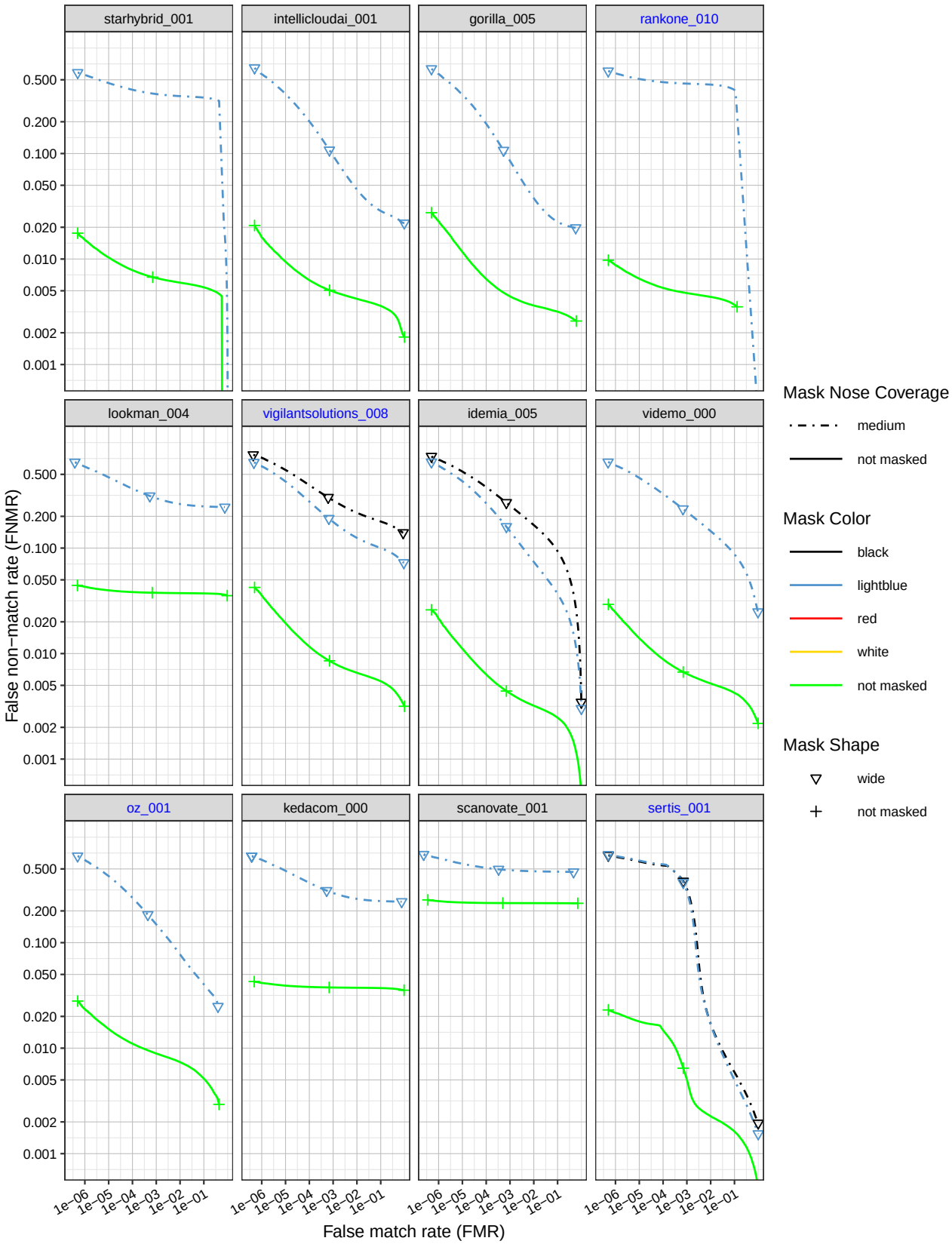


*Figure 32: DET curves showing error rates on unmasked and masked probe images, broken out by mask color. Algorithms in black were submitted prior to mid-March 2020, and algorithms in blue were submitted thereafter.*



FNMR(T) "False non-match rate"
FMR(T) "False match rate"

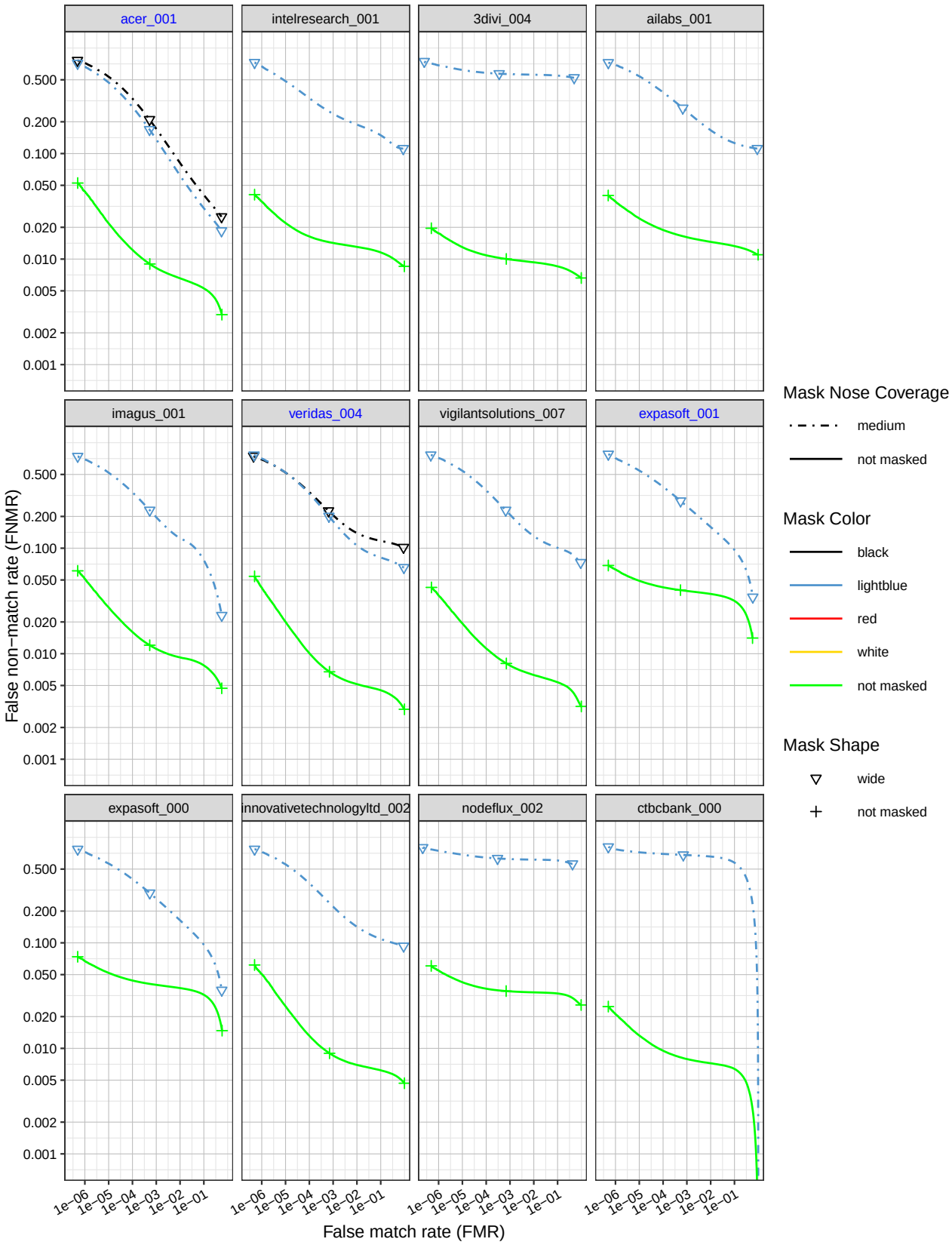


*Figure 33: DET curves showing error rates on unmasked and masked probe images, broken out by mask color. Algorithms in black were submitted prior to mid-March 2020, and algorithms in blue were submitted thereafter.*



FNMR(T) "False non-match rate"
FMR(T) "False match rate"

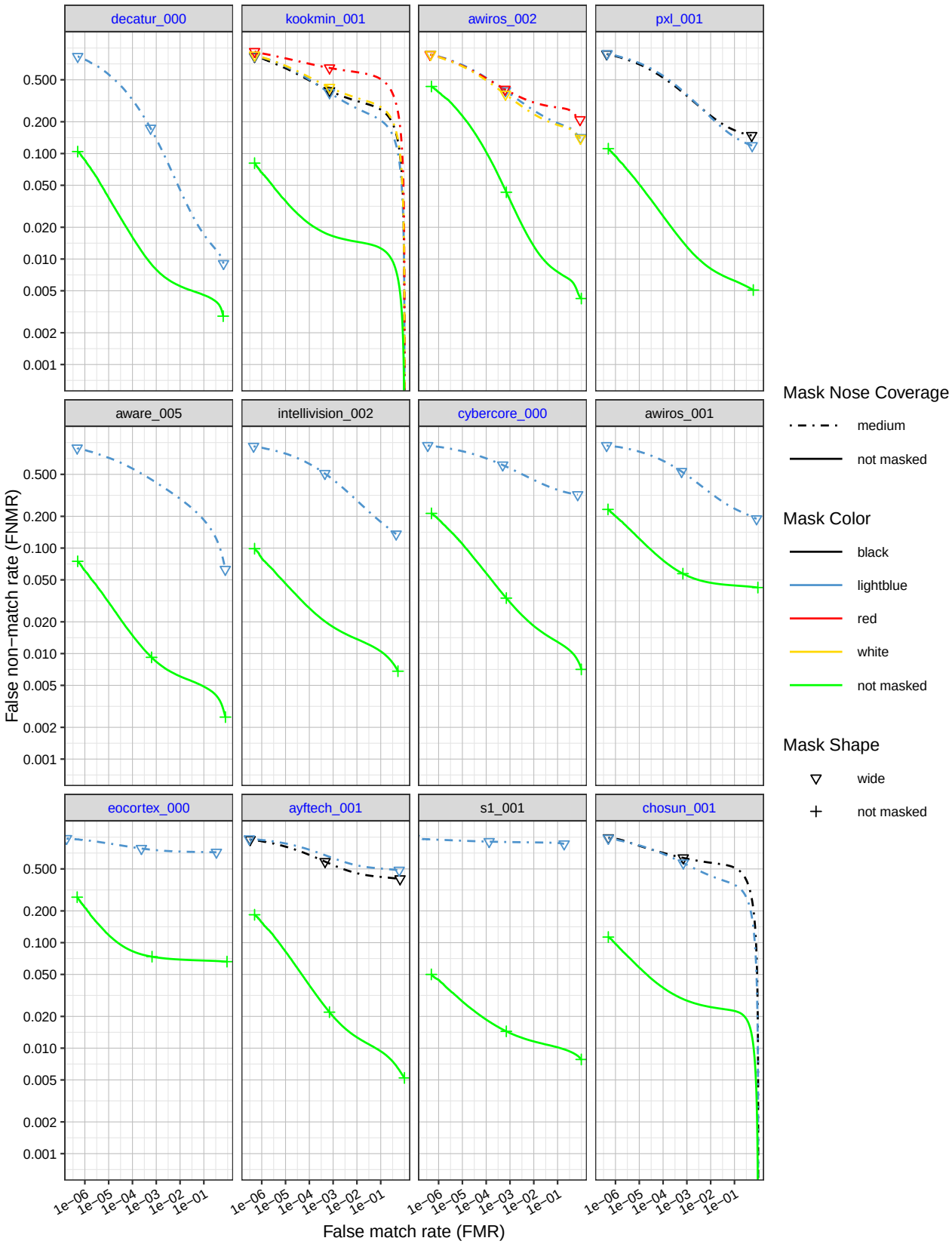


*Figure 34: DET curves showing error rates on unmasked and masked probe images, broken out by mask color. Algorithms in black were submitted prior to mid-March 2020, and algorithms in blue were submitted thereafter.*



FNMR(T) "False non-match rate"
FMR(T) "False match rate"

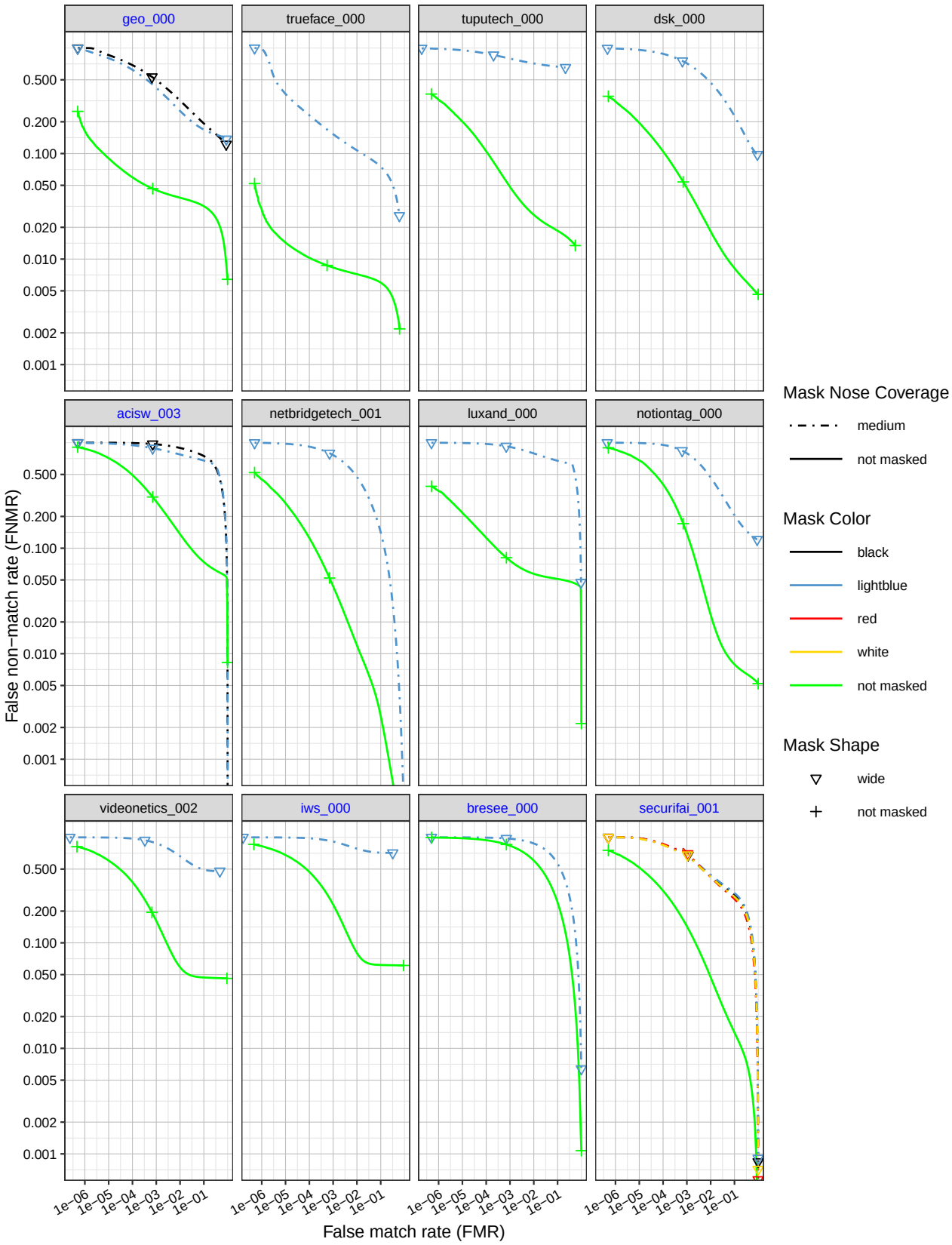


*Figure 35: DET curves showing error rates on unmasked and masked probe images, broken out by mask color. Algorithms in black were submitted prior to mid-March 2020, and algorithms in blue were submitted thereafter.*



FNMR(T) "False non-match rate"
FMR(T) "False match rate"

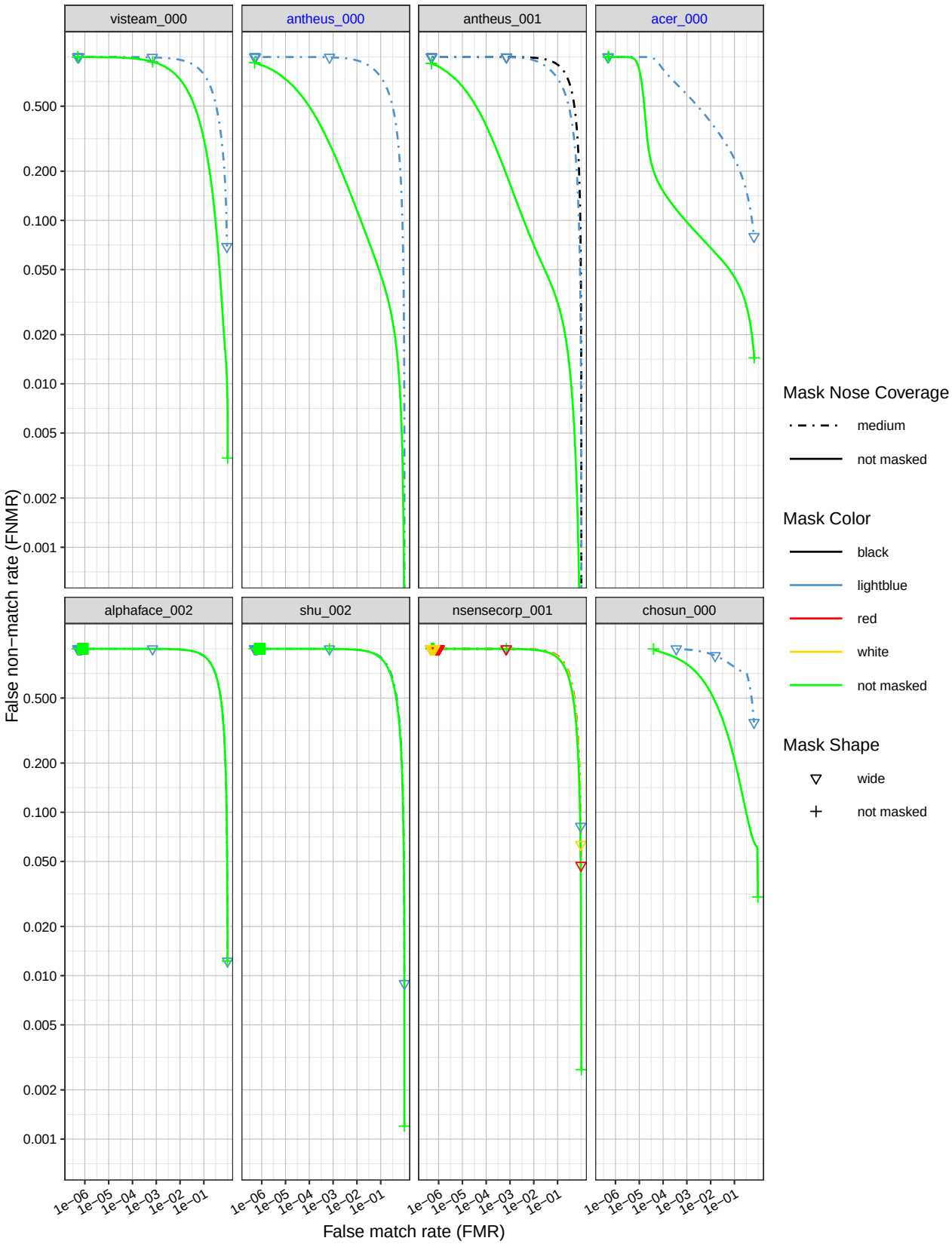


*Figure 36: DET curves showing error rates on unmasked and masked probe images, broken out by mask color. Algorithms in black were submitted prior to mid-March 2020, and algorithms in blue were submitted thereafter.*



FNMR(T) "False non-match rate"
FMR(T) "False match rate"

The following plots show the explicit dependence of false non-match rate (FNMR) and false match rate (FMR) on score threshold for each algorithm, across different masked/unmasked combinations.



FNMR(T) "False non-match rate"
FMR(T) "False match rate"

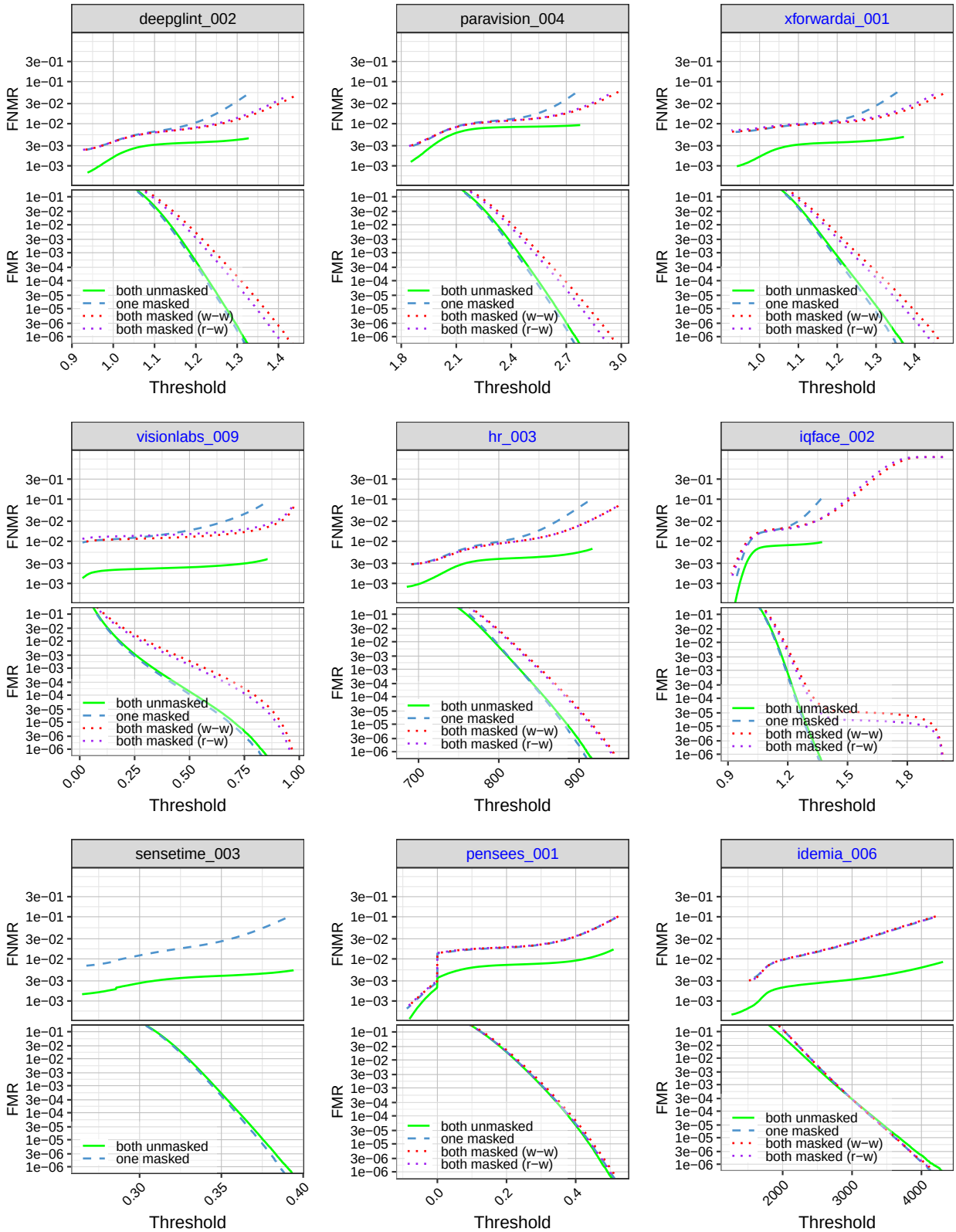


*Figure 37: FNMR and FMR calibration curves on unmasked-to-unmasked (both unmasked), masked-to-unmasked with medium, wide, lightblue masks (one masked), masked-to-masked with medium, wide, lightblue masks (both masked (w-w)), and masked-to-masked with medium, round, white masks (enrollment image) and medium, wide, lightblue masks (verification image) (both masked (r-w)). Algorithms in black were submitted prior to mid-March 2020, and algorithms in blue were submitted thereafter.*



FNMR(T) "False non-match rate"
FMR(T) "False match rate"

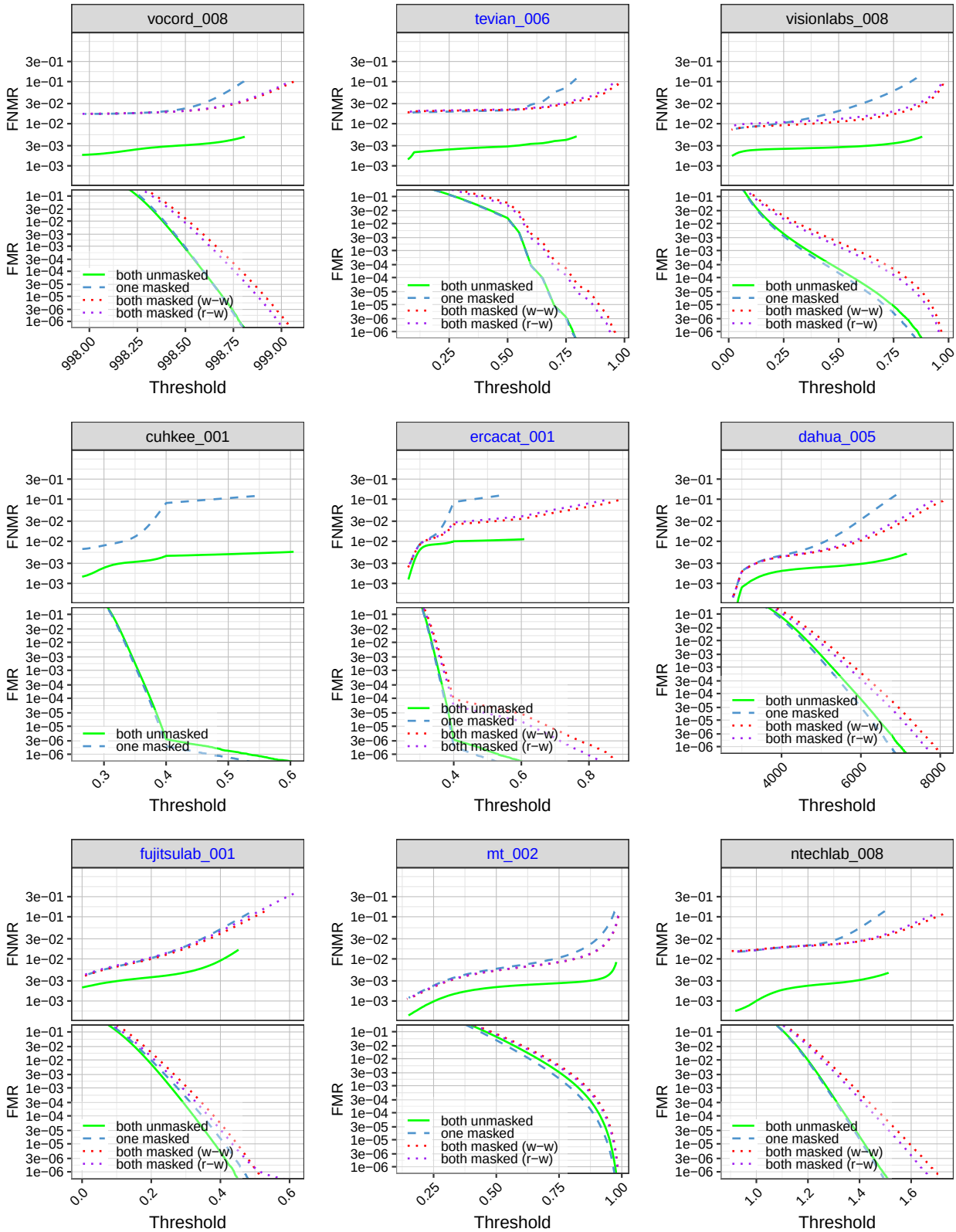


*Figure 38: FNMR and FMR calibration curves on unmasked-to-unmasked (both unmasked), masked-to-unmasked with medium, wide, lightblue masks (one masked), masked-to-masked with medium, wide, lightblue masks (both masked (w-w)), and masked-to-masked with medium, round, white masks (enrollment image) and medium, wide, lightblue masks (verification image) (both masked (r-w)). Algorithms in black were submitted prior to mid-March 2020, and algorithms in blue were submitted thereafter.*



FNMR(T) "False non-match rate"
FMR(T) "False match rate"

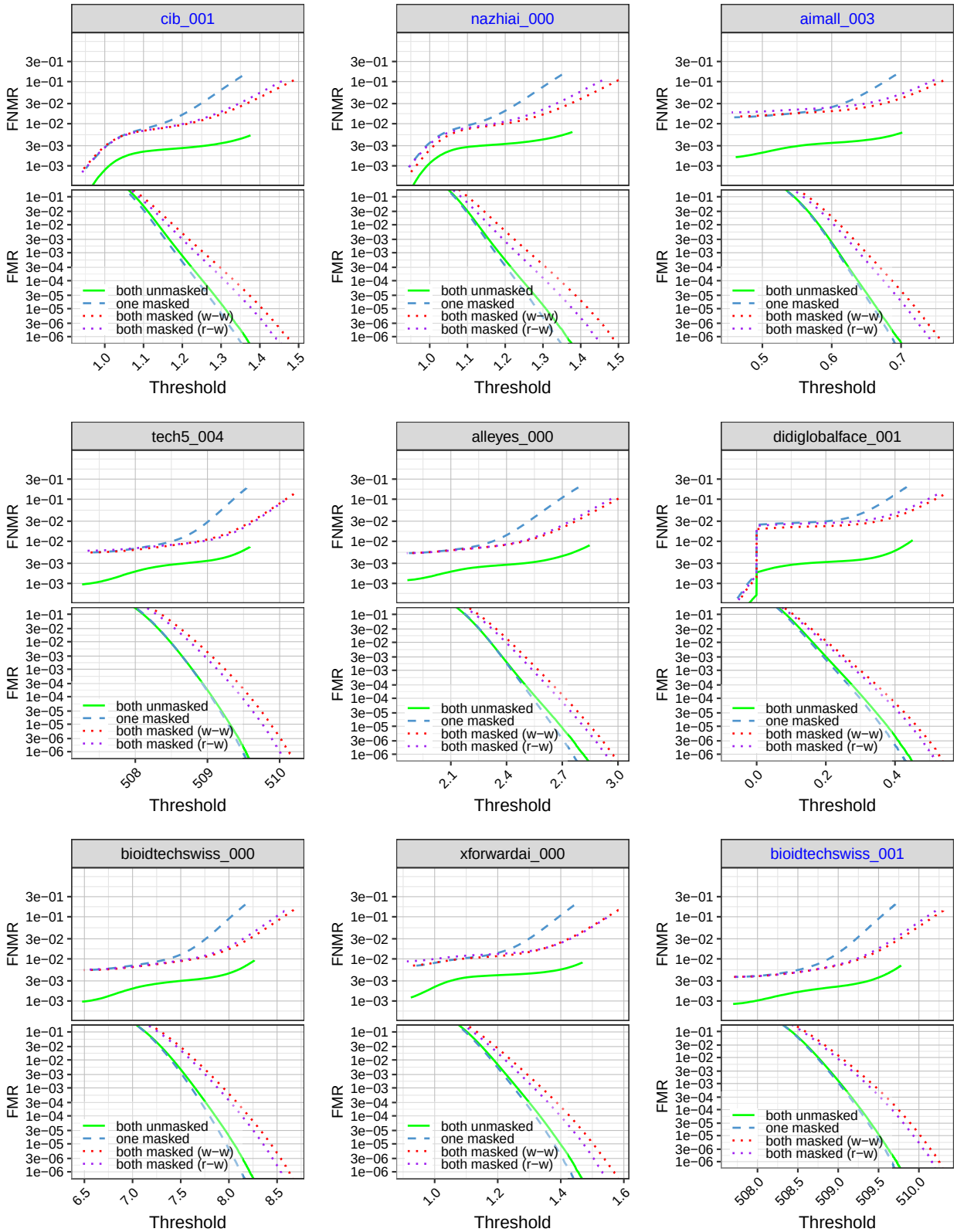


*Figure 39: FNMR and FMR calibration curves on unmasked-to-unmasked (both unmasked), masked-to-unmasked with medium, wide, lightblue masks (one masked), masked-to-masked with medium, wide, lightblue masks (both masked (w-w)), and masked-to-masked with medium, round, white masks (enrollment image) and medium, wide, lightblue masks (verification image) (both masked (r-w)). Algorithms in black were submitted prior to mid-March 2020, and algorithms in blue were submitted thereafter.*



FNMR(T) "False non-match rate"
FMR(T) "False match rate"

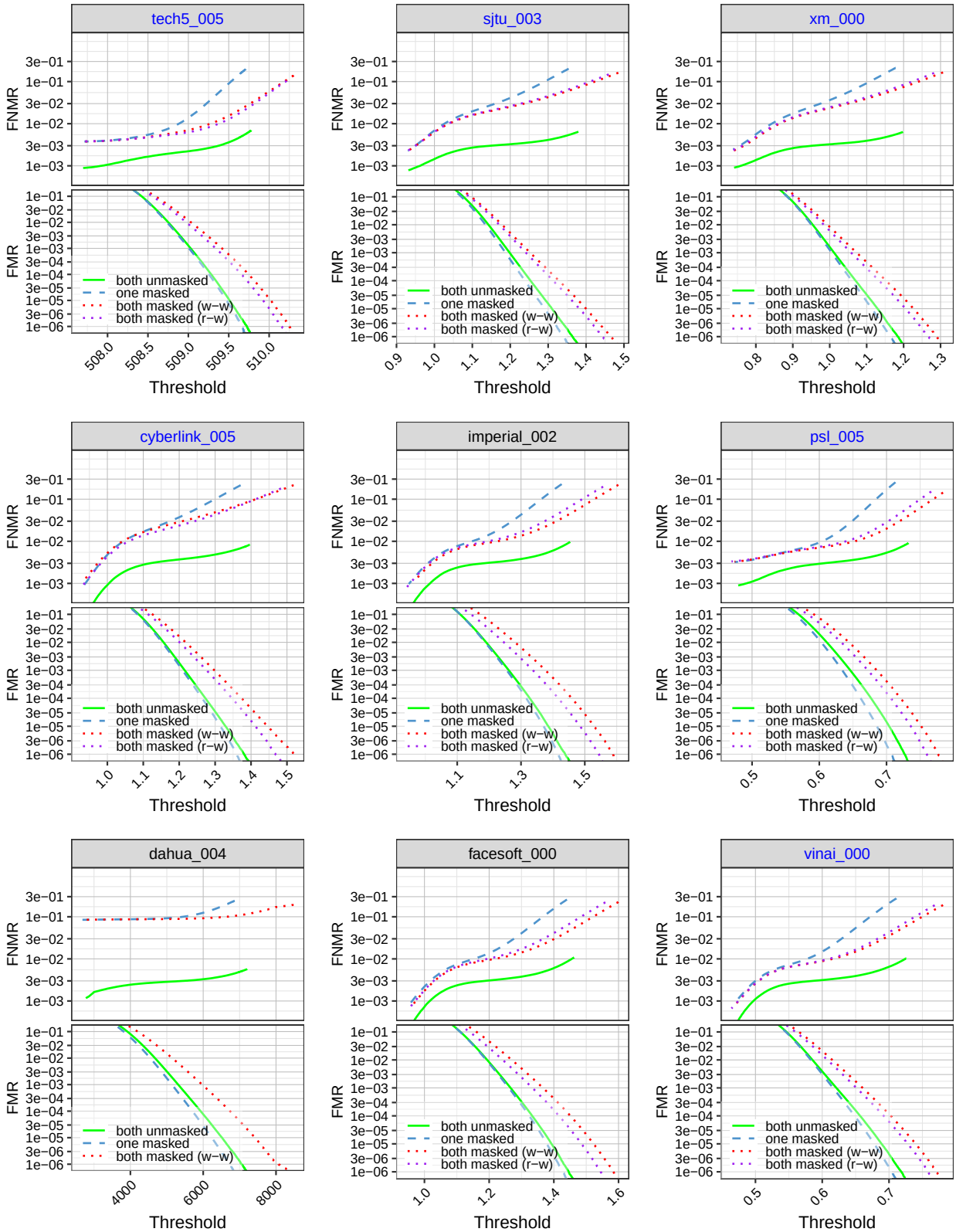


*Figure 40: FNMR and FMR calibration curves on unmasked-to-unmasked (both unmasked), masked-to-unmasked with medium, wide, lightblue masks (one masked), masked-to-masked with medium, wide, lightblue masks (both masked (w-w)), and masked-to-masked with medium, round, white masks (enrollment image) and medium, wide, lightblue masks (verification image) (both masked (r-w)). Algorithms in black were submitted prior to mid-March 2020, and algorithms in blue were submitted thereafter.*



FNMR(T) "False non-match rate"
FMR(T) "False match rate"

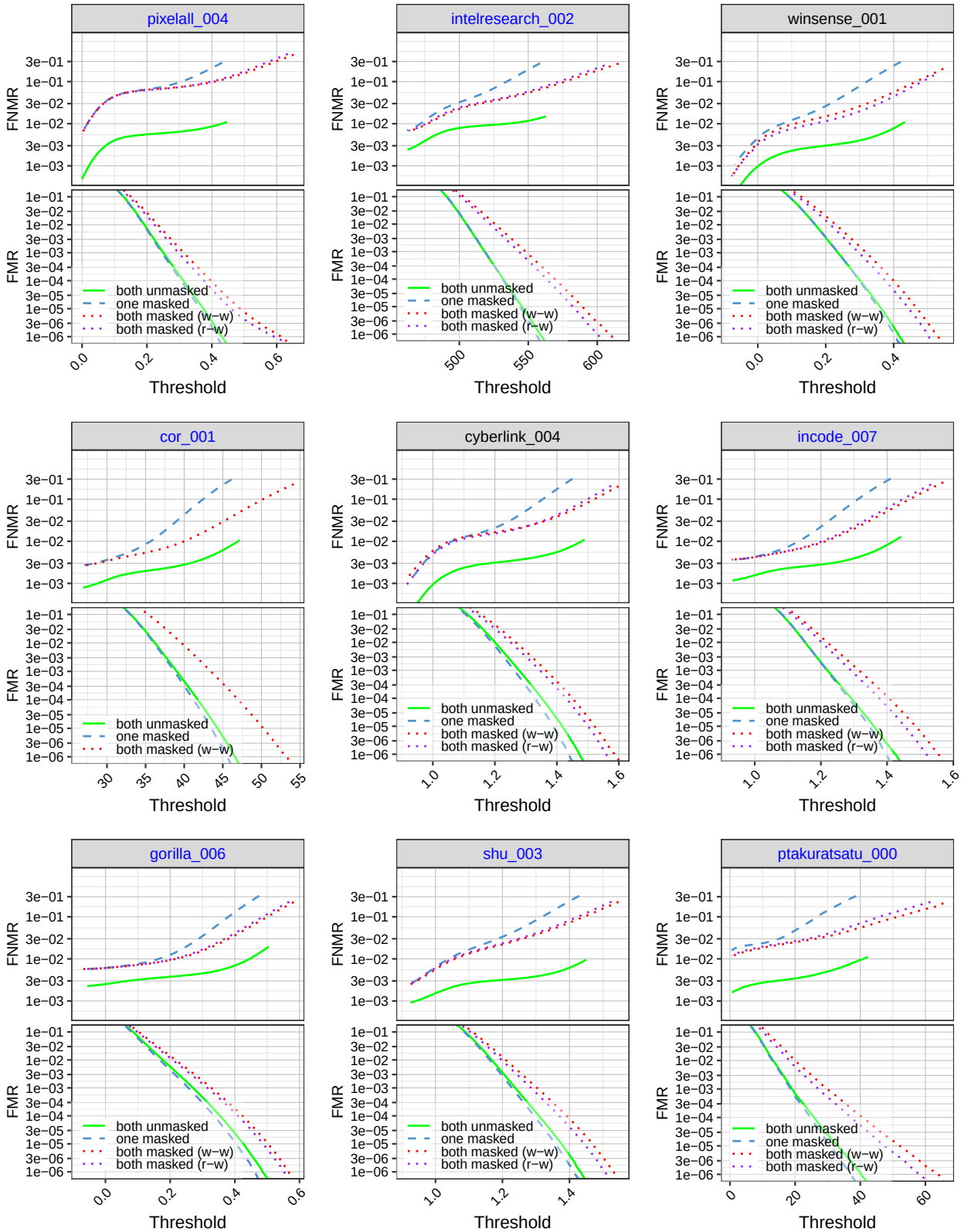


*Figure 41: FNMR and FMR calibration curves on unmasked-to-unmasked (both unmasked), masked-to-unmasked with medium, wide, lightblue masks (one masked), masked-to-masked with medium, wide, lightblue masks (both masked (w-w)), and masked-to-masked with medium, round, white masks (enrollment image) and medium, wide, lightblue masks (verification image) (both masked (r-w)). Algorithms in black were submitted prior to mid-March 2020, and algorithms in blue were submitted thereafter.*



FNMR(T) "False non-match rate"
FMR(T) "False match rate"

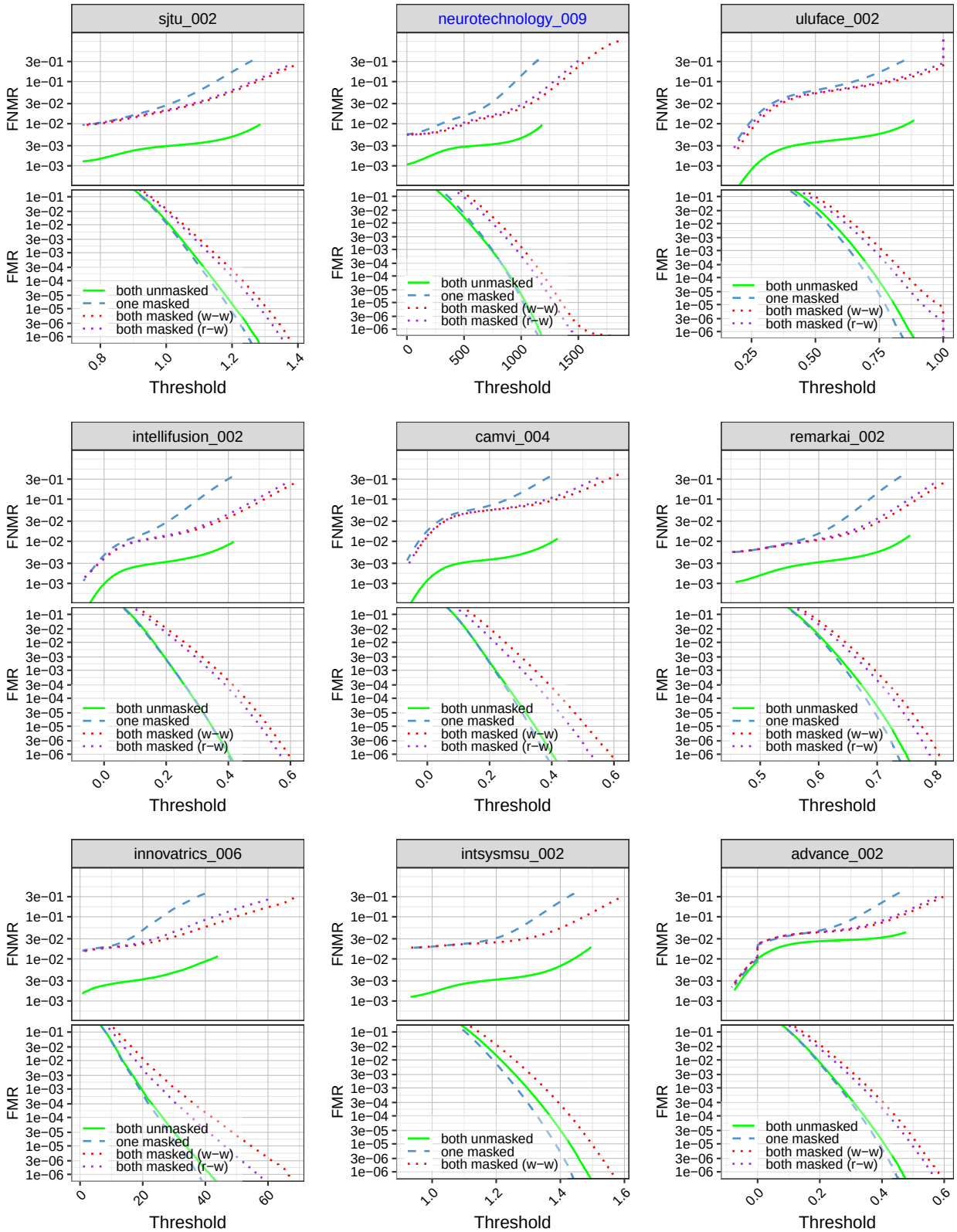


*Figure 42: FNMR and FMR calibration curves on unmasked-to-unmasked (both unmasked), masked-to-unmasked with medium, wide, lightblue masks (one masked), masked-to-masked with medium, wide, lightblue masks (both masked (w-w)), and masked-to-masked with medium, round, white masks (enrollment image) and medium, wide, lightblue masks (verification image) (both masked (r-w)). Algorithms in black were submitted prior to mid-March 2020, and algorithms in blue were submitted thereafter.*



FNMR(T) "False non-match rate"
FMR(T) "False match rate"

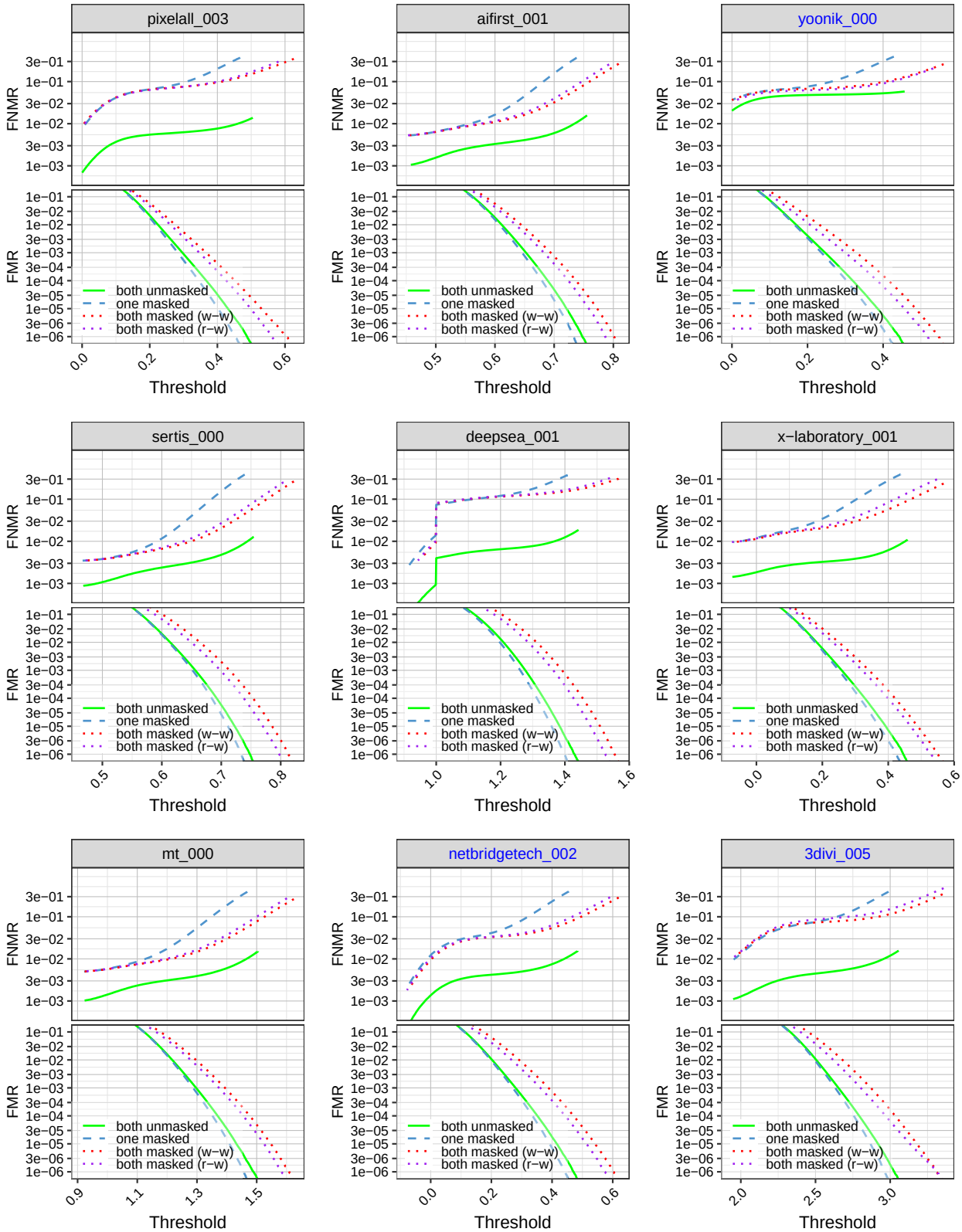


*Figure 43: FNMR and FMR calibration curves on unmasked-to-unmasked (both unmasked), masked-to-unmasked with medium, wide, lightblue masks (one masked), masked-to-masked with medium, wide, lightblue masks (both masked (w-w)), and masked-to-masked with medium, round, white masks (enrollment image) and medium, wide, lightblue masks (verification image) (both masked (r-w)). Algorithms in black were submitted prior to mid-March 2020, and algorithms in blue were submitted thereafter.*



FNMR(T) "False non-match rate"
FMR(T) "False match rate"

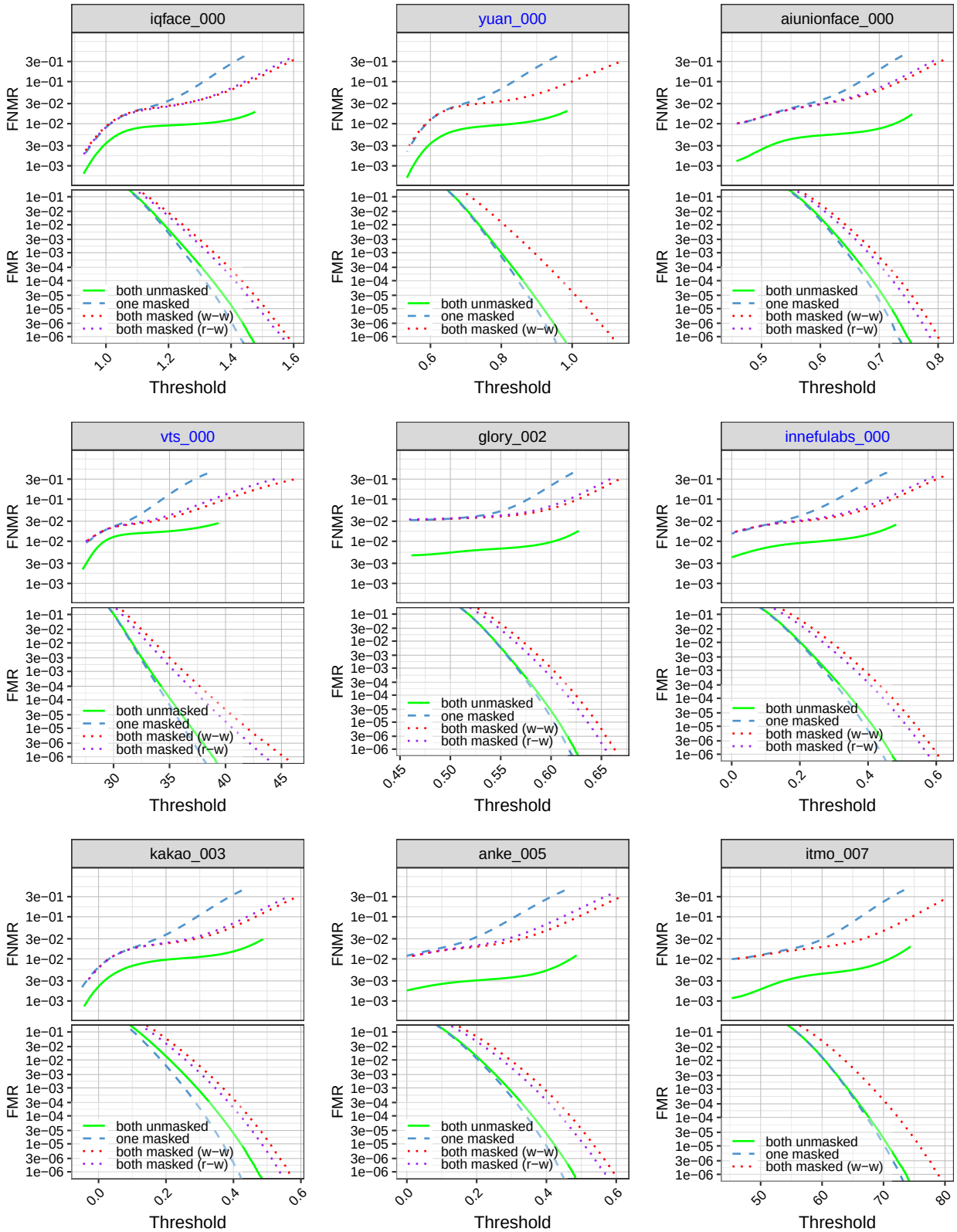


*Figure 44: FNMR and FMR calibration curves on unmasked-to-unmasked (both unmasked), masked-to-unmasked with medium, wide, lightblue masks (one masked), masked-to-masked with medium, wide, lightblue masks (both masked (w-w)), and masked-to-masked with medium, round, white masks (enrollment image) and medium, wide, lightblue masks (verification image) (both masked (r-w)). Algorithms in black were submitted prior to mid-March 2020, and algorithms in blue were submitted thereafter.*

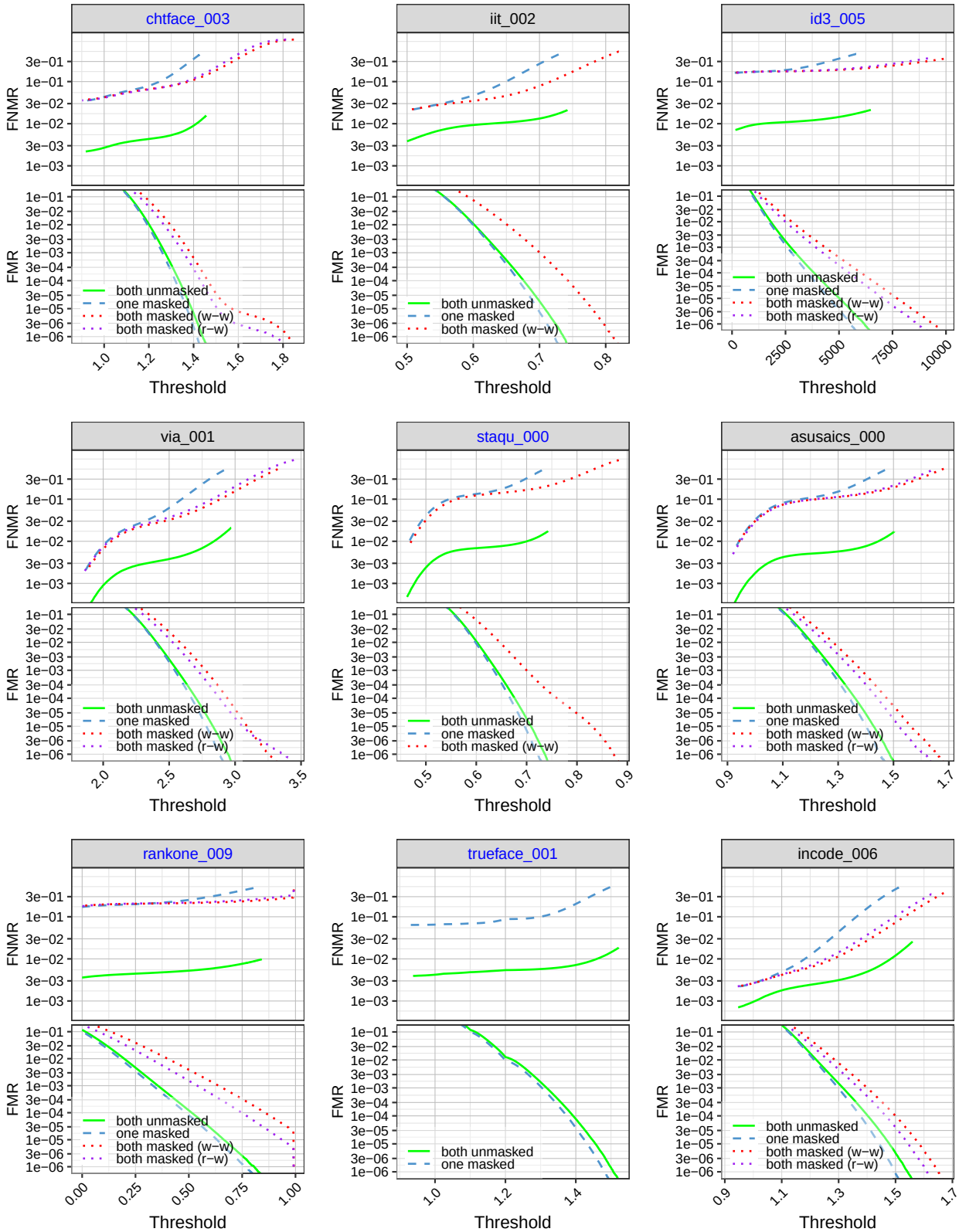


*Figure 45: FNMR and FMR calibration curves on unmasked-to-unmasked (both unmasked), masked-to-unmasked with medium, wide, lightblue masks (one masked), masked-to-masked with medium, wide, lightblue masks (both masked (w-w)), and masked-to-masked with medium, round, white masks (enrollment image) and medium, wide, lightblue masks (verification image) (both masked (r-w)). Algorithms in black were submitted prior to mid-March 2020, and algorithms in blue were submitted thereafter.*



FNMR(T) "False non-match rate"
FMR(T) "False match rate"

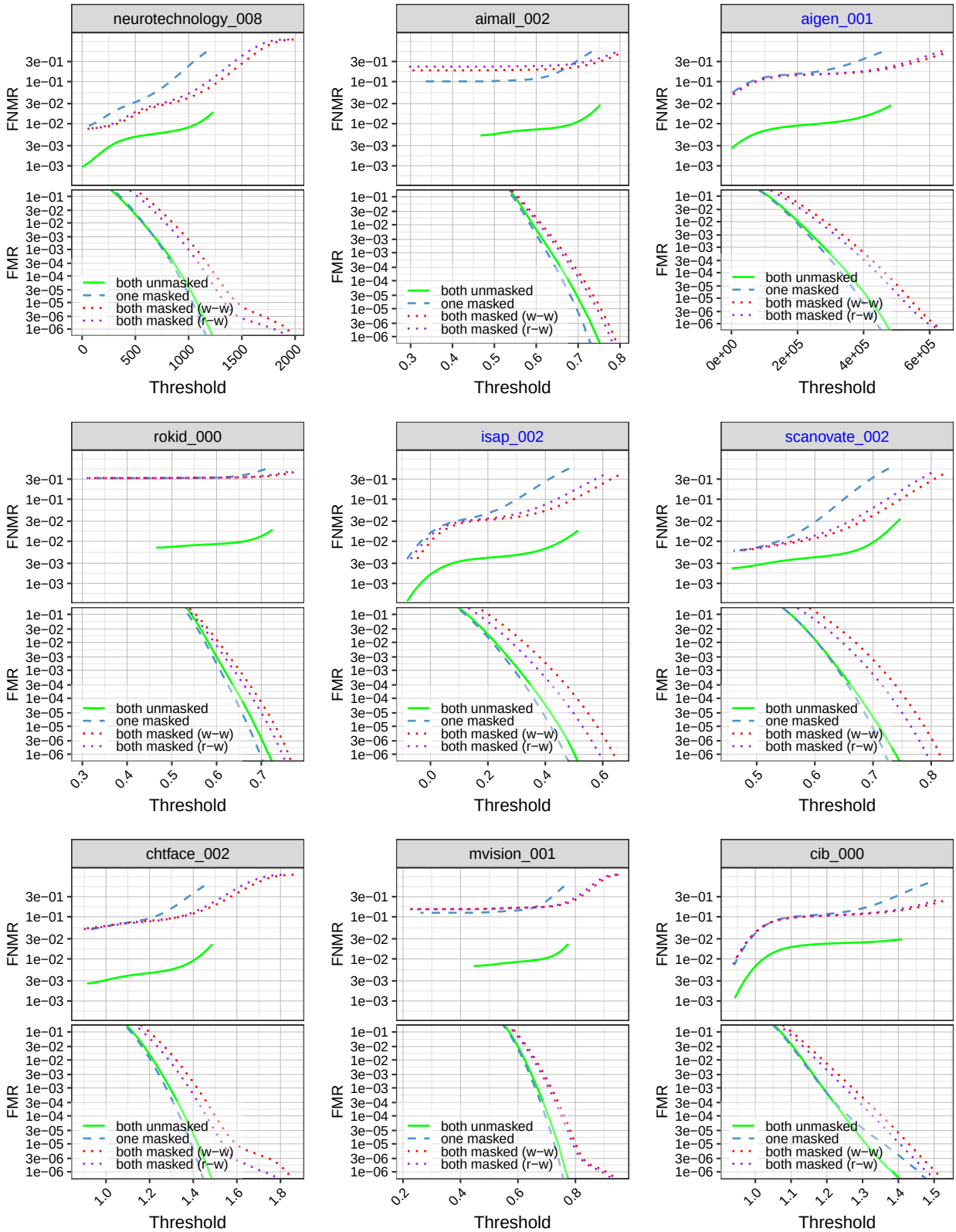


*Figure 46: FNMR and FMR calibration curves on unmasked-to-unmasked (both unmasked), masked-to-unmasked with medium, wide, lightblue masks (one masked), masked-to-masked with medium, wide, lightblue masks (both masked (w-w)), and masked-to-masked with medium, round, white masks (enrollment image) and medium, wide, lightblue masks (verification image) (both masked (r-w)). Algorithms in black were submitted prior to mid-March 2020, and algorithms in blue were submitted thereafter.*



FNMR(T) "False non-match rate"
FMR(T) "False match rate"

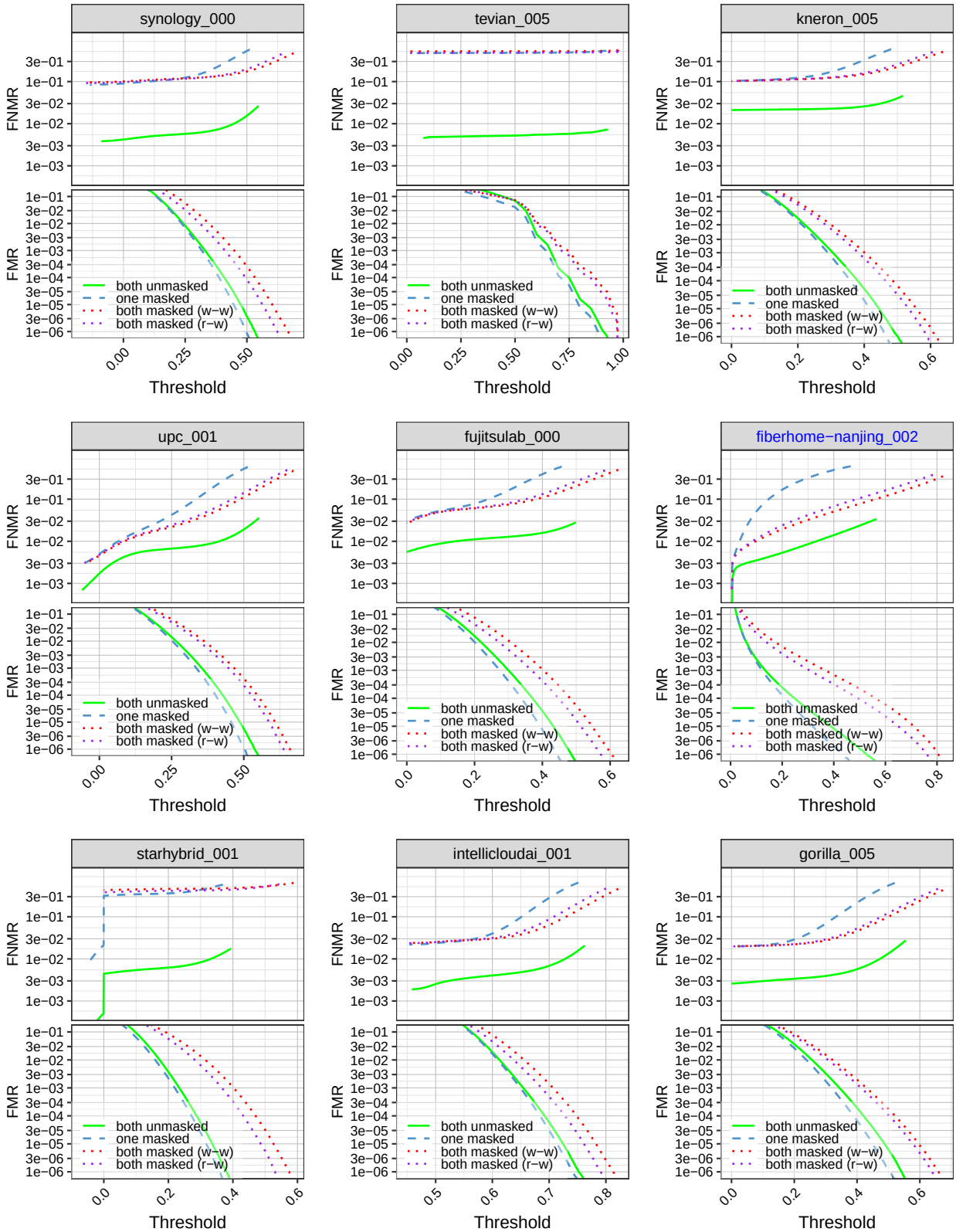


*Figure 47: FNMR and FMR calibration curves on unmasked-to-unmasked (both unmasked), masked-to-unmasked with medium, wide, lightblue masks (one masked), masked-to-masked with medium, wide, lightblue masks (both masked (w-w)), and masked-to-masked with medium, round, white masks (enrollment image) and medium, wide, lightblue masks (verification image) (both masked (r-w)). Algorithms in black were submitted prior to mid-March 2020, and algorithms in blue were submitted thereafter.*



FNMR(T) "False non-match rate"
FMR(T) "False match rate"

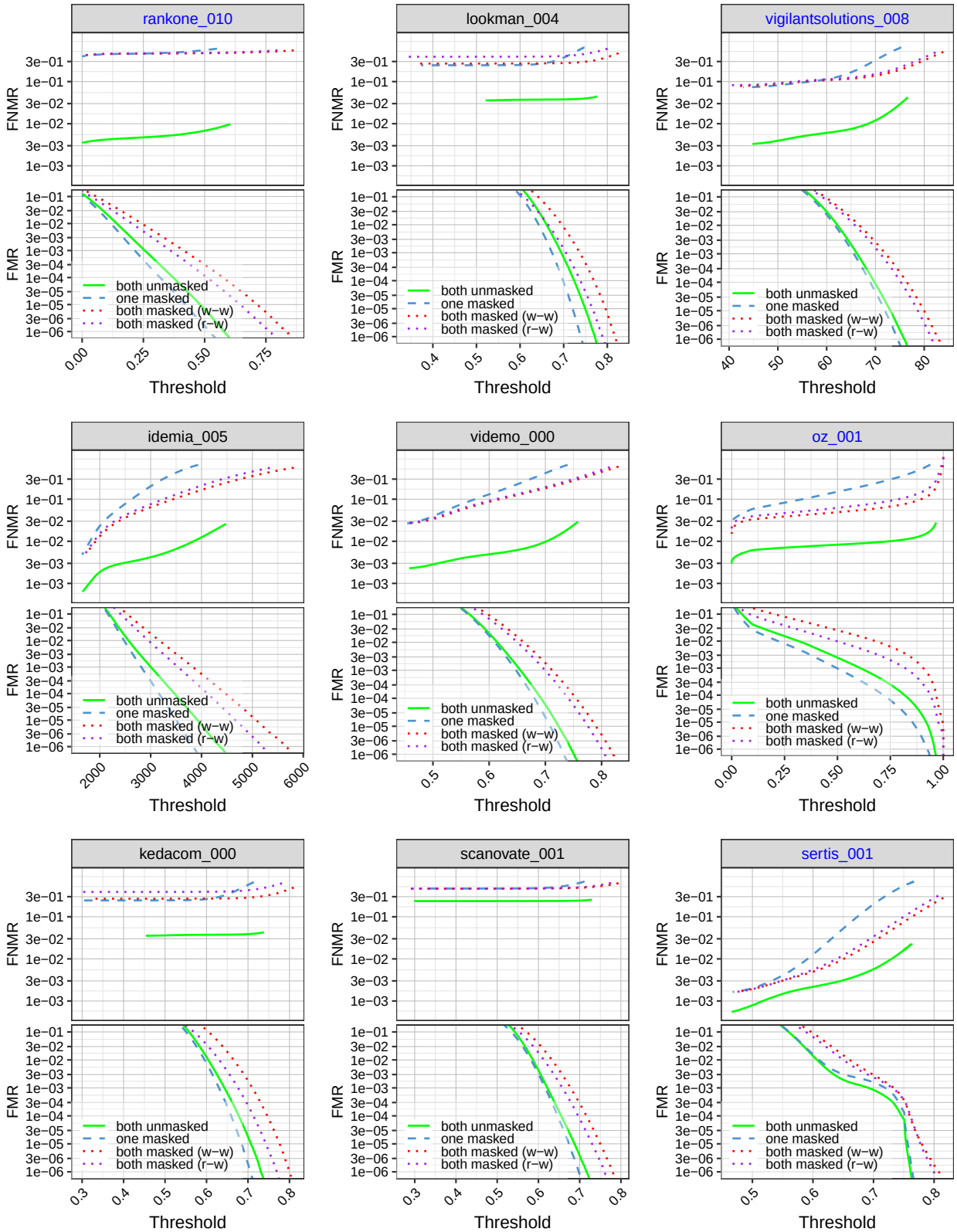


*Figure 48: FNMR and FMR calibration curves on unmasked-to-unmasked (both unmasked), masked-to-unmasked with medium, wide, lightblue masks (one masked), masked-to-masked with medium, wide, lightblue masks (both masked (w-w)), and masked-to-masked with medium, round, white masks (enrollment image) and medium, wide, lightblue masks (verification image) (both masked (r-w)). Algorithms in black were submitted prior to mid-March 2020, and algorithms in blue were submitted thereafter.*

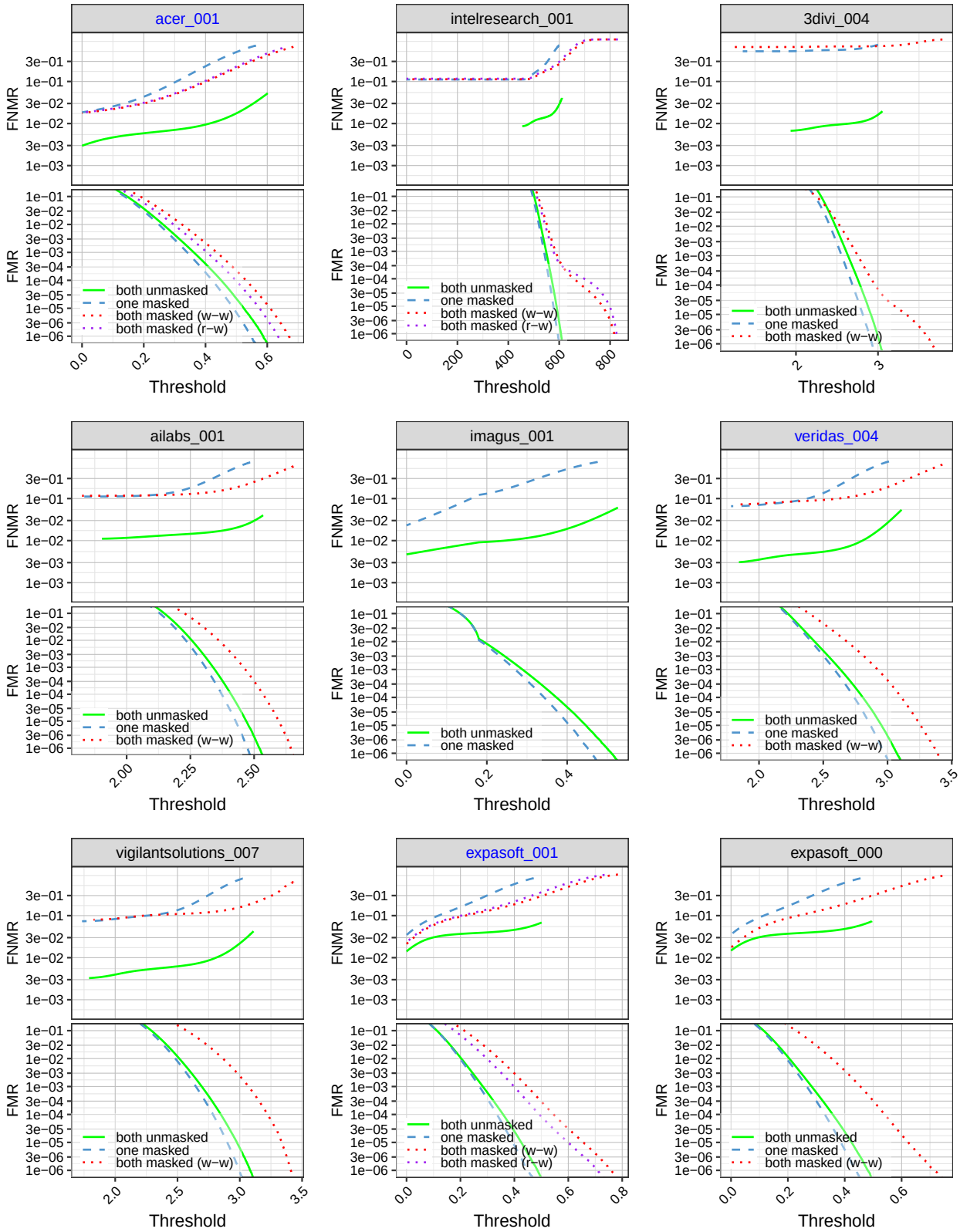


*Figure 49: FNMR and FMR calibration curves on unmasked-to-unmasked (both unmasked), masked-to-unmasked with medium, wide, lightblue masks (one masked), masked-to-masked with medium, wide, lightblue masks (both masked (w-w)), and masked-to-masked with medium, round, white masks (enrollment image) and medium, wide, lightblue masks (verification image) (both masked (r-w)). Algorithms in black were submitted prior to mid-March 2020, and algorithms in blue were submitted thereafter.*



FNMR(T) "False non-match rate"
FMR(T) "False match rate"

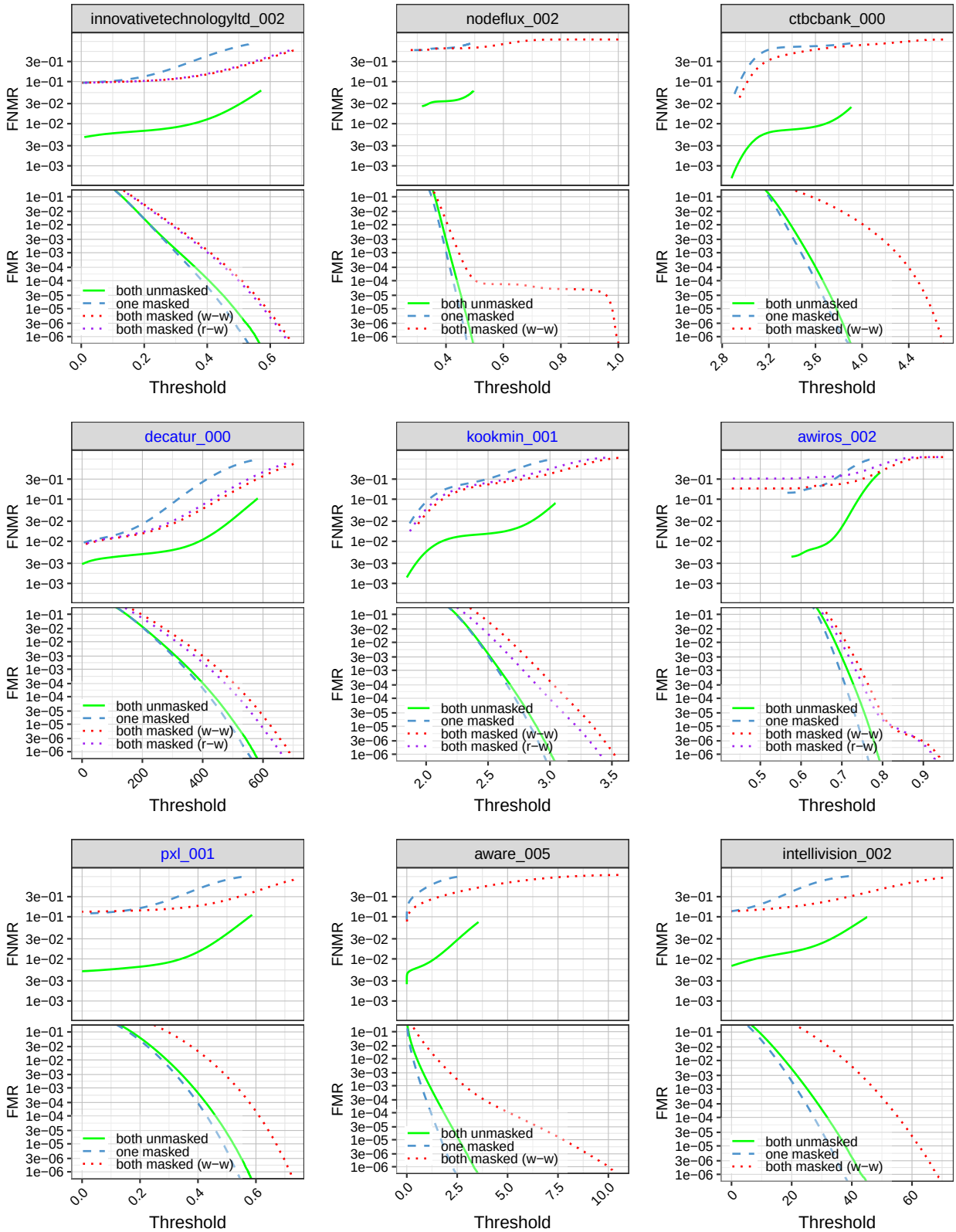


*Figure 50: FNMR and FMR calibration curves on unmasked-to-unmasked (both unmasked), masked-to-unmasked with medium, wide, lightblue masks (one masked), masked-to-masked with medium, wide, lightblue masks (both masked (w-w)), and masked-to-masked with medium, round, white masks (enrollment image) and medium, wide, lightblue masks (verification image) (both masked (r-w)). Algorithms in black were submitted prior to mid-March 2020, and algorithms in blue were submitted thereafter.*



FNMR(T) "False non-match rate"
FMR(T) "False match rate"

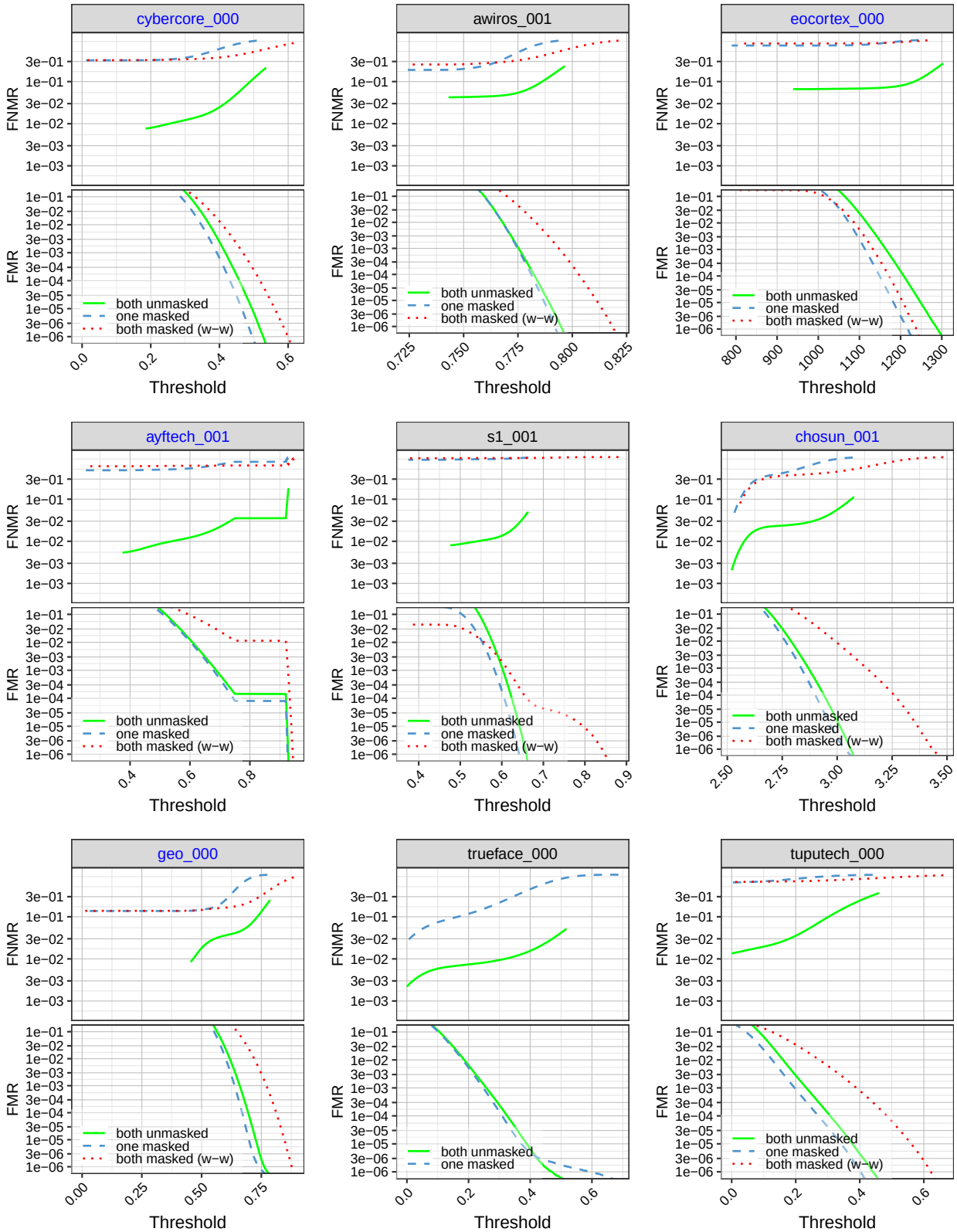


*Figure 51: FNMR and FMR calibration curves on unmasked-to-unmasked (both unmasked), masked-to-unmasked with medium, wide, lightblue masks (one masked), masked-to-masked with medium, wide, lightblue masks (both masked (w-w)), and masked-to-masked with medium, round, white masks (enrollment image) and medium, wide, lightblue masks (verification image) (both masked (r-w)). Algorithms in black were submitted prior to mid-March 2020, and algorithms in blue were submitted thereafter.*



FNMR(T) "False non-match rate"
FMR(T) "False match rate"

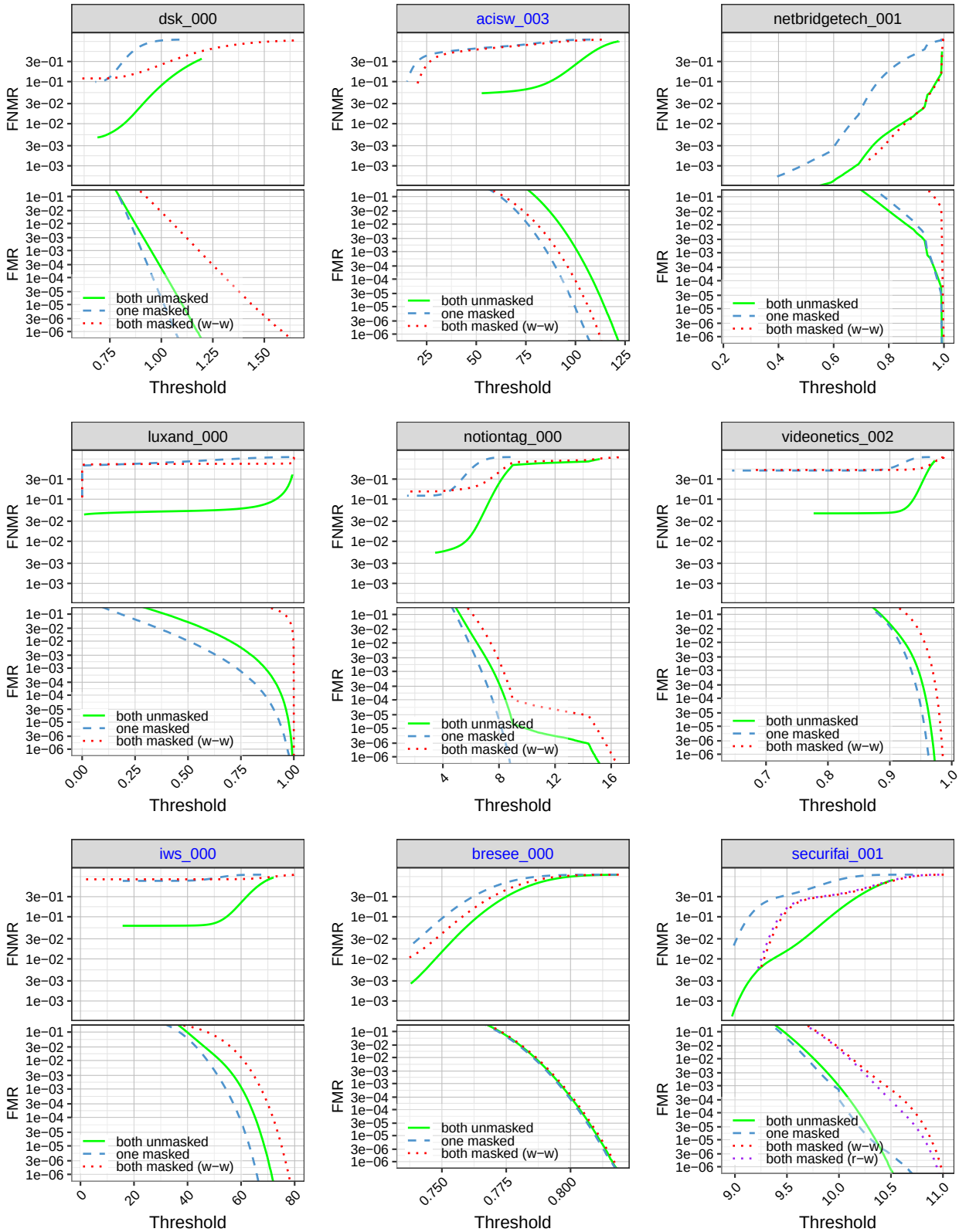


*Figure 52: FNMR and FMR calibration curves on unmasked-to-unmasked (both unmasked), masked-to-unmasked with medium, wide, lightblue masks (one masked), masked-to-masked with medium, wide, lightblue masks (both masked (w-w)), and masked-to-masked with medium, round, white masks (enrollment image) and medium, wide, lightblue masks (verification image) (both masked (r-w)). Algorithms in black were submitted prior to mid-March 2020, and algorithms in blue were submitted thereafter.*



FNMR(T) "False non-match rate"
FMR(T) "False match rate"

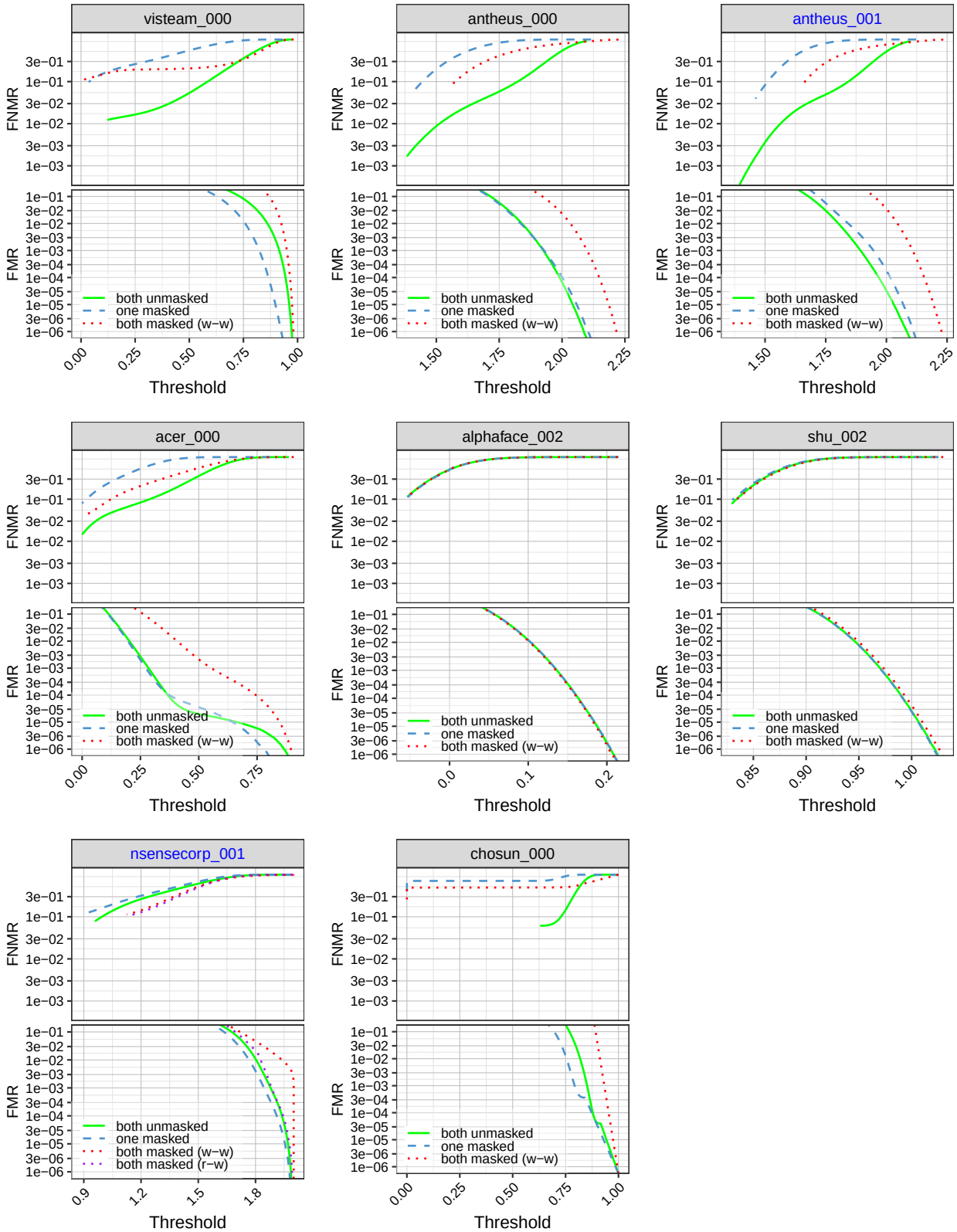


*Figure 53: FNMR and FMR calibration curves on unmasked-to-unmasked (both unmasked), masked-to-unmasked with medium, wide, lightblue masks (one masked), masked-to-masked with medium, wide, lightblue masks (both masked (w-w)), and masked-to-masked with medium, round, white masks (enrollment image) and medium, wide, lightblue masks (verification image) (both masked (r-w)). Algorithms in black were submitted prior to mid-March 2020, and algorithms in blue were submitted thereafter.*

# References


[1] ISO/IEC 19794-5:2011 - Information technology - Biometric data interchange formats - Part 5: Face image data.

[2] N95 Respirators, Surgical Masks, and Face Masks. https://www.fda.gov/medical-devices/personal-protective-equipment-infection-control/n95-respirators-surgical-masks-and-face-masks.

[3] NIST Special Database 32 - Multiple Encounter Dataset (MEDS-II). https://www.nist.gov/itl/iad/image-group/special-database-32-multiple-encounter-dataset-meds.

[4] Patrick Grother, Mei Ngan, and Kayee Hanaoka. NISTIR 8311 - Ongoing FRVT Part 6A: Face recognition accuracy with face masks using pre-COVID-19 algorithms. Interagency Report 8311, National Institute of Standards and Technology, July 2017. https://pages.nist.gov/frvt/reports/11/frvt_11_report_2017_07_29.pdf.

[5] Patrick Grother, George Quinn, and Mei Ngan. Face in video evaluation (five) face recognition of non-cooperative subjects. Interagency Report 8173, National Institute of Standards and Technology, March 2017. https://doi.org/10.6028/NIST.IR.8173.

[6] J. Hanley and A. Lippman-Hand. If nothing goes wrong, is everything all right? interpreting zero numerators. *JAMA*, 249 13:1743–5, 1983.

[7] Davis E. King. Dlib-ml: A machine learning toolkit. *Journal of Machine Learning Research*, 10:1755–1758, 2009. http://dlib.net.

[8] Mei Ngan, Patrick Grother, and Kayee Hanaoka. NISTIR 8311 - Ongoing FRVT Part 6A: Face recognition accuracy with face masks using pre-COVID-19 algorithms. Interagency Report 8311, National Institute of Standards and Technology, July 2020. https://doi.org/10.6028/NIST.IR.8311.

[9] Patrick Grother and Mei Ngan and Kayee Hanaoka. NIST Ongoing Face Recognition Vendor Test (FRVT) 1:1 Verification Application Programming Interface (API), April 2019. https://pages.nist.gov/frvt/api/FRVT_ongoing_11_api_4.0.pdf.

[10] Zhongyuan Wang, Guangcheng Wang, Baojin Huang, Zhangyang Xiong, Qi Hong, Hao Wu, Peng Yi, Kui Jiang, Nanxi Wang, Yingjiao Pei, Heling Chen, Yu Miao, Zhibing Huang, and Jinbi Liang. Masked face recognition dataset and application, 2020.

# Appendix A Dlib Masking Methodology

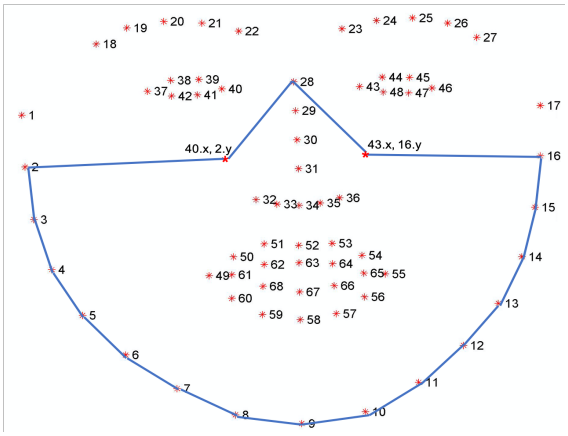


*(a) wide, high coverage*

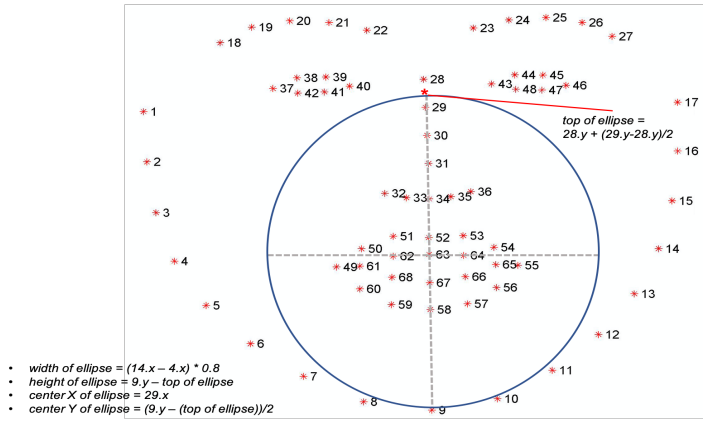


*(b) round, high coverage*

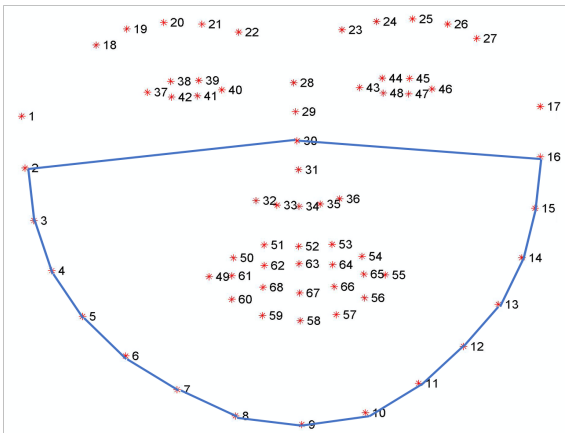

*(c) wide, medium coverage*

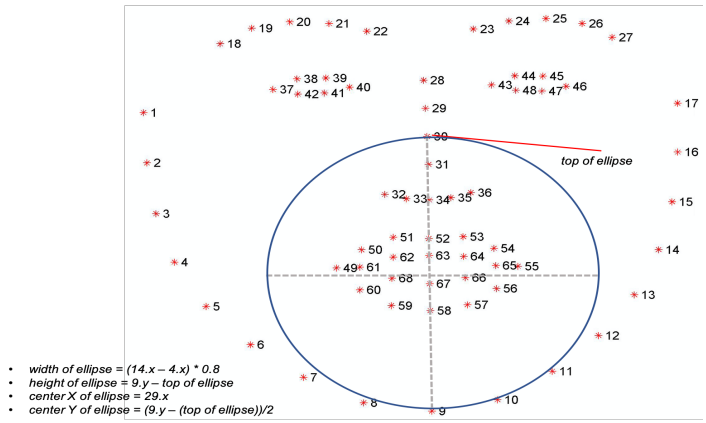


*(d) round, medium coverage*

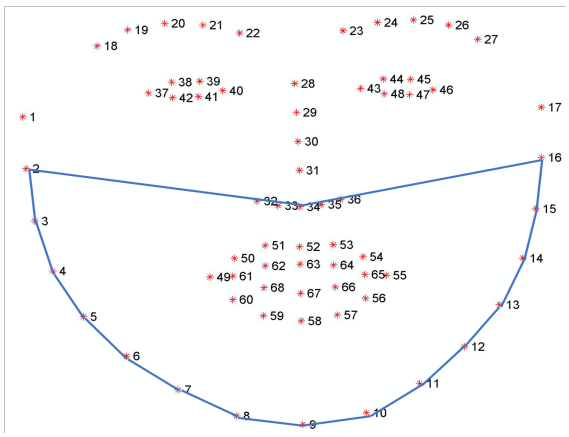

*(e) wide, low coverage*

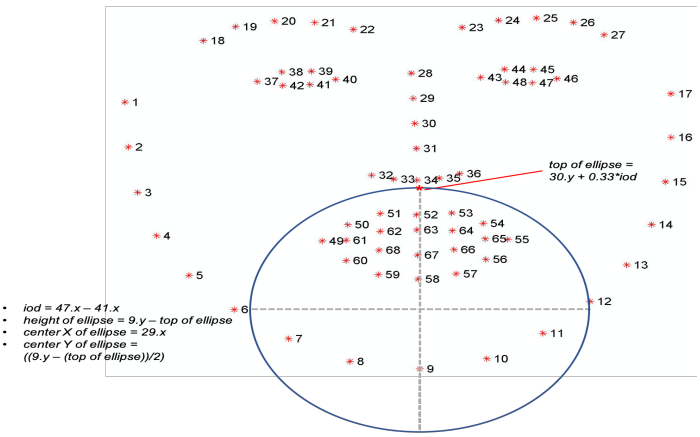


*(f) round, low coverage*

*Figure 54: This figure shows the Dlib facial points used to create the various synthetic masks used in this report. For wide masks, the specified Dlib facial points were used to generate a closed polygon and two additional points were interpolated between each dlib facial point used for smoothing purposes. For round masks, the specified Dlib facial points were used to generate an ellipse. The Dlib C++ toolkit version 19.19, configured with the common histogram of gradients (HoG)-based face detector and 68 face landmark shape predictor was used to generate the 68 facial landmarks.*





FNMR(T) "False non-match rate"
FMR(T) "False match rate"